M. A. MINOR

M.S.

This is to certify that the

thesis entitled

USING TOP DOWN MULTIPORT MODELING FOR
AUTOMOTIVE APPLICATIONS

presented by

Mark Andrew Minor

has been accepted towards fulfillment
of the requirements for

M.S. degree in Mechanical Engineering

R C Rosenberg
Major professor

Date 8/16/96

USING TOP DOWN MULTIPORT MODELING FOR AUTOMOTIVE APPLICATIONS

By

Mark Andrew Minor

A THESIS

Submitted to
Michigan State University
in partial fulfillment of the requirements
for the degree of

MASTER OF SCIENCE

Department of Mechanical Engineering

1996

ABSTRACT

USING TOP DOWN MULTIPORT MODELING FOR AUTOMOTIVE APPLICATIONS

By

Mark Andrew Minor

The objective of this research is to explore the development and use of a model library by simulating the powertrain and rigid body dynamics of a typical automobile. A top down hierarchical structure of an automobile system is developed and used as a foundation for a model library. The multiport macro node is used as the building block that allows the iconification of components or effects. Component models are developed, verified, then stored in the library. A vehicle model is constructed from the iconified component models. Issues raised by this exercise include multiport connectivity, valid operating range, parameter management, initial condition management, and standard model verification tests. As a result of the connectivity issues, causality and power flow must also be considered.

Dedication

I would like to dedicate this work to my Grandparents and Parents. Their support and guidance have made this possible.

ACKNOWLEDGMENTS

Special thanks to the guys is in the Computational Design Laboratory at Michigan State University. Dr. Rosenberg, Giuseppe DeRose, Michael Hales, and Wei-Wen Deng have given me tremendous support throughout the process of completing this thesis. Without their assistance, this would not be possible.

Table of Contents

List of Tables

List of Figures

1. Introduction

1.1 Problem Definition

Mathematical modeling of systems and components is now an accepted strategy for improving the efficiency of product design. A recognized tool for constructing mathematical models of complicated systems is the bond graph language. Bond graphs are typically constructed from a fundamental set of elements which are used to describe mixed domain systems and components. (Karnopp, 1990)

In the past few years an element known as Macro node has come into use. Macro nodes are used to describe complex behavior associated with a device or component, such as a pump or motor, using a single node to represent the device. A Macro node is displayed as an icon with connection ports which allow communication. The icon represents an underlying structure which typically is constructed of basic elements and possibly macro nodes. An intricate machine can be broken down by its subsystems and Macro nodes can be used to represent each subsystem. This compact representation simplifies system modeling and naturally leads to the reuse of models. A library of component/system models naturally follows.

Software applications, such as CAMAS (Broenink, 1995) and OLMECO (Top, 1995), have adopted the Macro node style of modeling. The problem is that the ENPORT (Hales, 1995) environment to date does not fully incorporate the hierarchical mentality associated with multiport modeling. In order to move forward the ENPORT group must further explore issues related to the use of Macro node modeling and the creation of a model library.

1.2 Statement of Objective

The objective of this research is to develop a general powertrain and rigid body kinematic model library for an automobile and investigate its use. The structure of the library will be based upon a top-down perspective of an automobile. The top down perspective dissects the automobile until all the systems can be modeled in terms of components such as the transmission, engine, or tire. The framework of the model library will be based upon the classifications which the top down structure creates. For each component an appropriate Multiport Macro node is created and it holds a place within the model library structure.

The model library will serve future researchers with a selection of models to use and build upon. The top-down structure guides the implementation and connection of the multiport nodes. The user is not to be burdened with the task of developing each individual model from scratch and deciding how they should communicate. Yet, if a user needs to customize a component model it is only a matter of editing the underlying structure of the multiport node. Further, the modified model can be saved as a new model in the library and reused at a later date.

In an industrial setting, the library and model structure also grant greater flexibility. Given that a model structure has been defined separate teams can work simultaneously on modeling different components or they can develop variations of the same component. In either case the multiport model allows faster development with more options for design alternatives. Vehicle models can be produced faster and component model interchangability is guaranteed by the clearly defined interface.

1.3 Thesis Structure

The structure of this thesis begins with a brief introduction to the problem definition and research objectives. Section 2 is dedicated to discussing the fundamentals of Hierarchical Multiport modeling. Section 3 discusses reusability and provides requirements for a model library. A sample library entry is given. Section 4 presents the top down model structure that the library will be based upon. A case study applied to an automobile will be examined in section 5 which explores the use of Macro nodes and a model library. Finally, in section 6 conclusions will be made based upon the case study results. Appendix A contains a more complete model library and Appendix B contains the subroutines used in this work.

2. Multiport Modeling

In this chapter we explore the issues associated with multiport modeling. There are three basic elements associated with multiport modeling which we will present and discuss. Then we examine how these elements fit together in a hierarchical structure.

2.1 Nodes

A node is a general term used to describe an object which graphically represents some mathematical model of a component, system, or phenomenon. There are two types of nodes: the Atom node and the Macro node. The Atom node is the most basic type and is used as a building block. They are used to describe physical or mathematical phenomenon and are the only node capable of directly stating a mathematical relationship. Figure 1 illustrates two cases of Atom nodes. Figure 1a represents a typical atom node

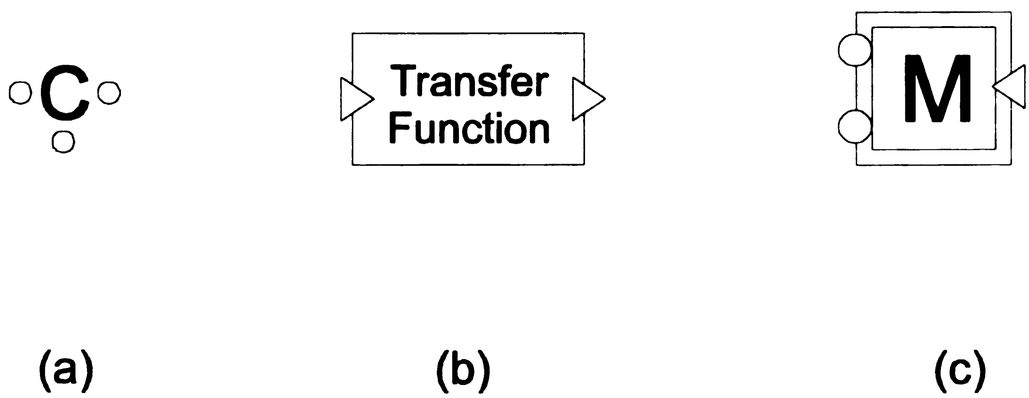

Figure 1: Node Examples. (a) Typical Atom node. (b) Special Atom node. (c) Macro node.

from the bond graph language (Karnopp, 1990) and Figure 1b represents a specialized atom node for a transfer function. The Macro node, shown in Figure 1c, is used to iconify an underlying graphical node structure. This graphical structure may consist of both Atom and Macro nodes in conjunction. Figure 2b illustrates this point.

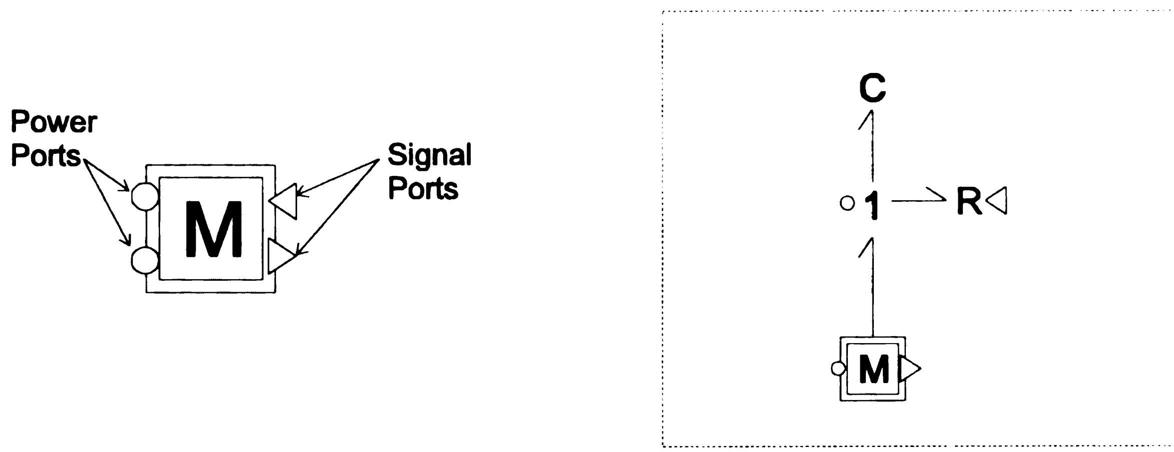

(a) (b)

Figure 2: Macro Node Illustration. (a) Macro node appearance. (b) Macro node contents.

2.2 Ports and Connectors

A port is an object associated with a node that allows the node to communicate with its environment. There are two primary types of ports and a node may posses multiples of each. The first type of port is the Power port and it allows other nodes to communicate with the node. This implies that the port exchanges effort and flow data, but causality may also be a concern. Causality is determined by the underlying model which may have indifferent, constrained, or restricted causality amongst its power ports. The Signal port is the other type of port. It allows one variable to flow through the port and the direction of that flow is indicated by the direction it points. Figure 2 illustrates the use of both Power and Signal ports. If a node has multiple ports it is referred to as a Multiport node. There are Multiport Macro nodes and Multiport Atom nodes. Figures 1 and 2 both illustrate Multiport nodes.

Connectors permit ports, and ultimately nodes, to communicate. Connector types include bonds and signals. Bonds carry effort and flow information between ports. Causality must be assigned to a bond to facilitate computability. In contrast, Signals only carry data and direction of data flow is indicated by the Signals' arrow. Observing Figure 2, note that a port symbol is only used when a port is not connected. It is implied that a port is present where a connector contacts a node.

2.3 Hierarchy

Top down modeling hierarchy views a model as consisting of multiple levels of information which vary in detail. At the highest level the model is viewed from its most simple perspective and as we move into lower levels of the model we zoom in on its structure. At the very highest level of this hierarchy, the model appears simply as a Macro node with Ports that allow the model to interface with its environment. The simplest perspective of an automobile is as a complete system which interfaces with the driver, road, and environmental conditions.

A convenient database has been developed by Hales (1995) which represents this structure. Rather than referring to parent and child levels, Figure 3 illustrates a hierarchical structure which numbers the various levels. Here the simplest perspective of the system is the System Graph, which is viewed at level 1. This is how the system would appear if used as a Multiport in a parent level. The system graph can be expanded to view the children at the next level in 1.1. Level 1.1 contains other Macro nodes which act as parents to their own subsequent underlying structure. Accordingly the child levels of these other macro nodes are referred to as 1.1.1 and 1.1.2. This same numbering scheme can be extended to the individual atoms which are used to build a sub level, but that aspect is not explored here.

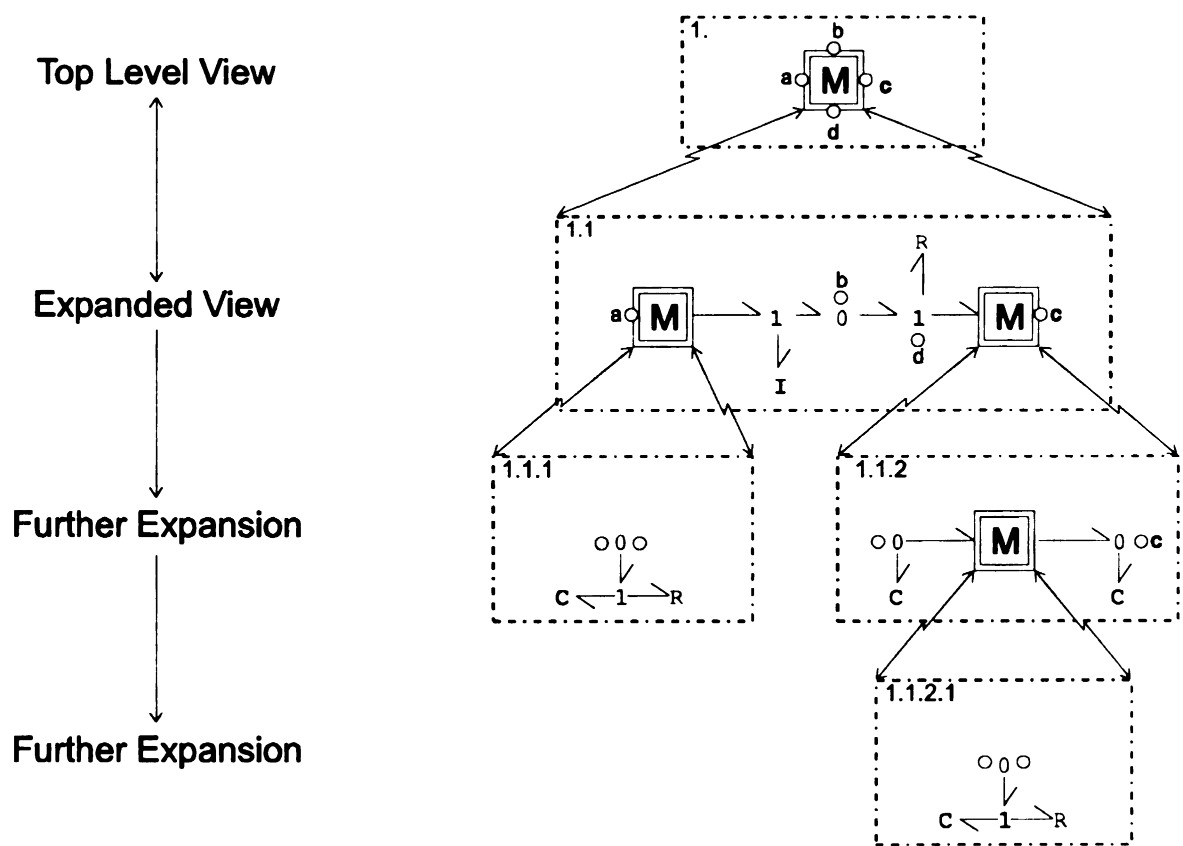

Figure 3: Sample Top Down Model Hierarchy

3. Design of a Model Library

3.1 Reusability and Libraries

Further observation of Figure 3 reveals that child levels 1.1 and 1.2.1 contain essentially the same sub-model. This is not an uncommon situation in modeling given that systems often contain multiple occurrences of similar components. For example, an automobile model requires four tire models that are similar. On a broader scale a component may be used in other models as well. That same tire model may be applicable over a wide range of applications. Much time and energy could be saved if a standard model of that tire was created and available for usage. The next issue which must be considered is the accessibility of those models.

Reusability of component models is only feasible if the models are stored and organized in structured manner. A library of component models would facilitate storage and organization of those models. The next question that has to be addressed is how to organize the library. There are many different schemes that are possible, but one scheme has to be chosen. The scheme selected in this research is based upon a top down perspective of the automobile. The top down hierarchy is presented in the next chapter, but its key features will be presented here to give the reader a better impression of the library structure. From the highest level the vehicle is viewed as a Multiport macro node which interfaces with its environment. We expand this macro node and discover that the automobile is considered in terms of its powertrain and kinematics. Each of these sub-systems can be further expanded until we are viewing the component models which make them up. The library developed here will be structured based upon this hierarchical viewpoint.

The refinement of the hierarchical breakdown is determined by the requirements of the users. If the modeler is interested in the general performance of a vehicle then the breakdown should consider major components such as the engine and transmission. Different combinations of engine and transmission could be examined for affect on vehicle performance. If the user is interested in building transmission models then the library should have smaller scale models for pumps and valves. In either case the refinement of the library is determined by the requirements of the user. This research is directed towards exploring the development of a model library for the kinematics and powertrain of a vehicle. Development of larger component models, such as the engine, which fit within this hierarchy are sufficient for exploring the issues involved with developing and implementing such a library.

3.2 Background

This section of the paper discusses the fundamental concepts and information required to build a library of component models. Currently, there are two primary schools of thought regarding model libraries. Stein (1995) supports the development of a two level modeling approach which utilizes an expandable component model library. The first level of Stein's approach is equivalent to viewing a component model as a node. The second level views the physical model which describes the component. Expandability refers to the model's ability to capture varying levels of complexity. For example, a drive shaft could be viewed as a simple lumped mass torsional member or several lumped mass members. In his current work, the physical model which Stein refers to is a traditional bond graph model. Stein does not focus on the development of a multilevel library which can contain nested sub-models.

Similar to Stein, Top (1995) suggests that a model library needs to contain a variety of models varying in levels of complexity and validation status. However, Top further suggests that the models can be based upon generic building blocks and hence contain nested sub-models. This type of modeling structure is much more conducive to hierarchical modeling which should support the birth of new component models through the combination of existing models. For example, if a user is building a model of an automatic transmission (s)he should be able to select valves from a set of validated valve models and not have to build five identical valve models. Top also points out that if a model is to be reusable it has to be described in terms of what type of component it is, how the model is conceptually intended to be used, and what mathematical relations apply. Top's work is much more focused on developing a fundamental library structure which is adapted to reuse and growth.

3.3 A Proposed Library Structure

The author of this thesis agrees with Top that a library structure must support the reuse of component models in system models and in the development of hierarchical component models. Further, a component model should be able to be modified from its original form to support model refinements and modifications when an implementation of the model requires it. The library structure should also provide sufficient information to its users such that they can easily understand the intended use of the stored multiport models. Subjects such as energy domain, port type, range of valid usage, and units must not be neglected.

Clearly the component view point indicates that the library be divided by type of component. However, it is insufficient to state that a library of component models is available without further qualifying what energy domain(s) the models apply to and whether the models are mean value or dynamic in nature. Therefore the library structure must clearly indicate what the component is and what physical characteristics of the component are under consideration. A library should contain sufficient information regarding a model such that the user can evaluate the intended usage and applicability of a model. This means that a model's underlying assumptions and dynamic qualities must be clearly described. To assure proper implementation of a model library the port type, domain, and units must be indicated for every port; parameter usage, units, and range must be described as well. The developer of a component model must be aware that the model (s)he is developing is intended for reuse and take proper precautions in documenting assumptions, parameters, and intended qualitative behavior.

A summary of the relevant information which a library should contain is as follows:

- what component the model applies to
- what aspect of the component the model captures
- what assumptions were made in constructing the model
- port connection and domain data
- parameter usage, range, and units
- validation results

In the structure of the library developed here all of the above are addressed in three separate sections for each component. The first section is "Model Description and Assumptions" which describes what component the model applies to, what aspect of the component is considered, and what assumptions were made in the construction of the model. The second section is "Ports and Parameters." For each port this section indicates what information the port transfers, port type (signal versus power flow), and what units apply. This same section also indicates what parameters are used in the component model as well as what their corresponding units and relevant range of applicability are. The third section is "Verification Results." This section describes what verification tests a model had to pass in order to be deemed valid. A description of the tests and results is included as well as a discussion.

3.4 A Library Example: A Propelled Two Dimensional Rigid Ring Tire Model

A component model is presented as an example of how a typical component model should be described in a model library. Information associated with the component model is presented in the fashion prescribed above. A more useful model library is included in Appendix A which contains a set of component models sufficient to illustrate the use of a model library applied to an automobile's powertrain and kinematic dynamics.

3.4.1 Model Description and Assumptions

The tire model presented here is a combination of work by Pacejka (1991) and Zegelaar (1993). Work by Zegelaar is used to construct the interface between the tire carcass and the rim. (see Figure 4) His model is capable of capturing torsional, vertical, and longitudinal dynamics. The interface between the tire carcass and the ground is described by Pacejka's "Magic Tyre Formula" applied solely to longitudinal slip in conjunction with non-linear springs which consider tire contact with the road.

In the Zegelaar model it is assumed that the behavior of the tire acts as a linear spring about its equilibrium point and that damping is negligible. A rigid ring is used to represent the tire carcass and is connected to the rim via translational and rotational springs. The result is a model which is capable of capturing the zeroth and first modes of the tire and rim interaction in both translation and rotation. Since the model approximates the lower modes only, the model is only applicable to lower frequency usage up to 90 Hz. A small amount of damping has been introduced as shown in Figure 5 which represents the tire-rim interactions more realistically and provides for a numerically better conditioned model.

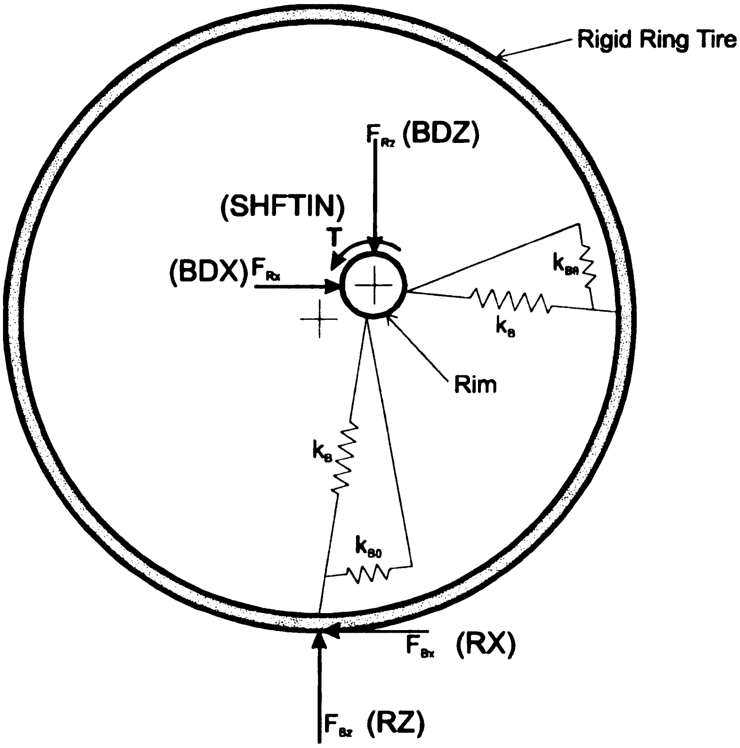

Figure 4: Diagram of Rigid Ring Tire Model

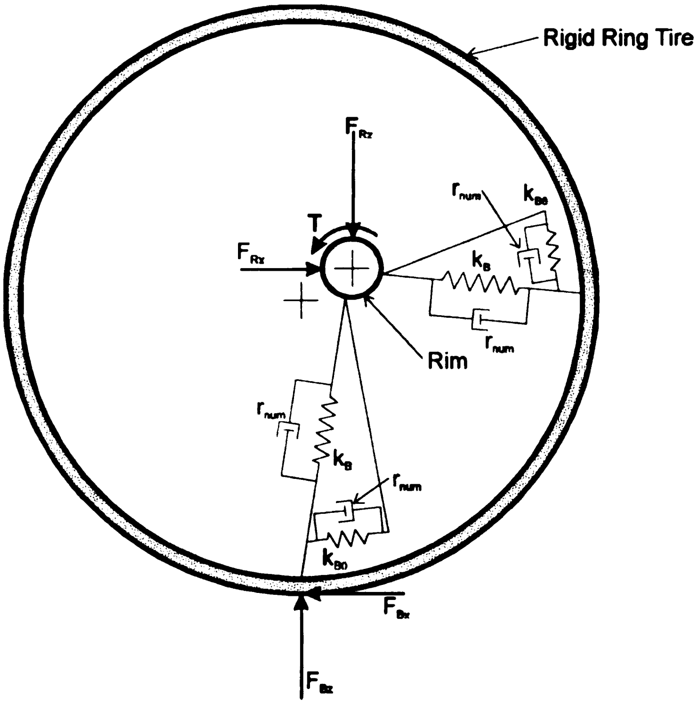

Figure 5: Diagram of modified Rigid Ring Tire Model

The Zegelaar model also suggests the use of a first order transfer function to approximate the tire carcass and longitudinal tractive interactions. However, since very small phase and amplitude effects are noted at lower frequencies, a steady state model presented by Pacejka is used which more accurately describes tractive force as a function of longitudinal slip. Here longitudinal slip, x, is described as,

$$x = \frac{r\Omega - V}{V} \tag{1}$$

where r is the rolling radius, Ω is the angular velocity of the tire, and V is the longitudinal velocity of the rigid rim. Figure 6 shows the fraction of normal force transferred to longitudinal force as a function of longitudinal slip, x, for a set of parameters characteristic of dry pavement. A more complete description of these parameters follows in the Ports and Parameters section.

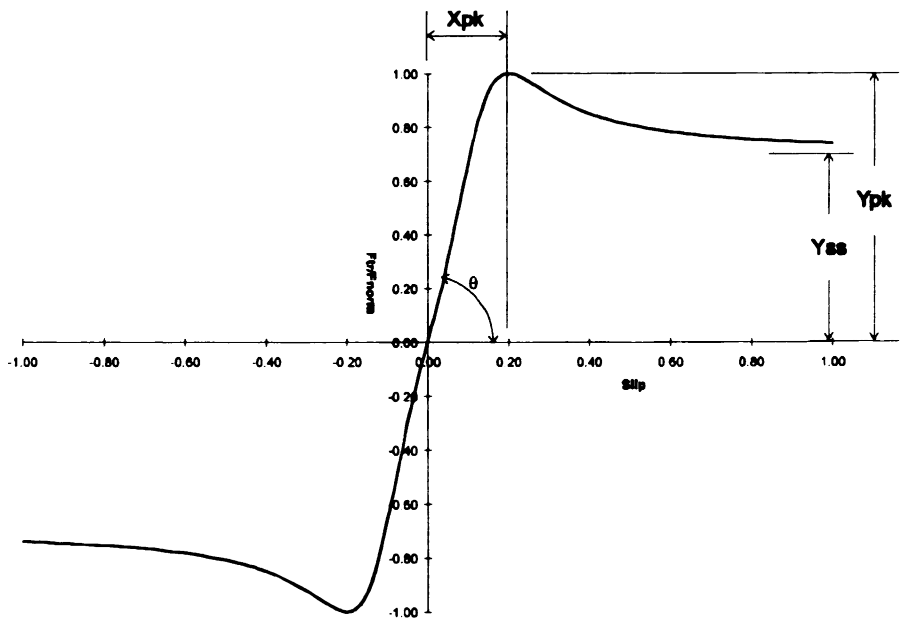

Figure 6: Fraction of transmitted Normal Force as a function of longitudinal slip, x.

Ground and tire contact is described by a non-linear spring which has a stiffness profile as shown in Figure 7. Note that the stiffness of the ground tire interaction is recommended to be at least ten times greater than the stiffness of tire itself. While this minimizes displacements as a result of road surface deformation, it creates a much stiffer model. The result is that the model is much more computationally intensive to solve but is more accurate regarding road contact. A slight amount of damping has also been included in the ground interface.

Figure 8 is the bond graph of the Rigid Ring tire model. The structure of the graph will not be examined but the meaning of the nodes, except 0's and 1's, will be explained in Table 1. There the node name, primary coordinate, type, relevant subroutines, and a brief description of the node are included. Several subroutines are referenced by the nodes and are as follows:

ZZSU01 - Multiplies several model parameters and a model variable.
ZZSU02 - Non-linear contact stiffness. See Figure 7.
ZZSU23 - Pacejka's longitudinal traction model as a function of slip. See Figure 6.

These user subroutines can be found in Appendix B.

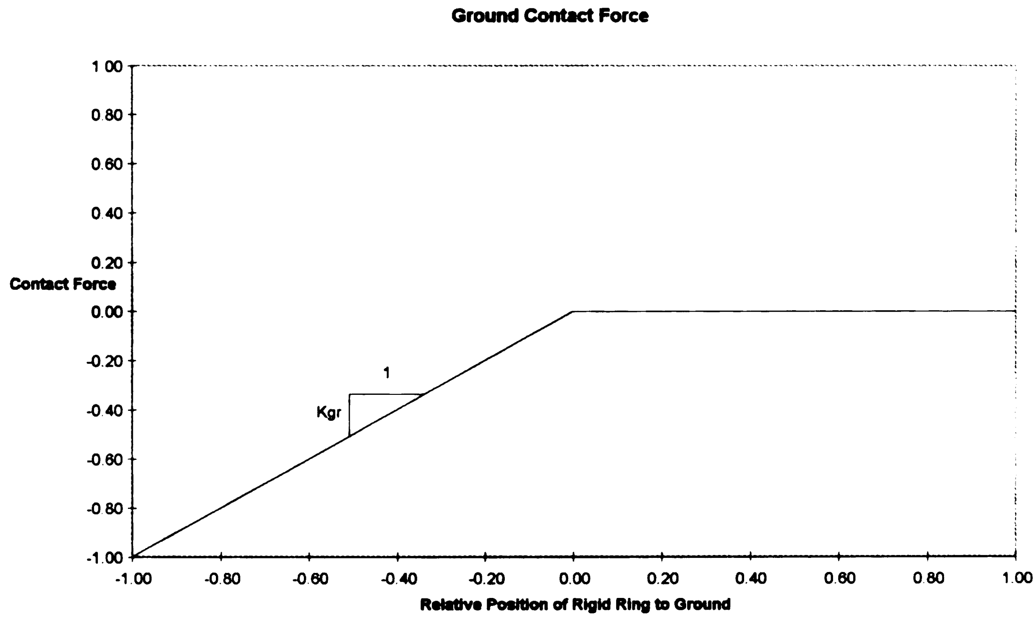

Figure 7: Non-linear Contact Force Function

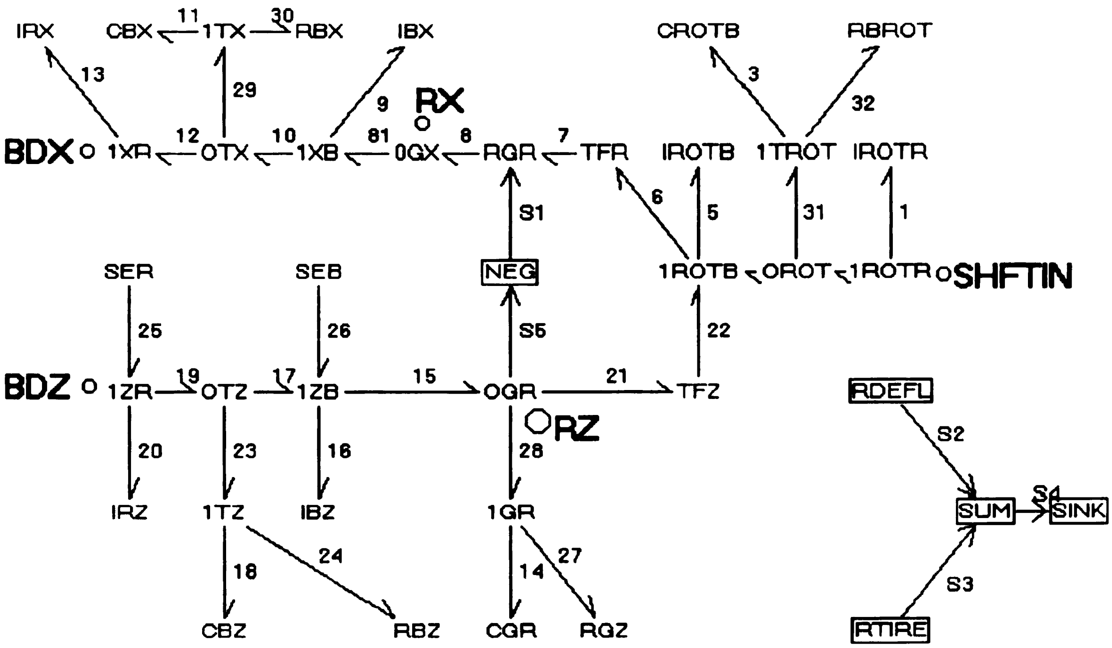

Figure 8: Bond graph submodel of a Rigid Ring tire model

Table 1: Rigid Rim Tire Model node descriptions

Name	Type	Primary Coordinate	Associated Subroutine	Description
1ROTB	1	θ		Sums the torques applied to the tire (rigid ring).
BDX	port	x		Rim connection to axle
BDZ	port	z		Rim connection to axle
CBX	C	x		Tire stiffness
CBZ	C	z		Tire stiffness
CGR	C	z	ZZSU02	Ground contact stiffness
CROTB	C	θ		Tire torsional stiffness
IBX	I	x		Tire Intertia
IBZ	I	z		Tire Inertia
IROTB	I	θ		Rotational Inertia of the tire
IROTR	I	θ		Rotational Inertia of the rim
IRX	I	x		Rim Inertia
IRZ	I	z		Rim Inertia
NEG	fcn	z		Conditions normal force signal such that it is positive when in compression
RBROT	R	θ		Tire/Numerical torsional damping
RBX	R	x		Tire/Numerical Damping
RBZ	R	z		Tire/Numerical Damping
RDEFL	src	z		Deflection of tire from free radius
RGR	R	x	ZZSU23	Pacejka Magic Tyre model slip function
RGZ	R	z		Ground contact damping
RTIRE	src	z		Free radius of tire
SEB	SE	z	ZZSU01	Gravitational force of tire
SER	SE	z	ZZSU01	Gravitational force of rim
SFGRND	port	z		Road profile
SHFTIN	port	θ		Rim connection to axle
SUM	sum	z		Sums RDEFL and RTIRE to give actual tire radius
TFR	TF	$x \leftrightarrow \theta$		Effect of longitudinal force on torque applied to rim
TFZ	TF	$z \leftrightarrow \theta$		Effect of normal force on torque applied to rim

Table 2: Port description for a Rigid Rim tire model

Port	Type	Units	Description
BDX	Bond	N m/s	Longitudinal force to rim Longitudinal velocity of rim
BDZ	Bond	N m/s	Vertical force to rim Vertical velocity of rim
SHFTIN	Bond	N-m rad/sec	Torque to rim Angular velocity of rim
RX	Bond	N m/s	Traction Force transmitted to ground Velocity of ground profile
RZ	Bond	N m/s	Vertical Force transmitted to ground Velocity of ground profile

Table 3: Parameter description for a Rigid Rim tire model.

Parameter	Node	Units	Typical Value	Description
YSS	RGR	-none-	0.84	Asymptotic F-traction/F-normal for tire at high slip
YPK	RGR	-none-	0.95	Peak value of F-traction/F-normal
XPK	RGR	-none-	0.22	Slip value where YPK occurs
THETA	RGR	-none-	80° - 87°	Initial slope of traction curve.
KBθ	CROTB	N-m/rad	70100	Torsional stiffness of tire.
KB	CBX, CBZ	N/m	1.47×10^6	Translational stiffness of tire
MRIM	IRX, IRZ	kg	5.0	Mass of rim
MTIRE	IBX, IBZ	kg	4.52	Mass of tire
JRIM	IROTR	kg-m^2	.100	Rotational Inertia of rim
JTIRE	IROTB	kg-m^2	.375	Rotational Inertia of tire
RTIRE	RTIRE	m	.288	Undeformed tire radius
RNUM	RBZ, RGZ, RBROT		100	Tire/Numerical Damping
G	SER, SEB	m/s^2	9.81	Acceleration due to gravity
KGR	CGR	N/m	7.35×10^7	Contact stiffness with ground
RG	RGZ		1×10^4	Contact damping with ground

3.4.2 Ports and Parameters

The external ports of the Rigid Ring tire model are indicated in Figure 8 as BDX, BDZ, SHFTIN, RX, and RZ. Since each port is connected to a bond there are two pieces of information associated: effort and flow. For each port Table 2 indicates the name, port type, a brief description, and units associated with that port.

Parameters associated with the Rigid Rim tire model are described in Table 3. The parameter name, associated node, units, a brief description, and a typical range have been indicated for each parameter. The parameters ranges listed for the node RGR are typical for the longitudinal slip-traction characteristics of a tire on dry pavement. (Wagner, 1995) The remaining parameters describe the linear characteristics of a smaller tire with a 70% aspect ratio. (Zegelaar, 1993)

3.4.3 Model Verification

Verification of the Rigid Ring tire model must be a multistep process since the model is relatively complicated and certain aspects of the model's performance must be verified methodically to insure proper performance of the model as a whole. The following tests must be completed:

Test 1 - Tire deflection in the z-direction.
Test 2 - Effective tire radius passed to TFR
Test 3 - Torque resulting from longitudinal deflection and normal force
Test 4 - Steady state longitudinal velocity of tire.

For Test 1, tire deflection in the z-direction can be tested by applying a load to port BDZ with all other inputs and initial condition set to zero. The anticipated result is an initial transient, which with the added tire/numerical damping will damp out to a steady state equilibrium without oscillations. If tire/numerical damping was not present the oscillations would result in steady harmonic equilibrium. Figure 9 demonstrates the effect of added damping on tire deflection with a 2000N load which is appropriate for most cars, applied to port BDZ. Special care must be taken when simulating this model because of stiff ground contact. For example, since the stiffness of the ground contact is 50 times greater that the tire stiffness the simulation time-step must be set appropriately to capture the affects of 460 Hz rather than 90 Hz, which is the natural frequency of the tire. Further, the benefit of added damping can be observed by viewing the Undamped response in Figure 9 as compared to the Damped response and noting the steady state behavior of the two. Clearly, the Damped response is much more realistic and both have a mean steady state deflection of 0.139 cm. If we compute the expected deflection of the tire given the net 2050N load and 1.47 MN/m tire stiffness, we also get 0.139 cm. While this deflection seems a bit small for an initial load application, we have to keep in mind that the stiffness we are using is intended to be implemented about an equilibrium point.

Given that the steady state deflection is accurate and that the numerical damping seems to be of benefit, we can assume that the damped vertical deflection of the model is valid.

Test #2 of the model is intended to assure that the effective radius of the tire is accurate after a load is applied. The tire radius is calculated by a summing node, SUM, and two signal source nodes, RDEFL and RTIRE. This test is to assure that the calculated radius is of the expected value. Given that the same 2000N load is applied as in Test 1, we know that the tire radius should be 0.139 cm smaller resulting in a new radius of 0.2866m. Figure 10 illustrates the actual effect of the applied load on tire radius. It can be observed that the tire radius does decrease as expected and that the response has a transient dynamic nature. We can therefore assume that the results of this test are valid.

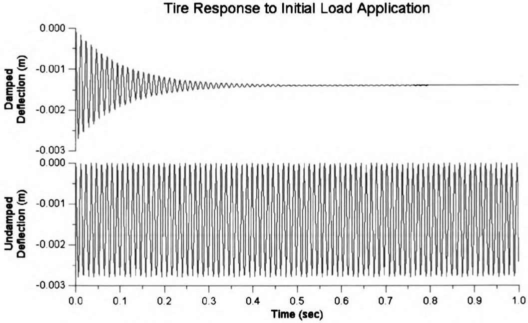

Figure 9: Test 1 - Damped and undamped response of vertical tire deflection to initial load application.

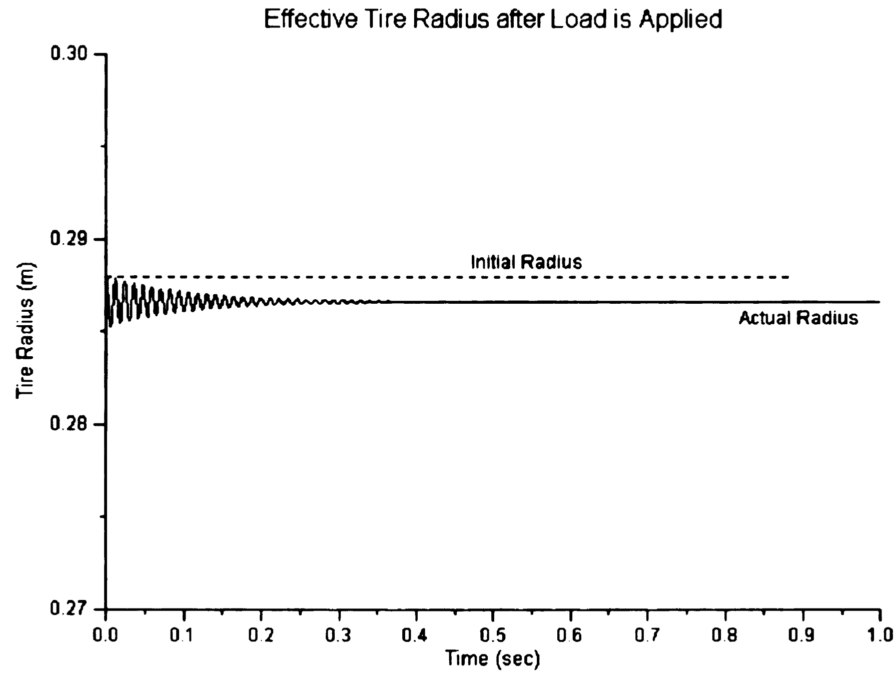

Figure 10: Test 2 - Effective Tire Radius after a 2000N load is applied.

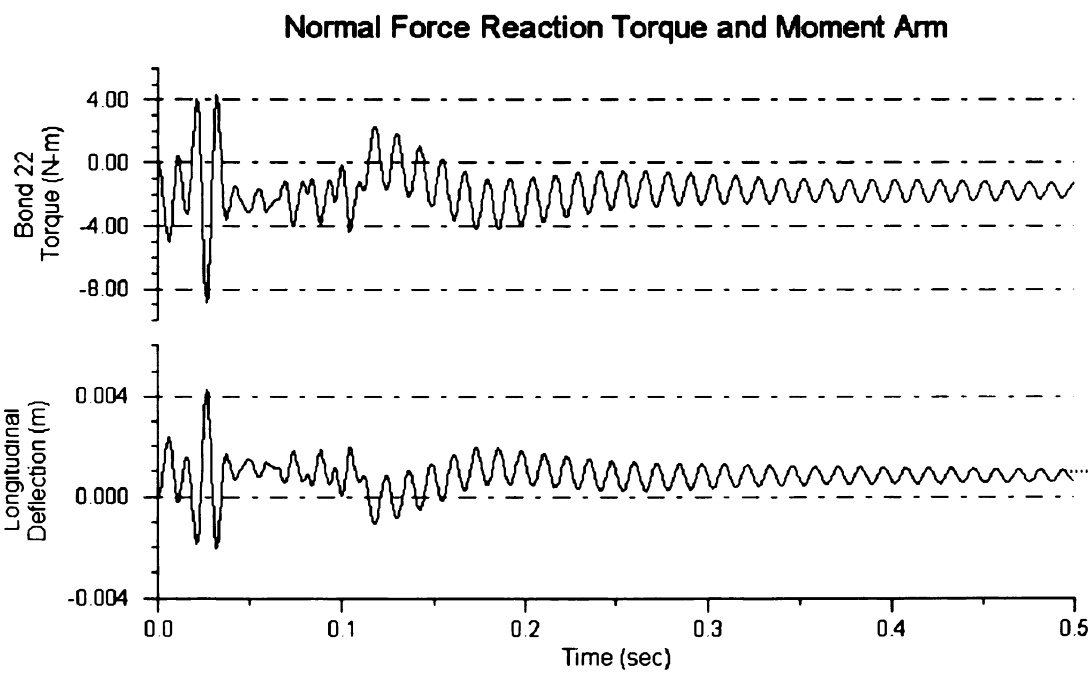

Figure 11: Test 3 - Torque as a result of longitudinal deflection and vertical forces.

Test #3 is intended to verify the torque applied to the rim and axle as a result of vertical forces and longitudinal deflection. It is anticipated that this torque will counteract the positive input torque at SHFTIN being applied to the rim. We can confirm this by inputting a step torque to SHFTIN and observing the longitudinal deflection and the effort associated with bond 22. Figure 11 illustrates that as the tire pulls the inertia of the vehicle there is a negative reaction torque resulting from the vehicle lagging behind the tire and generating a torque proportional to the longitudinal deflection. Based upon these results it is confirmed that the normal force resultant torques are valid.

Test #4 verifies the longitudinal velocity of the tire to a given input shaft speed. In this test the input shaft speed is 20 radians/second and it is anticipated that the final longitudinal velocity of the wheel will be 5.73 m/s given the steady state tire radius of 0.2866 m. Figure 12 shows the angular and longitudinal velocities of the tire when the angular velocity is ramped up from zero to 20 rad/sec in a one second time period. Note that the longitudinal velocity goes through a transient and then reaches its steady state velocity of 5.73 m/s in around 1.2 seconds. The final speed is as expected and it is concluded that the model is verified.

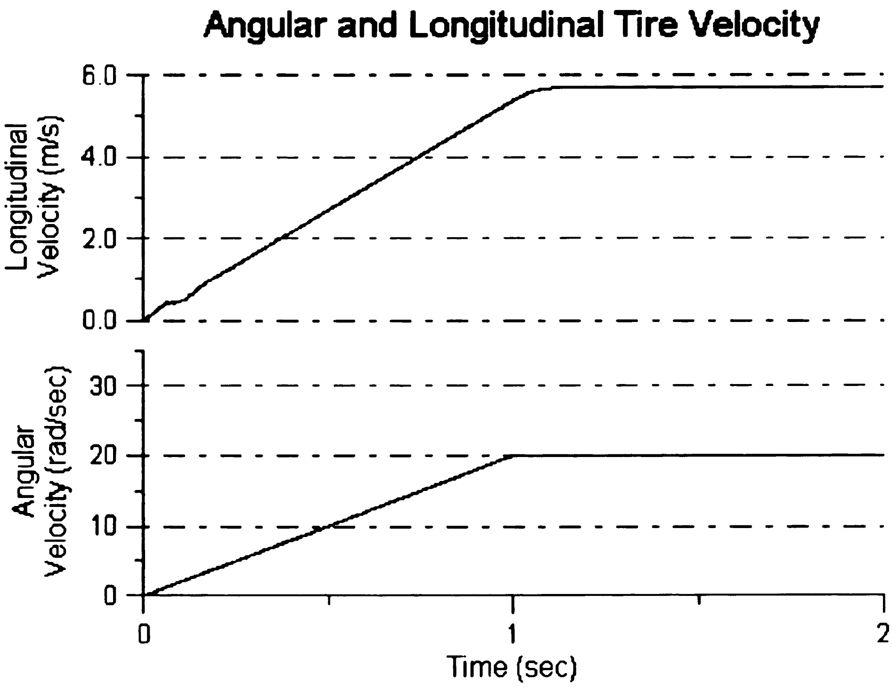

Figure 12: Test 4 - Longitudinal and angular velocity of the tire.

4. Top Down Model Structure

The structure of a mathematical model describing the propulsion/braking characteristics of a typical automobile is presented here. The model focuses on the powertrain and rigid body kinematics of the automobile. The structure of the model is presented from a top down perspective where the major systems under consideration are subdivided into sub-systems. This top down perspective of the automobile will serve as a hierarchical structure for the model library created by this research. Since our goal is to explore the development and use of a model library we will only explore the hierarchical structure of the major systems and components in the vehicle. We will not be examining the structure and details of a particular engine or transmission. This structure will be more general and applicable to a wide range of configurations.

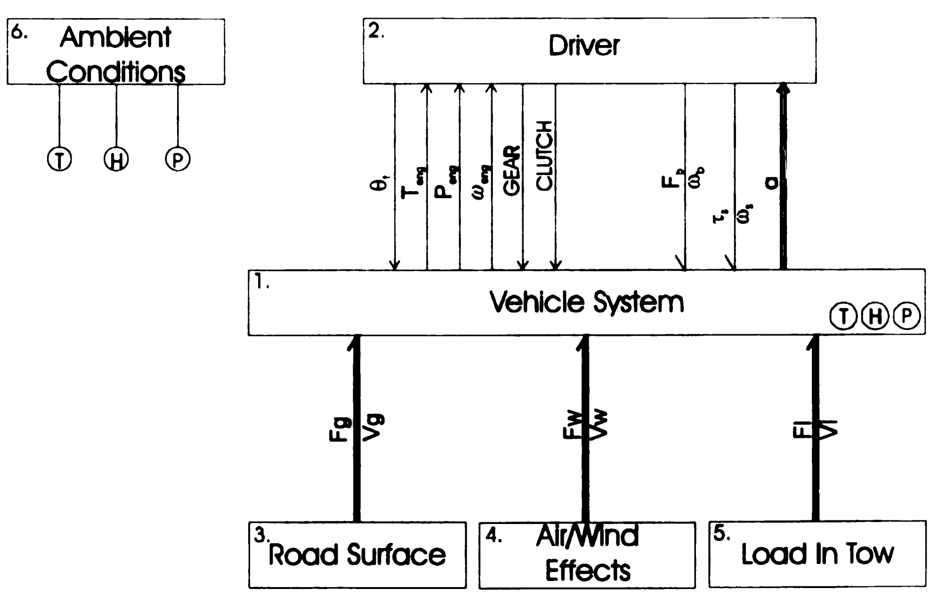

Figure 13: Top Level System Graph

4.1 Top Level

The top level model structure is shown in Figure 13. This level describes the interface between the vehicle system and its external environment; namely the driver, road surface, wind effects, and load in tow. Note that at this level, the vehicle system is shown as a macro node and is labeled "1. Vehicle System." The ports are not drawn here, but it is understood that where a connector is adjacent to a macro node a port is present. Further note that "6. Ambient Conditions" shows connectors draw to symbols such as T which indicate that this information may be used elsewhere in the model rather than drawing a signal to the necessary ports. The symbol can then be inserted where necessary and connected appropriately. Connections between many of these sub-systems are made using multiport vector bonds and vector signals. (Margolis, 1989) Such a connector type is a convenient means of simplification and generalization. Table 4 describes the connectors from Figure 13, and their type and units.

4.2 Vehicle System

The vehicle system is shown in Figure 14 below. Note that the Macro node "1. Vehicle System" has been opened to show its child level. Further note that it has two children; macro nodes "1.1 Power Train" and "1.2 Vehicle Dynamics." The child levels of these macros will be shown later. While it is not necessary to show sub-systems external to the macro node, the Driver, Road Surface, Air/Wind Effects, and Load in Tow are shown here to assist the reader in visualizing the Vehicle System's external connections. Further use has also been made of vector bonds and signals here to exploit their compactness and generality. Table 5 below details the connector internal to this macro node at this level.

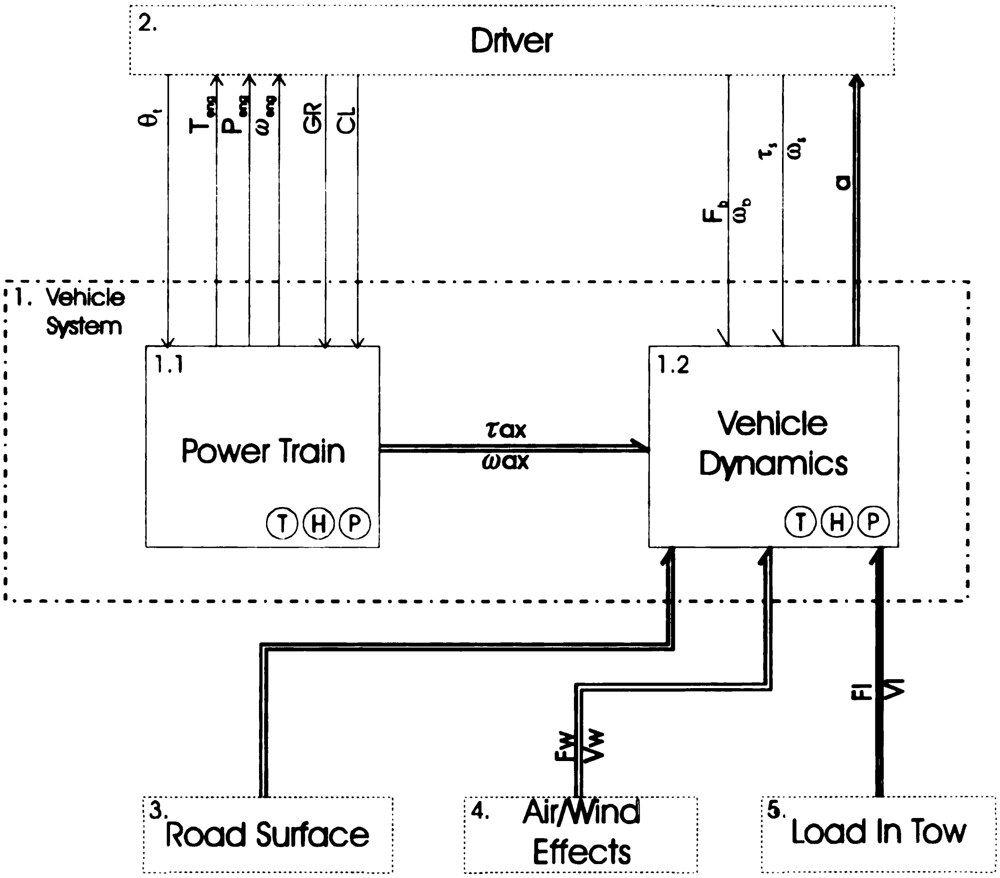

Figure 14: Vehicle System, Level 1.

Table 4: Top Level Variables

Symbol	Description	Connector Type	Units
ω_{eng}	Engine Speed	Signal	rad/sec
τ_s	Steering torque	Bond	N-m
ω_s	Steering Angular velocity		rad/sec
θ_t	Throttle angle	Signal	radians
CLUTCH	Clutch engagement	Signal	-
F_b	Applied brake force	Bond	N
V_b	Brake velocity		m/s
F_g	Force of ground	Vector Bond	N
V_g	Velocity of ground		m/s
F_l	Force of load	Vector Bond	N
V_l	Velocity of load		m/s
F_w	Force of wind	Vector Bond	N
V_w	Velocity of wind		m/s
GEAR	Gear selection	Signal	-
P_{eng}	Engine oil pressure	Signal	kPa
T_{eng}	Engine Temperature	Signal	°C
a	Driver perceived acceleration	Vector Signal	m/s^2

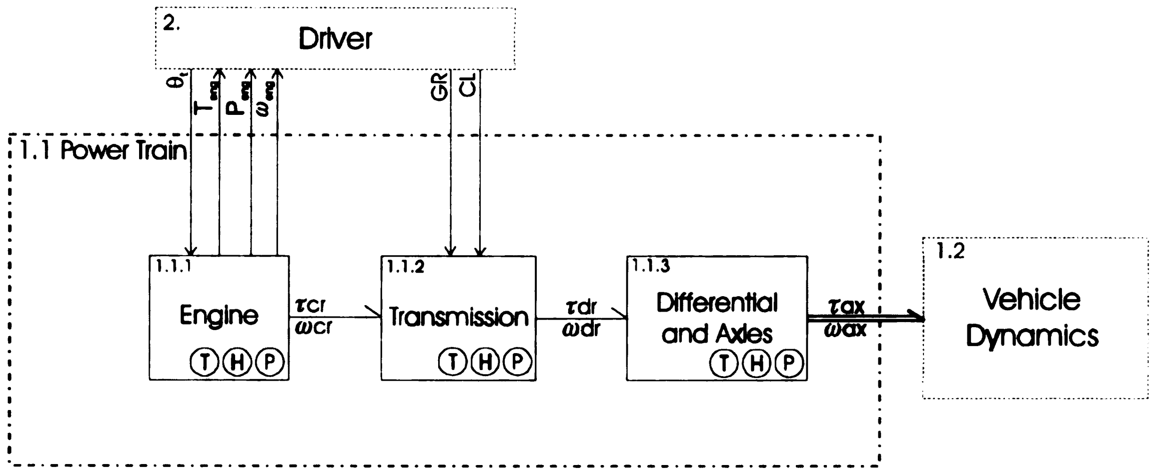

Figure 15: Powertrain, Level 1.1

Table 5: Vehicle System Level Connectors.

Symbol	Description	Connector Type	Units
τ_{ax}	Axle/body torques	Vector Bond	N-m
ω_{ax}	Axle/body relative angular velocity		rad/sec

Table 6: Powertrain Level Connectors.

Symbol	Description	Connector Type	Units
τ_{cr}	Crankshaft/Transmission Torque	Vector Bond	N-m
ω_{cr}	Crank/Trans relative angular velocity		rad/sec
τ_{dr}	Transmission/Differential Torque	Vector Bond	N-m
ω_{dr}	Trans/Diff relative angular velocity		rad/sec

4.3 Power Train

Figure 15 shows the child level of the "1.1 Powertrain" macro node from Figure 14 above. This level details the structure of the Powertrain macro node. Note that the children of this level are "1.1.1 Engine", "1.1.2 Transmission", and "1.1.3 Differential and Axles." This division was chosen because each of these sub-systems interacts as a set of distinct components with well defined modes of interaction. This correlates well with the preferred library structure discussed in Chapter 2. Table 6 below describes the connectors in this level.

4.4 Vehicle Dynamics

The internal structure of the "1.2 Vehicle Dynamics" macro node is shown in Figure 16. The children of this macro node include "1.2.1 Vehicle Body/Frame", "1.2.2 Front Suspension", "1.2.3 Brake System", "1.2.4 Rear Suspension", "1.2.5 Tire 1", "1.2.6 Tire 2", "1.2.7 Tire 3", and "1.2.8 Tire 4". Unique to this level is the connector distribution box, shown as  which signifies that a vector bond or signal is split into components. In this case those components include the connectors between the ground and the tires. The tires in this case are numbered one through four. Figure 17 illustrates the numbering of the tires with reference to a typical automobile as well as the SAE standard vehicle coordinate system (Gillespie, 1992). This coordinate system will be used in the simulations and sub-models following.

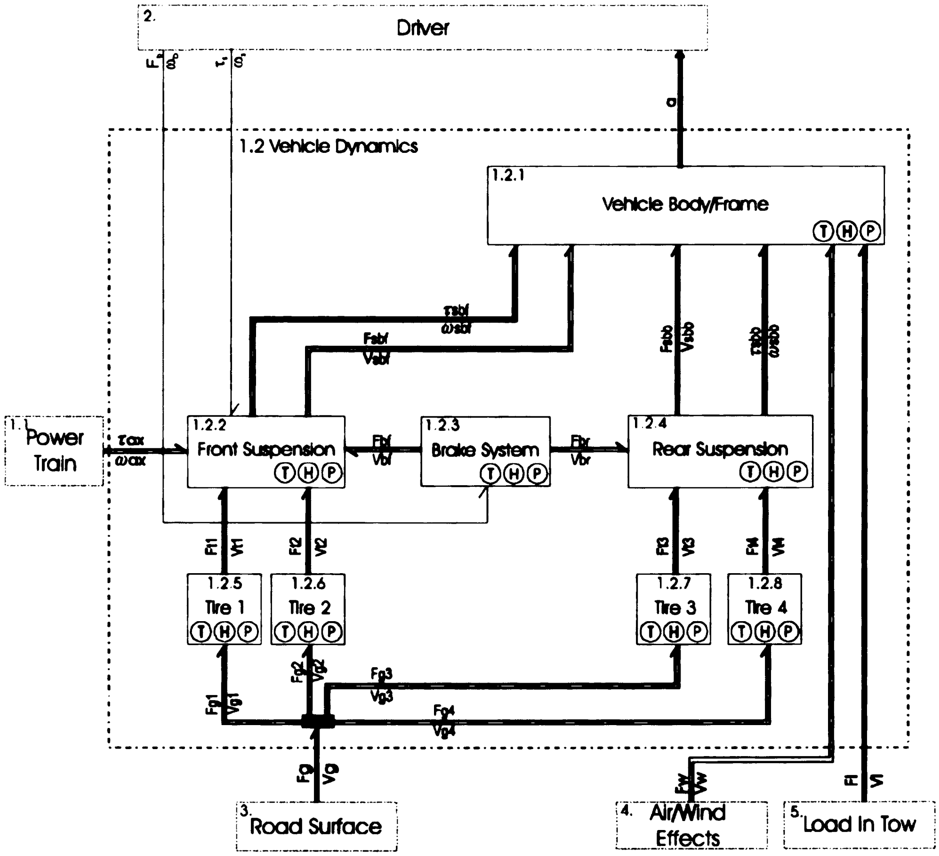

Figure 16: Vehicle Dynamics

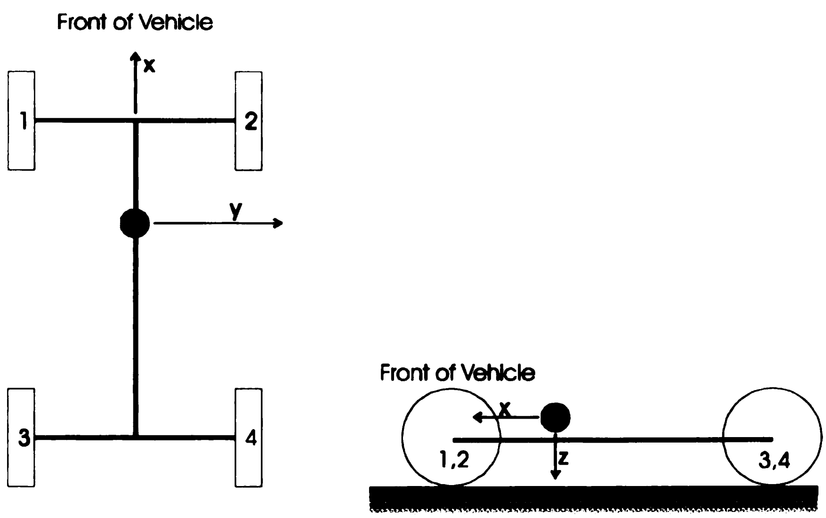

Figure 17: Vehicle Coordinate System and Tire Numbering

5. Case Study: An Automobile Powertrain and Rigid Body Kinematics Model

To this point we have shown that a model library aimed towards modeling the kinematics and dynamics of an automobile can be created. The structure of this library is based upon the hierarchical structure of an automobile's powertrain and kinematics. Now we will use the model library to construct a powertrain and rigid body kinematics model of an automobile. The model constructed here is based upon the model library developed by this research which is shown in Appendix A. Enport/PC 5.4 Professional was used to build, simulate, and debug all of the models shown in Appendix A as well as the vehicle model constructed here.

The version of Enport implemented here does not fully support hierarchical modeling. Enport facilitates traditional "flat" system models which consist of the basic bond graph elements and user defined subroutines. It does not support the usage of multiport macro nodes nor does it support hierarchical structuring. However, many aspects of multiport modeling can be explored through the construction of a large scale flat model which imitates the structure of a hierarchical model. This technique lacks the benefits of multiport modeling software, but it does force the researcher to thoroughly consider issues related to the construction of a hierarchical model. The researcher is forced to consider issues which must be anticipated in the design of library software.

5.1 Model Introduction

The vehicle model constructed here is based upon one published by Hrovat (1991). Hrovat's model was intended to show that simple bond graphs are capable of modeling basic vibration characteristics of an automobile. For example, in his paper Hrovat points out that his model predicts that there will be a mode of vibration where the engine, clutch, and longitudinal vehicle kinematics oscillate together. This is the shuffle mode of vibration and Hrovat points out that the frequency and amplitude of oscillation are dependent on transmission gear and vehicle speed. In this research we will be examining these modes as well as demonstrating that the model can be easily extended and applied to a much broader range of applications.

The model developed by Hrovat and the one developed here are similar in nature but different in structure and applicability. Hrovat's model is generally linearized about specific operating ranges, such as shift points. The models used in this research are generally non-linear and applicable over a broader range of problems. Another difference is that Hrovat's makes many simplifications in the form of model reductions which cannot be duplicated easily using a multiport model. Hrovat's model reductions result in a much simpler model, but no attempt is made to imitate them. While the underlying structure of the multiport vehicle model is very complex, the outward appearance of the model is much clearer than Hrovat's own simplified model. Hrovat's model is much less computationally intense though. His work serves us as a source of data, a general outline, and a baseline reference.

The vehicle model will now be presented. Since the major component models are developed and tested in the appendix A, we will not have a thorough discussion of the vehicle model. Rather, we will briefly present the major features of the vehicle. The system diagram of the vehicle is shown in Figure 18. The vehicle model is a propelled rigged body bicycle model of a rear wheel driven vehicle. Essentially rigged body means that the kinematic characteristics of the vehicle are summarized by the vehicle mass and inertia. Further, bicycle implies that the model has been simplified to being supported by two tires; the front and back. This assumes that any road effects, including traction, are felt equally by the passenger and driver side tires. Since the vehicle is rear wheel driven, the front tire is described by a simple tire model which only captures the vertical vibration of the tire, rim, and suspension. As the rear wheel is propelled by the powertrain, the vertical, longitudinal, and torsional vibrations of the tire and rim are modeled. The same applies for the rear suspension except that there are no torsional dynamics to consider. The engine is treated as a source of effort with inertia and rolling resistance. The transmission is treated similarly as a lumped mass inertia with damping and compliance. The clutch is fully considered as having torsional dynamics associated with the pressure and friction plate contact as well as the torsional compliance associated with the friction plate isolator springs. The drive shaft and axle shaft are each treated as single lumped masses with associated stiffness and inertia. The differential is considered as an ideal transformer with no energy loss.

The hierarchical multiport model of the vehicle is shown in Figure 19. The major components are labeled clearly in both Figures 18 and 19 and can be easily identified. As the reader may recall, the software implemented does not have the capability to construct a hierarchical model such as that shown in Figure 19. The hierarchical model shown is simply an illustration of what the model should appear as. The actual model is flat and is shown in Figure20. The components are not clearly labeled in the flat model, but their location in the figure corresponds relatively to the location of the components in the hierarchical model.

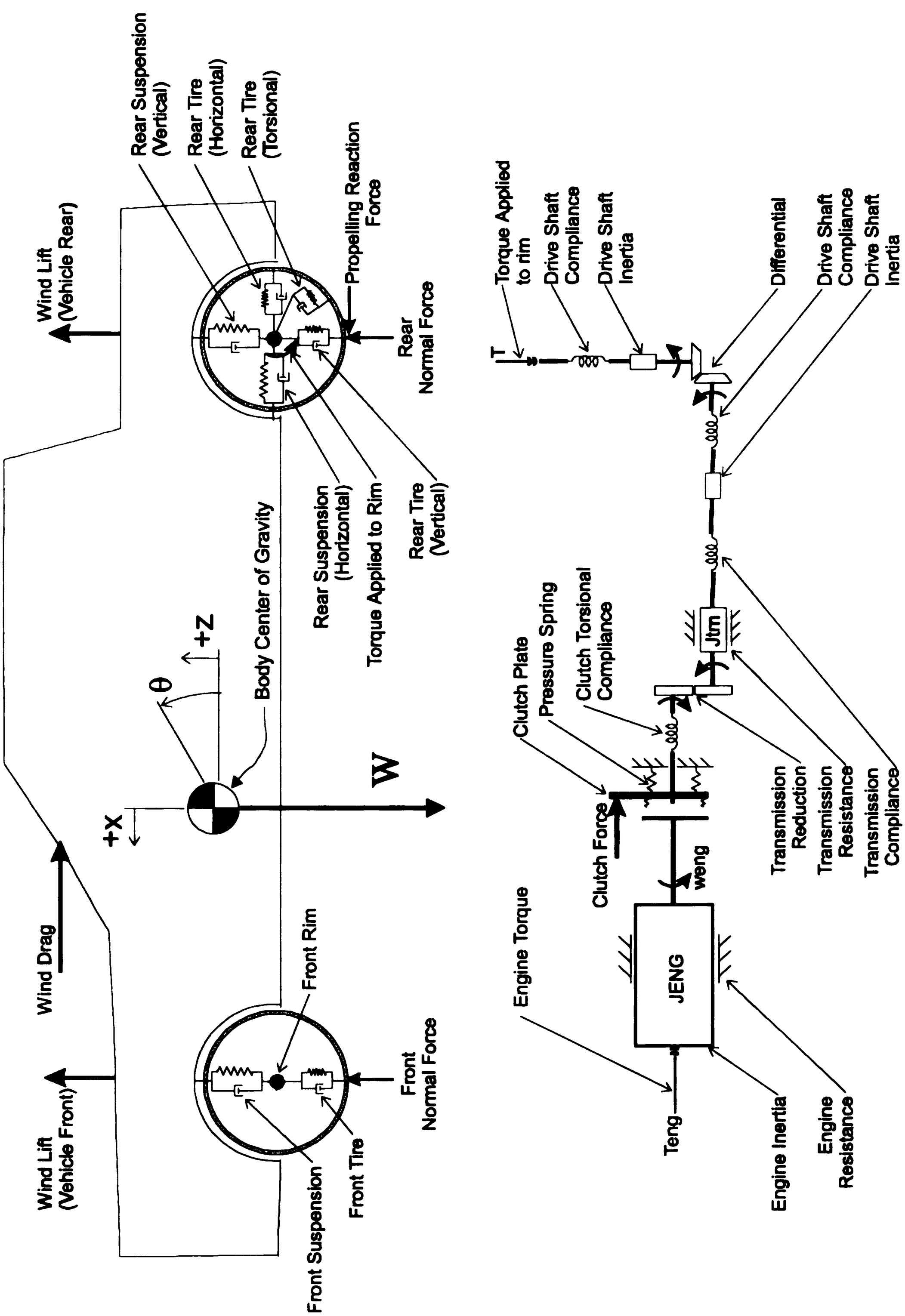

Figure 18: Vehicle System Diagram

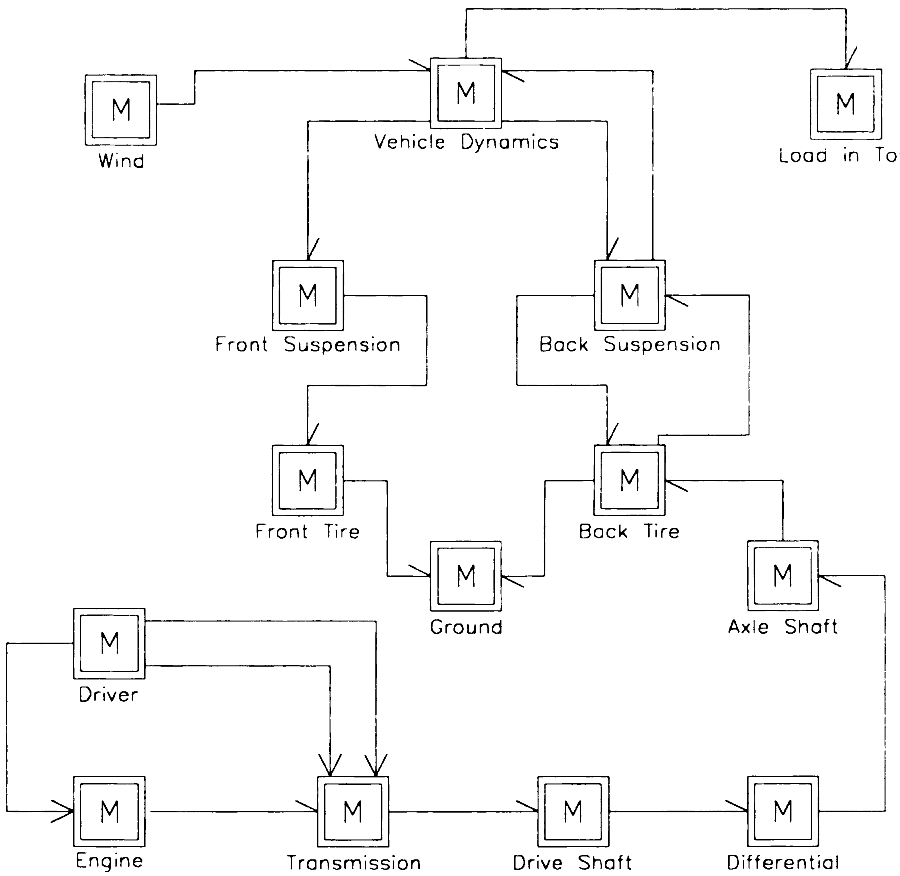

Figure 19: Hierarchical Automobile Model

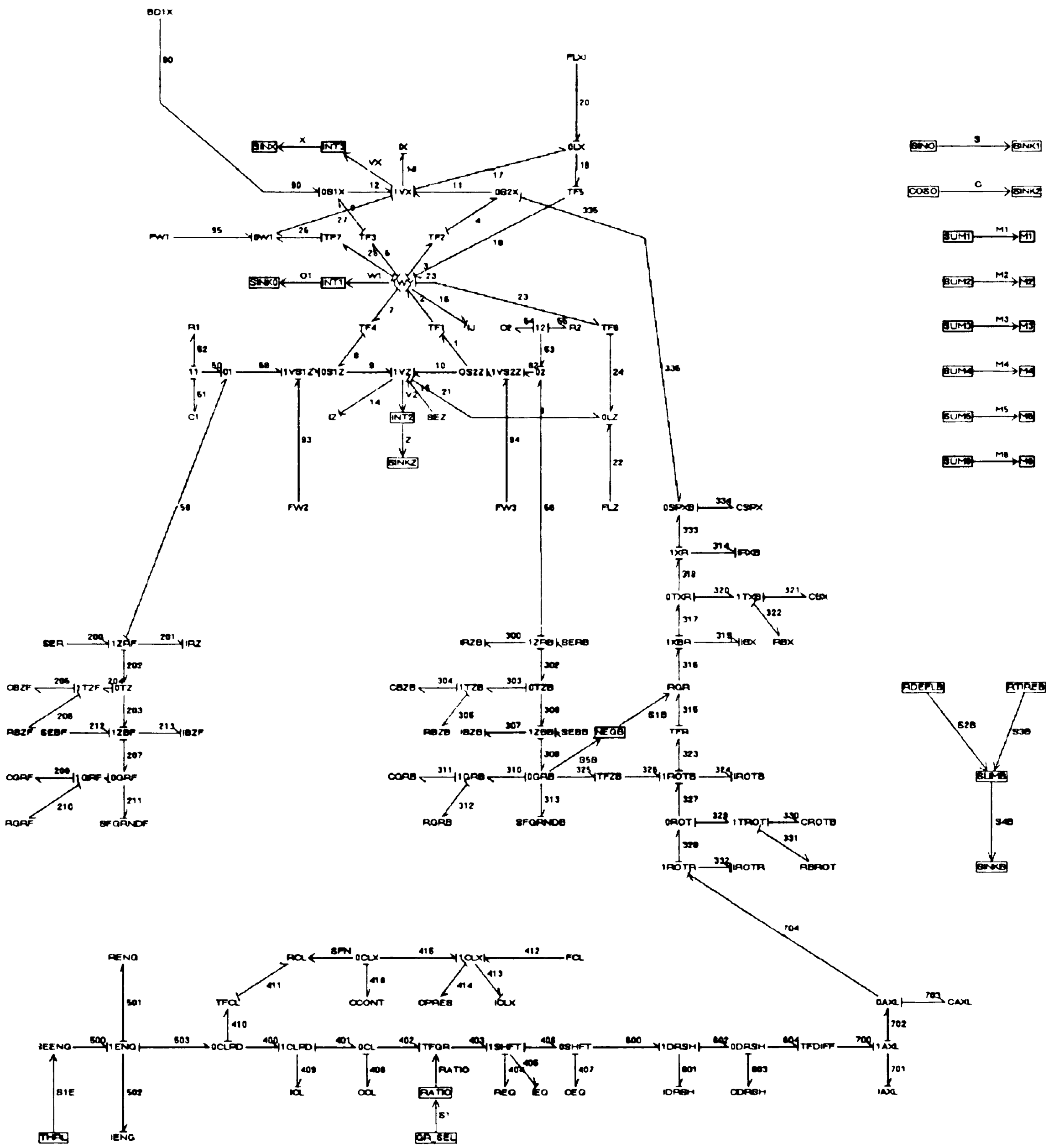

Figure 20: Flat Vehicle Model

5.2 Objectives

Typically a vehicle model like this is developed for the purpose of exploring a design alternative such as transmission gear ratios for optimal acceleration performance. In this case, the model has been developed for the purpose of exploring the usage of a model library and multiport macro nodes. So, rather than optimizing the vehicle performance through iterative solutions, we will only be solving the model a few times so that we can demonstrate the vehicle model's functionality.

What is intended by the functionality of the model is rather vague, so, we will begin by clarifying what we mean. First of all, by functionality we do not limit ourselves to just this model. We are interested in the applicability of multiport modeling to real problems. The baseline paper by Hrovat was chosen as a real problem because it presents a validated model that is accurate yet straight forward. His work presents a model that possesses the absolute minimum complexity to achieve a goal. Hrovat's goal was to show that bond graphs could easily be applied to the modeling of automotive powertrains. Our goal is similar in that we wish to show that multiport modeling and the use of a model library is applicable to real problems. Hrovat's paper gives us a baseline to aim for where we can achieve this goal and explore issues associated with this type of modeling without being muddled by a horribly complex system.

The vehicle model developed here is capable of more than imitating Hrovat's results. Hrovat's model is linear and as a result is only applicable over a narrow range of operating points. The model developed here is non-linear and applicable over a much broader operating range. For example, Hrovat's tire model required that he linearize the traction resistance at each shift point. The tire model implemented by this research is non-linear and is valid (Pacejka, 1991) over the entire operating range of the tire from full tire spin to steady-state propulsion. Simple parameter modifications can allow for varying road surfaces and environmental conditions. We will show that the vehicle model is capable of capturing the affects of a broader range of problems such as vehicle acceleration from a stand still. However, there are still inherent limitations to the model developed here. The largest limitation is the engine model, which as Hrovat points out, does not include any intake manifold or fuel delays. The engine model is most accurate at high speeds, which is where the model will spend the majority of its operating time.

We will further demonstrate and explore the ability of the vehicle model to undergo major design changes. In true multiport modeling this means that we are going to delete the icon representing a major component, such as the transmission, and insert a new component in its place. This is a true test of the applicability of the model library to a real problem. To facilitate this test we will delete the manual transmission in the vehicle and replace it with an experimental Constantly Varying Transmission (CVT). We will then perform several simulations to compare the vehicle performance with the manual transmission and the CVT. Discussion of the issues involved with this design change will follow.

In summary, we can state that the objectives that we have for this case study are to:

1. Show that the model library is capable of repeating previous work and explore the issues involved in developing the model.
2. Demonstrate that the model can easily capture a broader range of vehicle dynamics.
3. Demonstrate that major design changes are easily facilitated and explore issues which must be considered when modifying the model.

5.3 Results

5.3.1 Model Verification

First we must show that the model developed here is capable of repeating results accomplished by other authors. To facilitate this a vehicle model has been developed which is similar to one developed by Hrovat (Hrovat, 1991). As discussed above, Hrovat's model is quite fundamental and is intended to demonstrate the applicability of bond graphs to vehicle body and powertrain kinematics. One test implemented by Hrovat strives to predict the clutch torsional vibrations which result from a 41N-m engine toque step. Hrovat's model showed that the resulting oscillations would have a frequency of approximately 3 Hz with a damping ratio of 0.16 superimposed upon a slower first order decay. The first order response results from the vehicle acceleration counteracted by wind and rolling resistances. The harmonic component is a result of what is known as shuffle mode vibrations and is expected to be in the range of 2-10 Hz with a damping ratio below 0.20. Shuffle mode vibrations are largely associated with the engine inertia and powertrain compliance oscillations.

The vehicle model developed here is based upon the same vehicle configuration used by Hrovat. As we have discussed previously, our model is constructed from Multiport Macro nodes extracted from the developed model library. Hrovat's model has been reduced to an absolute minimum complexity and our's is in its full complex form represented by the multiport icons. To repeat Hrovat's results we have applied a 41 N-m engine torque step and we are observing the clutch spring deflections. The resulting deflections are shown in Figure 21. Interpretation of the figure reveals that the results posses a slow first order component and a faster harmonic component. The frequency of the harmonic component is about 3 Hz with a corresponding damping ratio of about 0.14.

The slower first order component does not decay as rapidly as the one in Hrovat's response. This can be explained by additional powertrain losses that are considered by our model. These losses require effort to overcome them and as a result do not allow the clutch deflection to decay as rapidly as Hrovat's. Further observation of Figure 21 also reveals that there is an additional high frequency component of about 50 Hz that becomes apparent after about 0.50 seconds. This is a result of additional torsional and inertial effects, such as the transmission and suspension, taken into consideration by our model. Hrovat's model neglects components which do not have a dominant effect on the powertrain dynamics. Comparison with Figure 22, which shows Hrovat's (1991) results, illustrates that our results match quite closely.

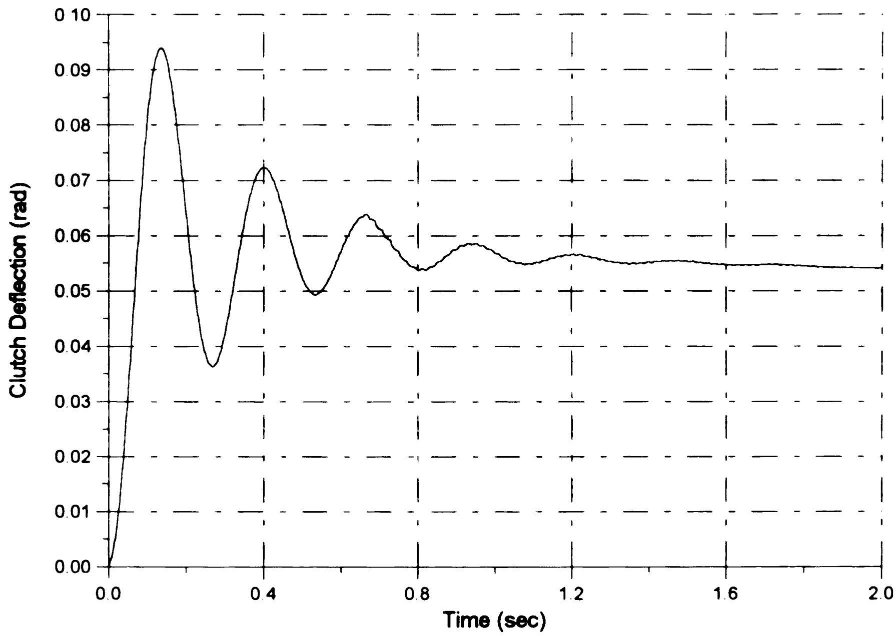

Figure 21: Axle deflection response to a 41N-m step in engine torque.

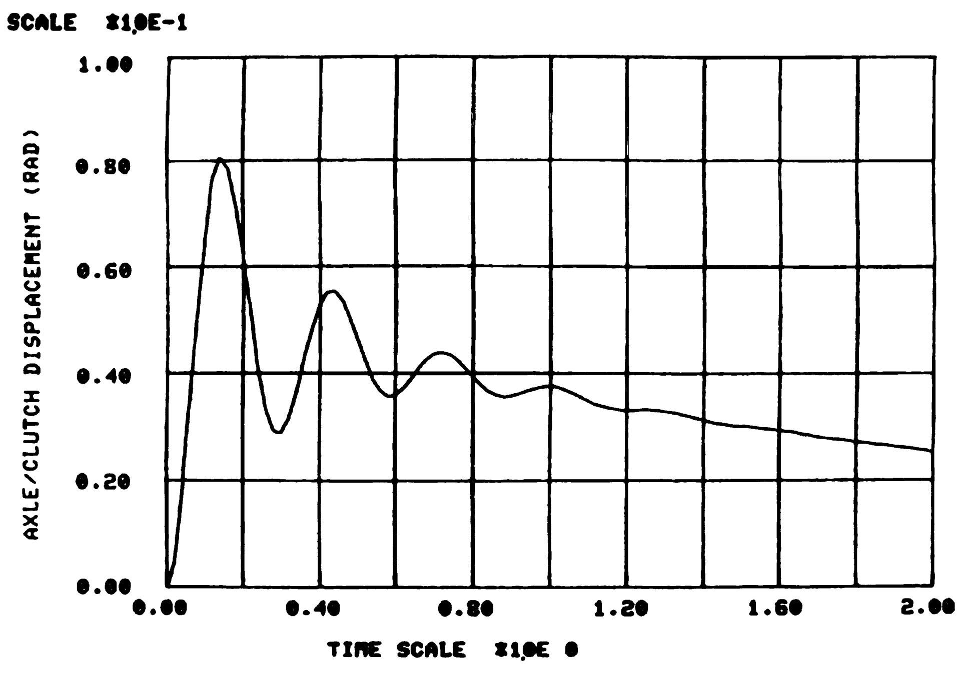

Figure 22: Test Case: Hrovat's (1991) Clutch/Axle response to a step in engine torque.

5.3.2 Additional Model Capabilities

Hrovat further verifies his model by estimating shuffle mode characteristics during a Wide Open Throttle (WOT) driveaway for a light duty manual transmission truck. The driveaway starts from a dead stop and the driver shifts aggressively through the first four gears of the transmission. Due to the linearized nature of Hrovat's model, he is limited to estimating powertrain behavior near the shift points. For his purposes that is sufficient. He is solely interested in demonstrating that bond graphs can be used to model dominant drivetrain oscillations. However, we are interested in demonstrating that our model can exceed the capabilities of a typical linearized model. We will actually predict the behavior of the vehicle during the WOT driveaway.

As just discussed, we will simulate the WOT driveaway behavior of a vehicle. The objective of this test is to demonstrate that the vehicle model developed is capable of functioning in a richer class of applications while still functioning well in basic environments. A basic environment requires that only the minimum functionality of a device is modeled. A basic transmission model is one where only the inertia and compliance of the transmission is considered. A richer transmission model would also allow the driver to operate the clutch and shift gears. The WOT driveaway provides a richer environment in that much more is expected of the model. To accurately capture a driveaway with shifting it is necessary that the driver is capable of operating the clutch, throttle, and shifting gears. The component models must be sufficiently general to accurately capture a device's dynamics while still being specific enough to imitate the operational characteristics of the component.

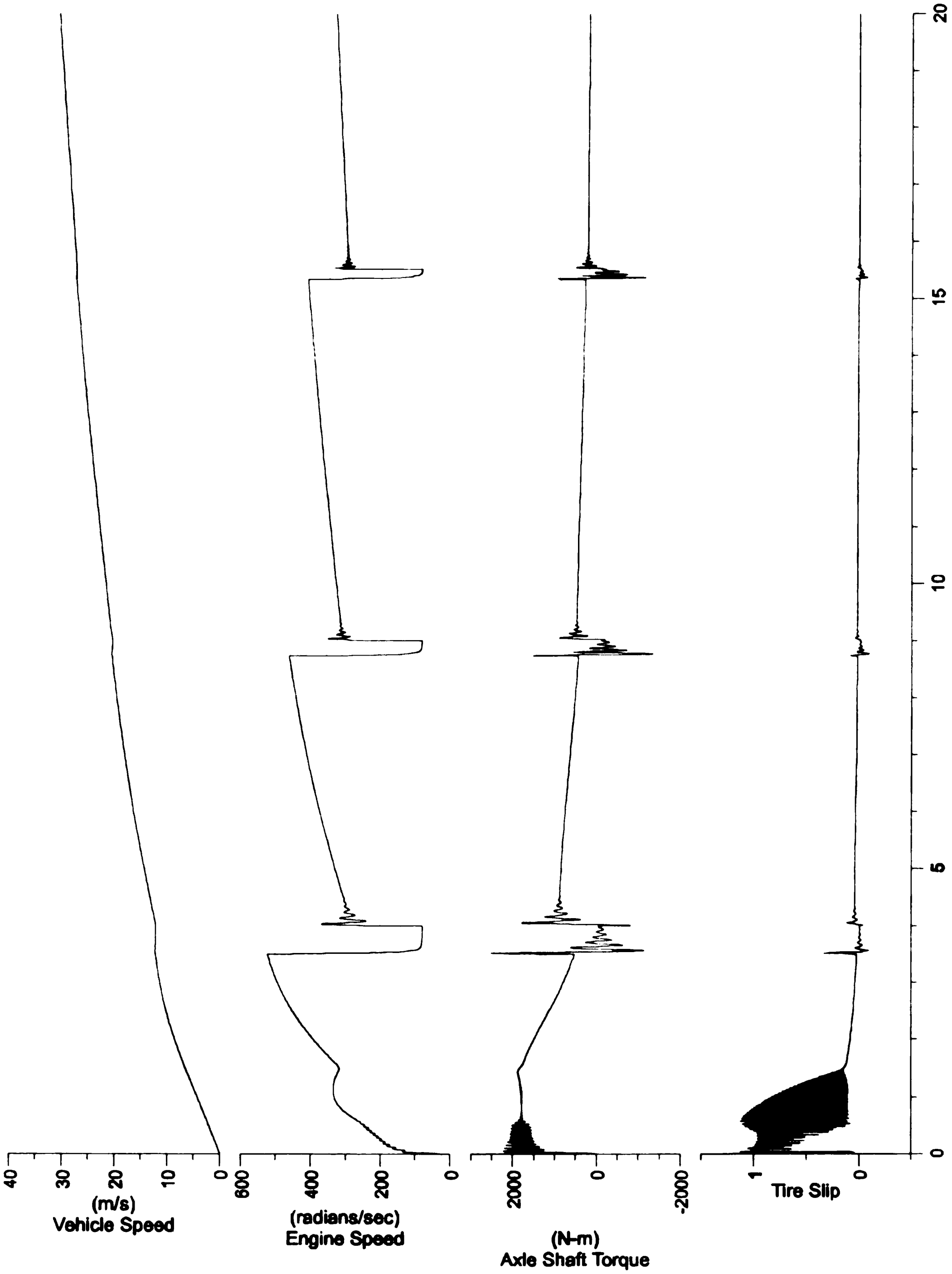

Figure 23: Wide Open Throttle Vehicle Driveaway Response

The model validation above demonstrates that the vehicle model is capable of basic implementations. Now we will replace the engine model used above with one that represents the WOT behavior of a six cylinder engine. In conjunction with a more elaborate driver model, the new engine will enhance the vehicle model sufficiently so that we can simulate the WOT driveaway. Modification of the other component models, such as the transmission, tires, and wind resistance, will not be necessary. Their sophistication is sufficient for our purposes.

Figure 23 represents our results of a WOT driveaway. In that figure we find the vehicle velocity, engine speed, axle shaft torque, and tire slip. These variables have been chosen since they characterize the behavior of the vehicle quite compactly. During a driveaway the prime concerns are whether we have sufficient traction, if the engine is over revving, and what our vehicle speed is. As a possible design issue, we are also interested in the dynamic torque applied to the axle shafts.

Our results indicate that during the first two seconds of driveaway there is a large amount of tire slip. This slip is associated with the initial acceleration of the vehicle from a stand still and the rapid engagement of the clutch. During this period the engine speed increases and the axle torque oscillates slightly about a maximum value. After 1.5 seconds the tire slip stabilizes and the axle torque and engine speed equilibrate. At each shift point (4, 9, and 15 seconds corresponding to 1st to 2nd gear, 2nd to 3rd, and 3rd to 4th gears) the engine and clutch are disengaged and the transmission gear is shifted. During this period, the engine speed decreases to idle and the vehicle speed decreases slightly. There is a transient in axle shaft torque and tire slip that occurs when the clutch is disengaged. This happens because the torque applied to the transmission by the engine is instantly discontinued when the clutch pedal force is applied. From a qualitative standpoint the transients seem too large. For the purpose of demonstration this transient is acceptable, but it is recommended that the shift timing involved in the driver model be examined. Approximately half a second after disengagement the engine and transmission are reengaged. There is a slight transient in slip, axle torque, and engine speed associated with this engagement. These transients that occur after reengaging the clutch and engine are associated with the shuffle mode of vibration. As Hrovat points out, the frequency of these oscillations should increase in higher gears, and our model indicates this.

5.3.3 Exploring Design Alternatives

So far we have shown that the vehicle model is capable of duplicating previous results. With slight modifications to the engine and driver models we have also shown that the model is capable of predicting a much richer class of vehicle performance. Now we will show that by replacing a component model, such as the transmission, we are capable of exploring design alternatives. In this case we will replace the manual transmission with a preliminary model of a Constantly Varying Transmission (CVT) coupled to the engine via a torque converter. We will simulate the driveaway performance of the vehicle with the new transmission and briefly compare the performance of the two vehicle configurations.

Figure 24 represents the performance of the vehicle during a WOT driveaway with a CVT installed. Figure 24 illustrates the vehicle and engine speeds. The figure represents the investigation of a design alternative to the manual transmission used above. In comparison with Figure 23, it can be seen that the manual transmission vehicle reaches a slightly higher speed after ten seconds (22 m/s) than the CVT vehicle (20m/s). Note however that the engine with the manual transmission reaches a maximum speed of nearly 500 rad/sec whereas the CVT vehicle reaches a maximum engine speed of 270 rad/sec. Further note that the acceleration of the CVT vehicle is not discontinuous like that of the manual transmission vehicle. We have explored a design alternative which has great potential for passenger comfort. Thanks to the multiport macro node it was simply a matter of replacing one node in our system diagram of Figure 19.

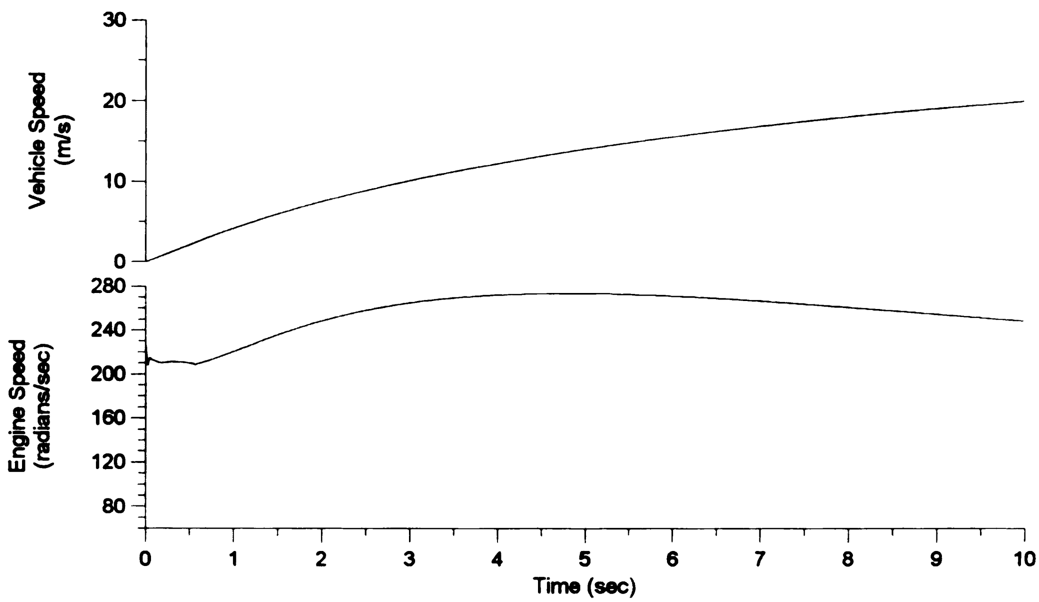

Figure 24: Wide Open Throttle Driveaway with CVT

5.4 Discussion

The objectives discussed above are aimed at exploring the use of a model library in a hierarchical multiport modeling environment. The first set of results proves that the automobile model we have developed yields reasonably accurate results. The second set of results demonstrates that our automobile model is capable of simulating more complex phenomena with minimal effort. The third set of results illustrates that multiport modeling simplifies exploring design alternatives. While our model managed to "jump through the hoops" provided by these tests, the real issue at hand was exploring what issues arose during these tests. We can list these issues as:

1. Connection of multiports
2. Model misuse
3. Parameter management
4. Initial condition management

One of the greatest difficulties encountered during the initial assembly of the vehicle model was the **connection of component** models. During the construction of the model library, each component model was built individually and tested. During this phase, power flow direction and causality at each port were determined by what seemed the most functionally logical form for each component and port. However, this logic rapidly decayed when it came time to assemble the component models. Issues of incompatible causality became evident and incompatible power flow soon resulted in sign errors. Essentially, even though each component model functioned very well individually there were no guarantees as to how they would function as a whole. Smart assembly procedures managed to remedy many of these problems, but the issues must be considered in software implementations.

Model misuse was an issue encountered during the use of the automobile model. It seems to occur in the form of using the model outside of its valid range. This can refer to excessive amplitude of effort, flow, power, or frequency at a port. The engine model implemented here is most subject to this misuse. The engine's torque source is derived from an eighth order polynomial fit through torque-speed data and is quite accurate in the range of 80 to 550 radians/second. However, outside of this range the engine model is very unreliable. A safety for this effect was provided by limiting the valid operating range of the model. This is an important issue in larger scale models. As hierarchical modeling tools develop larger models will become common place. It will be very difficult for the user to fully understand the underlying complexities of each multiport model. Large amounts of time will be saved if a safety feature is built into each component models which monitors its operating status.

Parameter management is another issue which needs to be addressed. As hierarchical tools develop model complexity will increase exponentially. With increased model sophistication comes greater parameterization. The issue is whether parameters should be local to each component model, or, whether parameters should be able to be passed through the hierarchical structure. In essence, the issue is whether models should be able to use global or local parameters. For greatest flexibility it is recommended that parameters originate at the local and global levels and that they can be linked to each other.

Initial conditions also require further attention. Much like parameters, as the model complexity increases, so does the number of initial conditions. Management and control of all these initial conditions can rapidly become very tedious. It is recommended that some sort of management tool be developed that streamlines the management of initial conditions.

6. Conclusions

A library of models supporting a powertrain and rigid body kinematics model of an automobile has been developed. The vehicle model has been assembled from component models stored in the library. Issues related to the construction of the library and hierarchical vehicle model have been explored. Following is a brief summary of the modeling and library environment design to which this exercise has led.

Software which manages model libraries of the type described here is not readily available at this time. If the hierarchical modeling and model libraries are going to be useful tools, software must be developed which manages the model libraries and makes them readily accessible. The user must be capable of selecting a model from a structured list where key characteristics of each model are available. Key characteristics include the contents of the model, port configuration, parameters, characteristics captured, and valid range of operation.

Intelligent hierarchical modeling tools must accompany good library management software for effective modeling. Good library management software provides the information discussed above to both the user and modeling software. The modeling software must be sufficiently intelligent to handle issues which arise during the structuring and assembly of the model. The issues faced by modeling software includes the connection of component models, assurance that a component model is operating within a valid range, parameter management, and initial condition management.

Connection of component models requires that causality and power flow be considered at every port. It is essential that these issues be handled appropriately or the resulting model will be useless. It is recommended that future library management software be capable of indicating a port's preferred or required causality. In some cases it may be necessary for software to manipulate the system equations into an appropriate form. In some cases the connection of component models may simply not be compatible. The issue of power flow direction is equally important at a port, but this issue can be handled much easier than causality.

It is also important that each component model function properly for a given operating range. It is easy to unknowingly allow a component model to operate outside of its valid range. It is recommended that the modeling software be made capable of monitoring the amplitude of effort, flow, power, and frequency range across any given component.

Parameter and initial condition management is also a point of key interest to the user. A local and global parameter management scheme is recommended where parameters can exist solely at the local level or they can be linked to global system parameters.

The reliability of reused models would benefit from a standard set of verification test conditions. A standard set of verification tests would improve the reliability of reused models by providing general operating specifications for a component. Significant deviation from specification would indicate that modifications made to the component model may be erroneous.

Appendix

Appendix A

Model Library

This section of the paper presents a brief library of component models critical to modeling and simulating vehicle kinematic and powertrain dynamics. While the library presented here does not provide a plentiful selection of models to choose from, it does provide a selection of models sufficiently large to illustrate hierarchical modeling and the use of a component model library. The following models are presented:

- A.1 Two Dimensional Rigid Body Vehicle Dynamics Model
- A.2 An Unpropelled Two Dimensional Rigid Ring Tire Model
- A.3 A Simple Open Differential
- A.4 A Lumped Mass Manual Transmission with Clutch
- A.5 Hollow Shaft Model
- A.6 Mean Torque Full Throttle Engine Model
- A.7 Longitudinal Wind Effects

A.1 Two Dimensional Rigid Body Vehicle Dynamics Model

Following is a two dimensional rigid body vehicle dynamics model designed to capture longitudinal, vertical, and pitch dynamics. The model considers the mass and inertia of the vehicle body to be concentrated at the center of gravity as a single lumped mass with inertial properties. It is further considered that there are two suspension connection points (see Figure 25) at the front and rear of the vehicle which can transmit both vertical and longitudinal forces. Wind drag forces are modeled as a point load applied to the vehicle in the longitudinal direction and wind lift forces are modeled as forces applied to each suspension point. A load in tow is treated as a pair of point loads applied to the rear of the vehicle in the longitudinal and vertical directions. The user of this model is required to know the vehicle mass, moment of inertia of the vehicle about the y-axis, and the location where all external loads are applied. External loads include wind drag, wind lift, suspension loads, and the load in tow.

The bond graph representing the system is shown below in Figure 26. Since this model is largely non-linear a series of sources and sinks have been used to calculate the module of the transformers. The sources in concern are SUM1 through SUM6, SIN0, and COS0. SUM1 through SUM6 actually calculate the corresponding moduli of TF1 through TF6. SIN0 and COS0 are used as a basis in the previously mentioned calculations. The sinks M1 through M7 simply act as destinations for the signals from the sources. Further explanation of the nodes associated with the model can be found in Table 7.

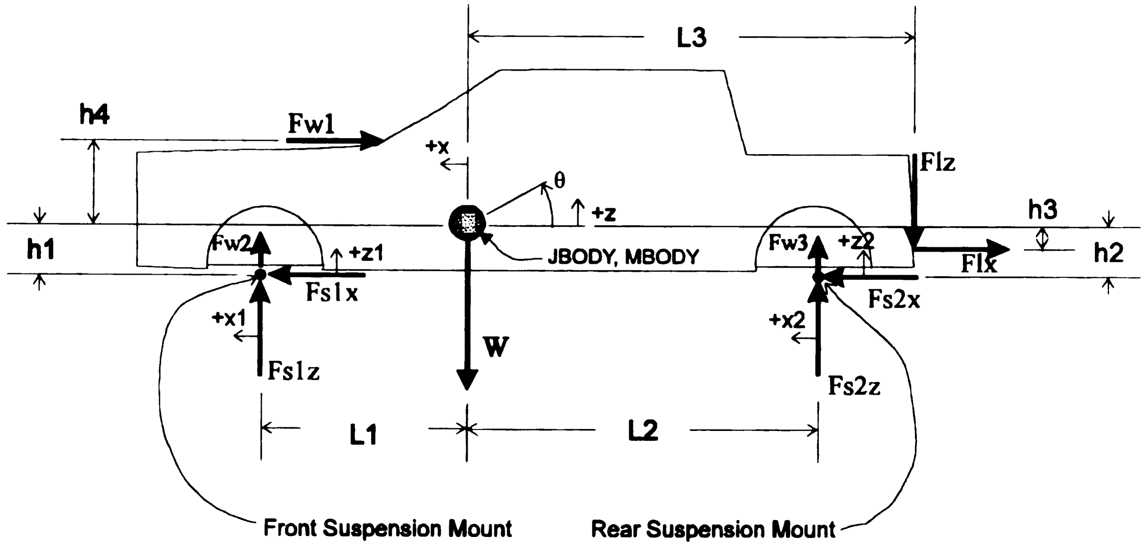

Figure 25: Diagram of a Two Dimensional Rigid Body Vehicle Model

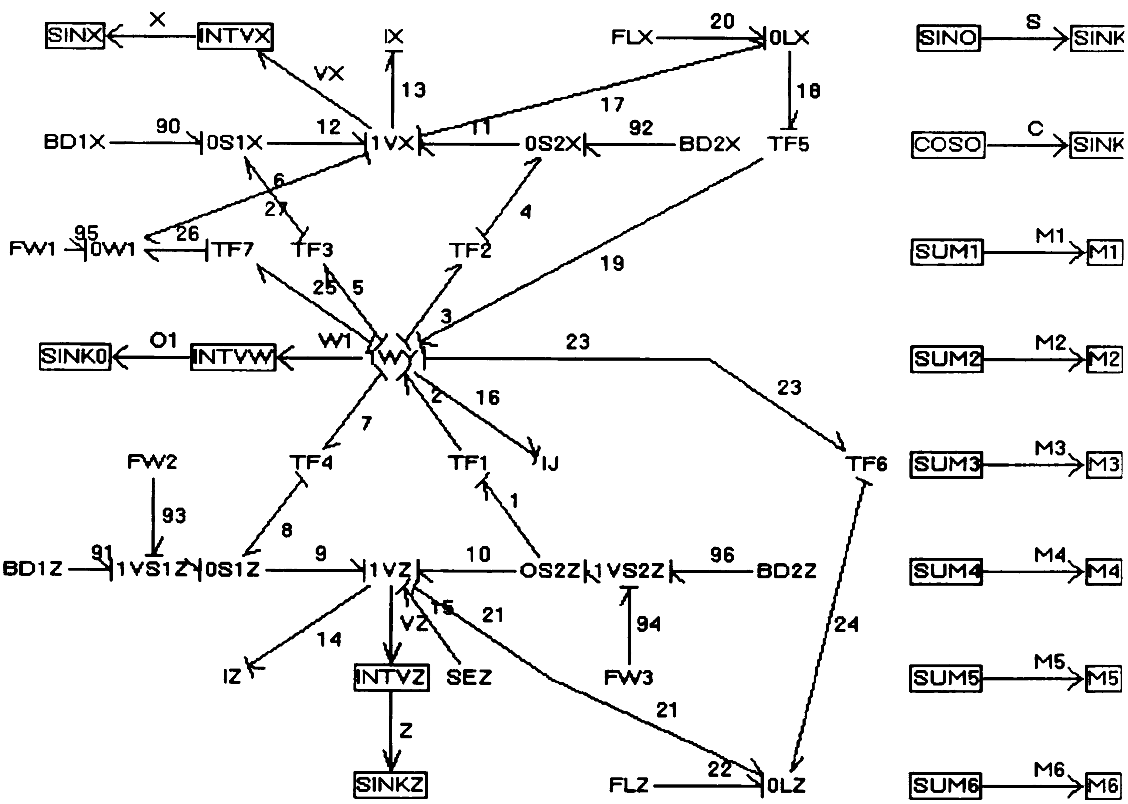

Figure 26: Bond graph submodel of a Two Dimensional Rigid Body Vehicle Model

Table 7: Nodes associated with the Rigid Body Vehicle Model

Name	Type	Primary Coordinate	Associated Subroutine	Description
BD1X	port	x		Suspension connection point 1
BD1Z	port	z		Suspension connection point 1
BD2X	port	x		Suspension connection point 2
BD2Z	port	z		Suspension connection point 2
FLX	port	x		Load in tow
FLZ	port	z		Load in tow
FW1	port	x		Longitudinal wind effects
FW2	port	z		Vertical wind effects at connection point 1
FW3	port	z		Vertical wind effects at connection point 2
IJ	I	θ		Vehicle in-plane rotational intertia.
INTVW	int	θ		Integrates angular velocity and gives angle.
INTVX	int	x		Integrates velocity and gives position
INTVZ	int	z		Integrates velocity and gives position
IX	I	x		Vehicle translational inertia
IZ	I	z		Vehicle translational inertia
SEZ	SE	z		Weight of vehicle
TF1-TF7	TF			Transmits effects of forces to the vehicle's rotational intertia

A.1.1 Ports and Parameters

The ports and parameters associated with this model are listed in Tables 8 and 9. Ports associated with this sub-model allow an interface with suspension forces, wind forces, and forces resulting from a load in tow. Parameters associated with this model determine the location of the forces interfacing with sub-model, vehicle mass, and vehicle inertia.

Table 8: Ports associated with the 2D Rigid Body Vehicle Model

Port	Location	Units	Description
BD1Z	Bond 91	N m/s	Vertical force at suspension point 1 Vertical velocity of suspension point 1
BD2Z	Bond 96	N m/s	Vertical force at suspension point 2 Vertical velocity of suspension point 2
BD1X	Bond 90	N m/s	Longitudinal force at suspension point 1 Longitudinal velocity of susp. point 1
BD2X	Bond 92	N m/s	Longitudinal force at suspension point 2 Longitudinal velocity of susp. point 2
FW1	Bond 95	N m/s	Longitudinal Wind Forces Velocity of wind relative to vehicle
FW2	Bond 93	N m/s	Vertical wind force (lift) at susp. point 1. Velocity of lift force
FW3	Bond 94	N m/s	Vertical wind force (lift) at susp. point 2. Velocity of lift force
FLX	Bond 20	N m/s	Longitudinal load in tow force Relative velocity of load in tow
FLZ	Bond 22	N m/s	Vertical load in tow force Relative velocity of load in tow

Table 9: Parameters associated with the 2D Rigid Body Vehicle Model

Parameter	Node	Units	Typical Range	Description
MBODY	IX, IZ, SEZ	kg	1400	Vehicle mass
L1	TF3, TF4	m	1.26	Longitudinal distance from C.G. to front suspension mount
L2	TF1, TF2	m	1.45	Longitudinal distance from C.G. to rear suspension mount
h1	TF3, TF4	m	.25	Vertical distance from C.G. to front suspension mount
h2	TF1, TF2	m	.25	Vertical distance from C.G. to rear suspension mount
g	SEZ	m/s^2	-9.81	Acceleration due to gravity
JBODY	IJ	$N{\cdot}m{\cdot}s^2$	1862	In plane inertia
h3	TF5, TF6	m	.25	Vertical distance from C.G. to point of load in tow connection
h4	TF7	m	.25	Vertical distance from C.G. to location of wind drag point load
L3	TF5, TF6	m	2.00	Longitudinal Distance from C.G. to point of load in tow connection

A.1.2 Verification Results

Verification of the Two Dimensional Rigid Body Vehicle Model must be a multistep process since there are multiple ports communicating with the model. Logically, the model must first be analyzed for settling performance with only the vehicle's weight and vertical suspension inputs. After this test has been completed then the performance of each of the other ports can be evaluated. The evaluation procedure will be implemented as follows:

Test 1 - Model settles properly under its own weight
Test 2 - Model response to a longitudinal impulse
Test 3 - Model response to wind affects
Test 4 - Effect of a load in tow on the model

Evaluation of Test 1 requires that suspension components are added to the ports BD1Z and BD2Z. Characteristic suspension parameters were used from a mid-size sedan. Namely, the spring stiffness was 13.8 kN/m and damping was 3.22kN·sec/m. The remaining parameters used are listed in Table 9. The evaluation consisted of starting with the vehicle at rest and level and the suspension undeformed. The vehicle was then allowed to settle upon the suspension and reach equilibrium. The results are shown in Figure 16. Upon analytical evaluation of the suspension deflection we first assume that the moment arms of the suspension are unaffected by angular displacement. While slight error is introduced, this serves as a good approximation for model verification. Inspection of Figure 16 indicates that the deflection of front suspension is 0.267m, the deflection of the rear suspension is 0.231m, and that the angular displacement of the center of gravity is 0.0133 radians. Our theoretical results are 0.266m, 0.231m, and 0.129 radians correspondingly. Given that nonlinearities were neglected we can assume that the results match and that the model has passed this test.

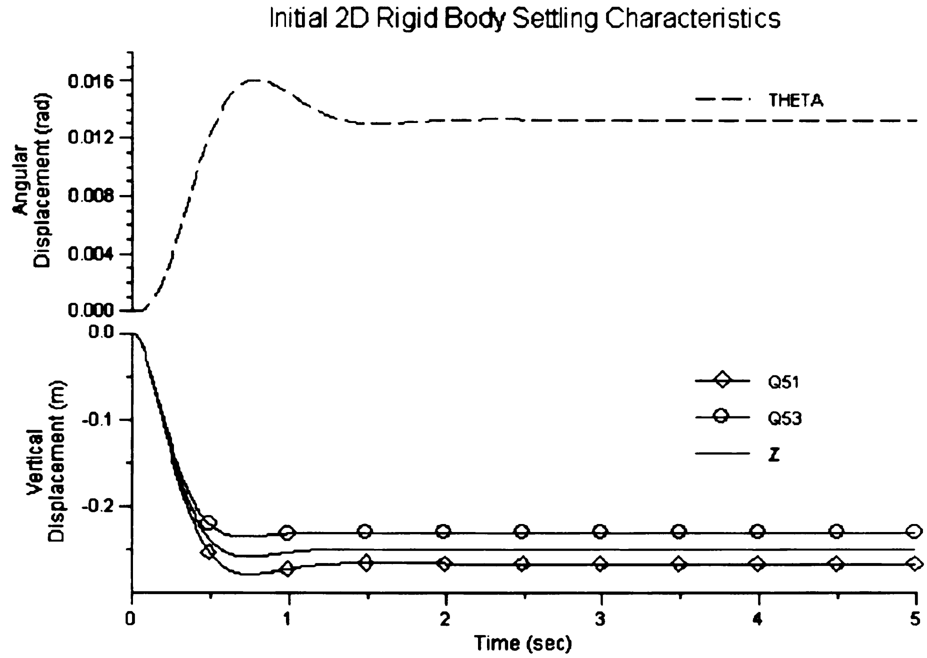

Figure 27: Test 1 - Initial Settling of the 2D Rigid Body Model

Test #2 requires that we now add a longitudinal step force to the vehicle and observe the vehicle's response. Two separate scenarios will be observed where a step force is first applied to the rear suspension point and then where the step is applied to the front suspension point. Here the qualitative behavior of the vehicle's pitch (in plane rotation), and corresponding deflection of the suspension will be observed. In either scenario of applying a step force we expect that the angular displacement will decrease, the rear suspension will compress further, and the front suspension will be extended. Further, we expect that since the force is a step force the vehicle will reach a new steady state orientation. Figure 28 illustrates the vehicle's response to a step force applied to the rear suspension. The vehicle responded as we expected and can assume that this portion of Test #2 is satisfied. Further examination of Figure 29 where a step is applied to front suspension reveals similar results to those in Figure 28. This is expected since both forces were applied at an equal distance below the center of gravity.

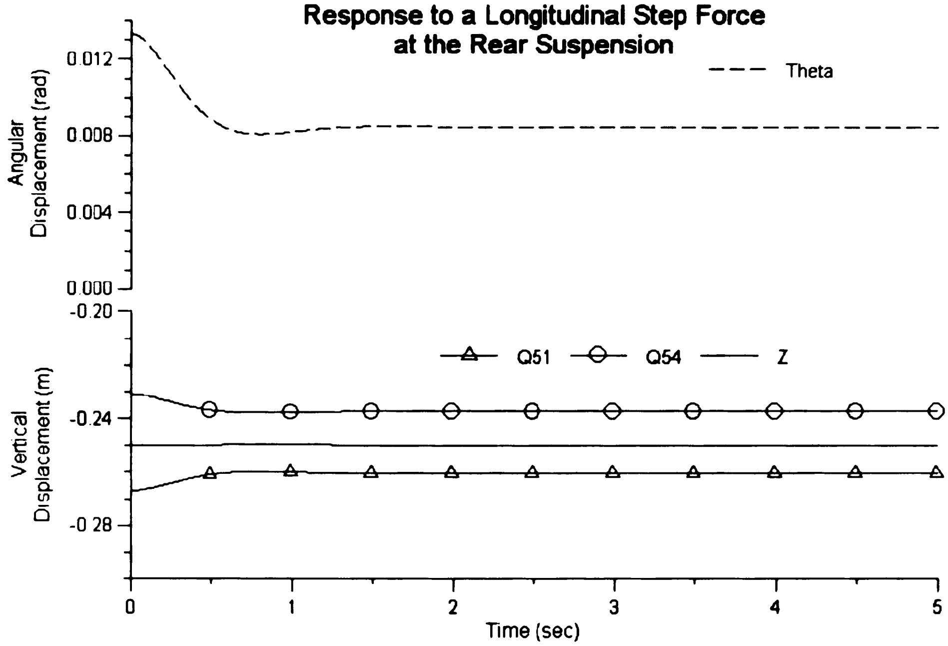

Figure 28: Test 2 - 2D Rigid body model subjected to a 1000N step force at rear suspension.

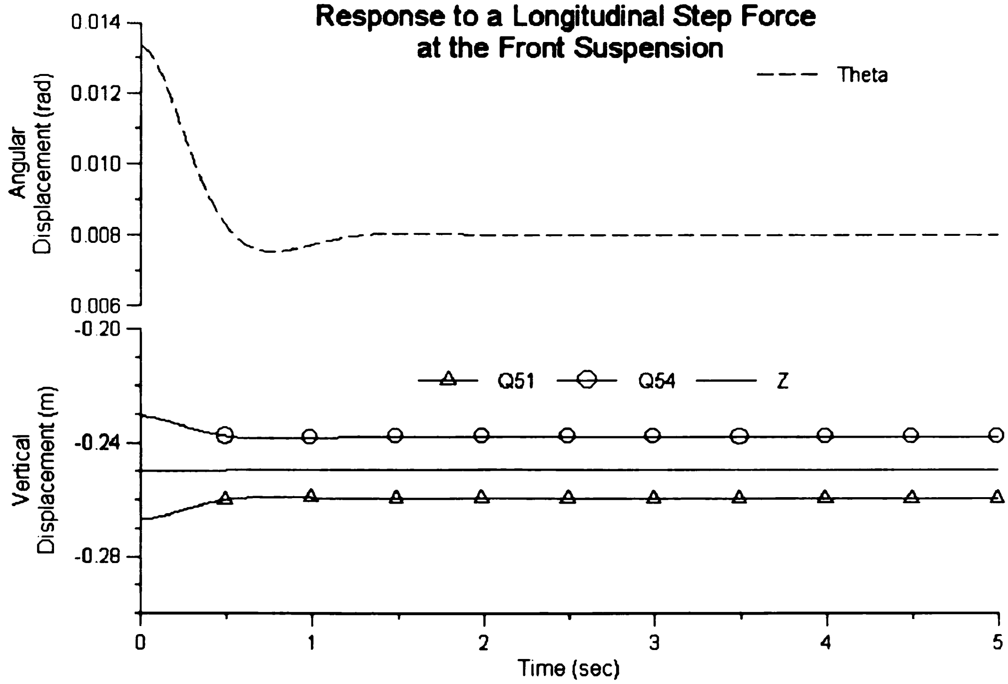

Figure 29: Test 2 - 2D Rigid Body model subjected to a 1000N step force at front suspension.

Test #3 evaluates the model's response to applied wind loads. Since there are multiple sources of wind load, longitudinal wind load will be evaluated first. For the sake of simplicity the longitudinal wind load will be modeled simply as linear viscous damping. A step load will be applied to the vehicle as in Test #2 and the model will reach a steady state velocity proportional to the damping coefficient and applied load. In this case a 375N step load will be applied to the vehicle while the wind drag coefficient of viscous damping will be 15N·sec/m. The resulting final speed is expected to be 25m/sec. Figure 30 illustrates that the vehicle speed exponentially approaches 25m/sec and we can conclude the model has passed this test.

Test #3 also requires that the effects of wind lift be tested. Using a similar test to the previous one, the vehicle's orientation will be monitored with and without wind effects included. If the wind affects are considered correctly the vehicle should lift slightly when wind affects are included and the force transmitted to the ground should decrease. For simplicity the lift affects will be considered to be linearly proportional to vehicle velocity. The lift coefficient for the front suspension will be considered to be 5N·sec/m and the rear suspension lift coefficient will be 13N·sec/m. The same 375N step load will be applied and the longitudinal viscous drag coefficient will again be 15N·sec/m. As it can be seen from Figure 31 the vertical forces at the front and rear suspensions both decrease due to wind lift. This is as expected and it is concluded that the wind lift interface is functioning correctly.

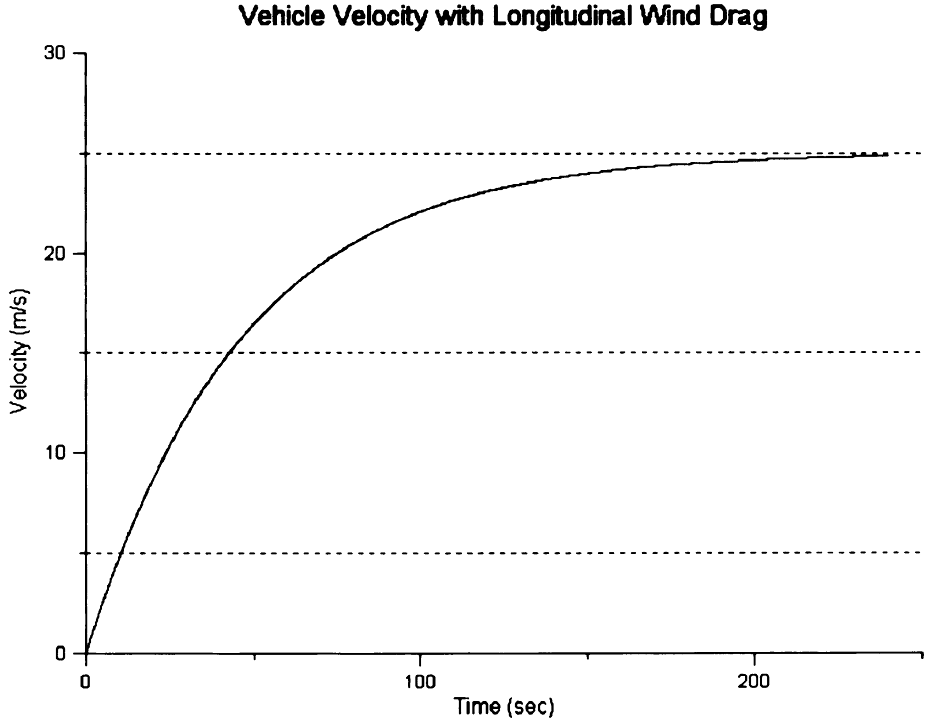

Figure 30: Test 3 - Vehicle Response to longitudinal wind drag.

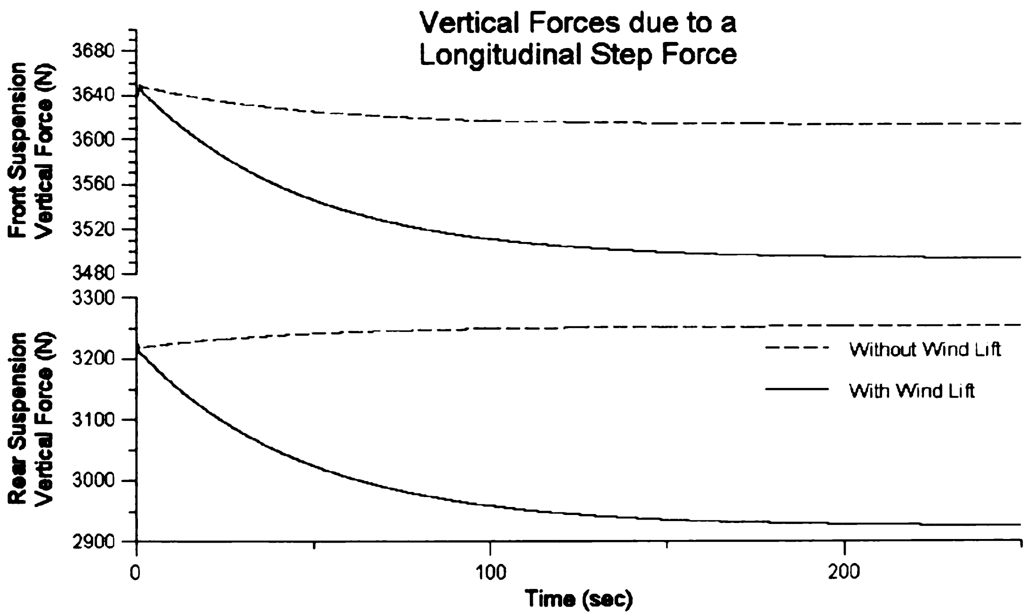

Figure 31: Test 2 - Vertical forces due to a longitudinal step force with and without Wind Lift Considered

Test #4 requires that the effect of a load in tow be examined. In order to evaluate this affect the vertical and longitudinal forces due to the load must be evaluated separately. The vertical forces will be investigated first by applying the load to the vehicle and observing the settling performance. Figure 32 shows the settling of the vehicle with and without the load in tow. As expected, the load in tow results in greater compression of the suspension and the vehicle pitch decreases.

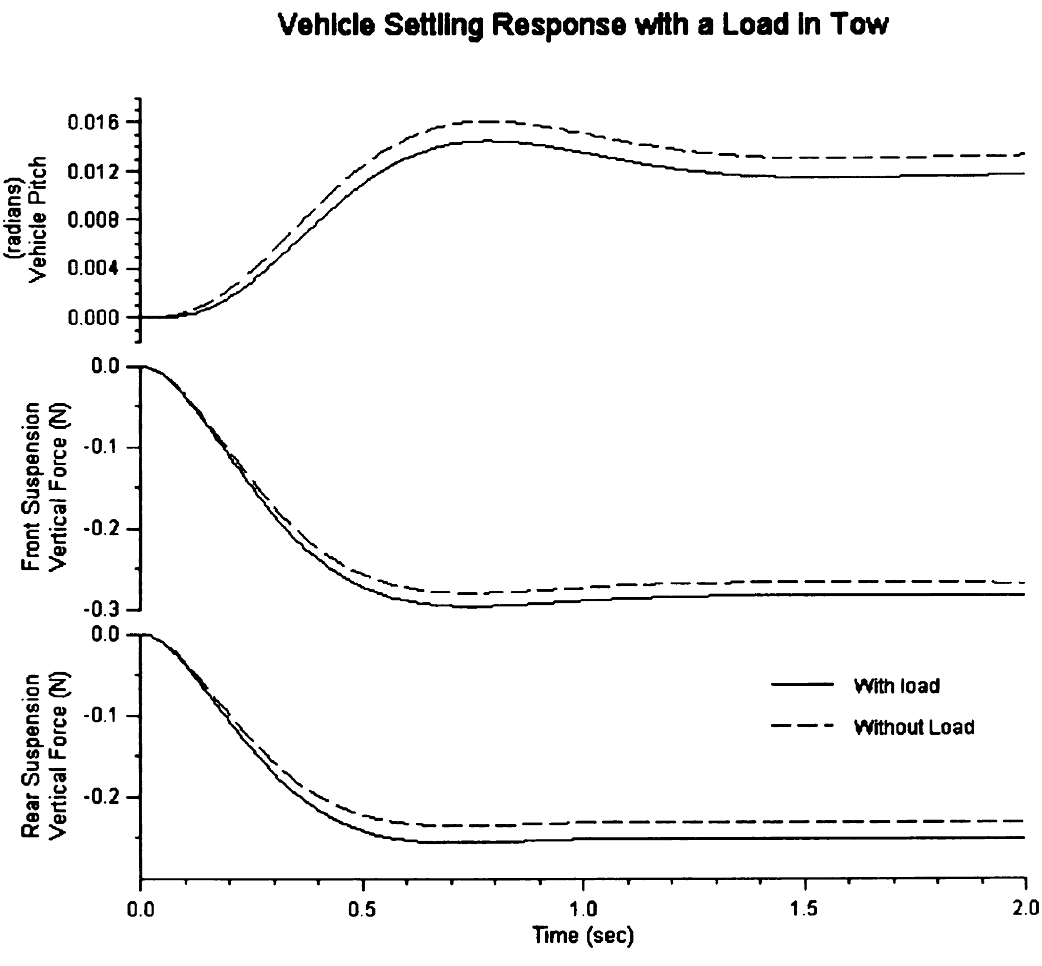

Figure 32: Test 4 - Vehicle Response due to application of load in tow

A.2 An Unpropelled Two Dimensional Rigid Ring Tire Model

A.2.1 Model Description and Assumptions

The tire model presented here is a much simpler version of the Propelled Two Dimensional Rigid Ring Tire Model based upon work by Zegelaar (Zegelaar, 1993). In this case though the tire model has been limited to only capture vertical translational dynamics of the rim and tire. The model does not include the ability to transmit torque from an input shaft to the ground and hence does not need to consider longitudinal forces. The model is purely concerned with normal forces between the tire and ground and between the rim and axle.

Much like the Propelled Rigid Ring Tire Model, this unpropelled tire model captures the zeroth and first modes of the tire and rim. The resulting limitation is that the model is only accurate up to 90 Hz. Further, since the tire-ground interface is modeled as a non-linear stiff spring there are computational limitations which require that solution strategies are capable of capturing frequencies up to 500Hz. A small amount of damping has also been added to this model which damps out otherwise present harmonic steady state motion and results in a steady state equilibrium. As mentioned previously, this is both more realistic and computationally desirable.

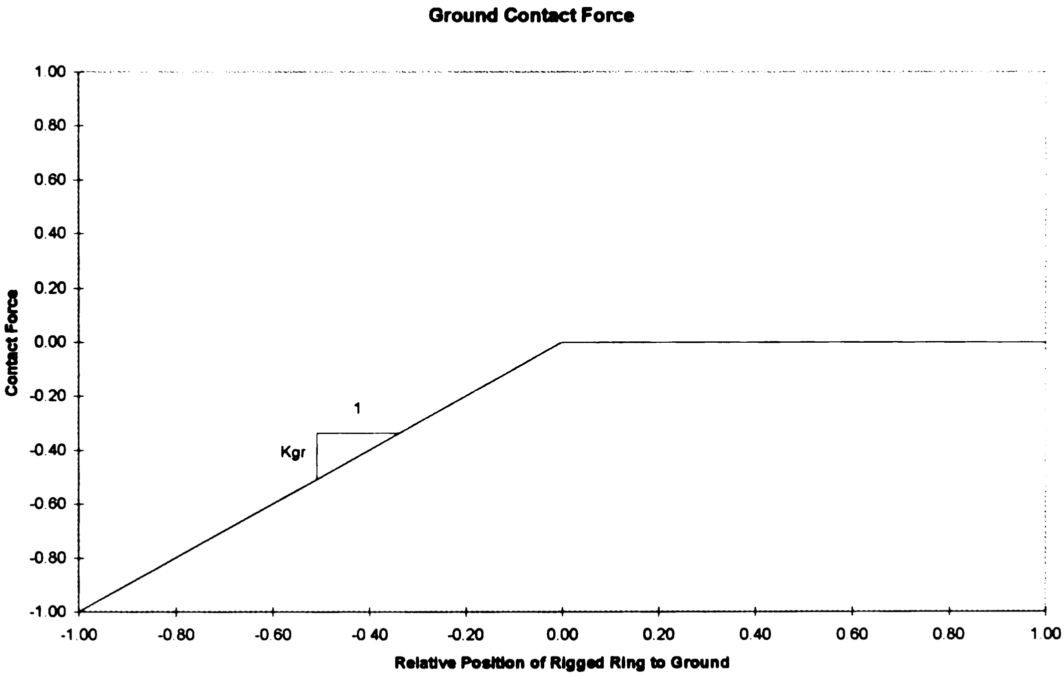

Figure 33: Non-Linear Contact Force Function

A diagram of the unpropelled tire model is presented in Figure 34. The tire model consists of a rigid ring which represents the tire carcass, the rim, and a linear spring in parallel with a damper which represents the tire side wall. As mentioned above, the damper is not an original part of Zegelaar's model, but has been added to damp out oscillations and make the model more numerically appealing. The bond graph of the model is shown in Figure 35. Table 10 describes the pertinent nodes of the model and their type, units, and associated subroutines. Note that the following subroutines are used in this model and can be found in Appendix A:

ZZSU01 - Multiplies several model parameters and a model variable
ZZSU02 - Non-linear contact stiffness. See Figure 33.

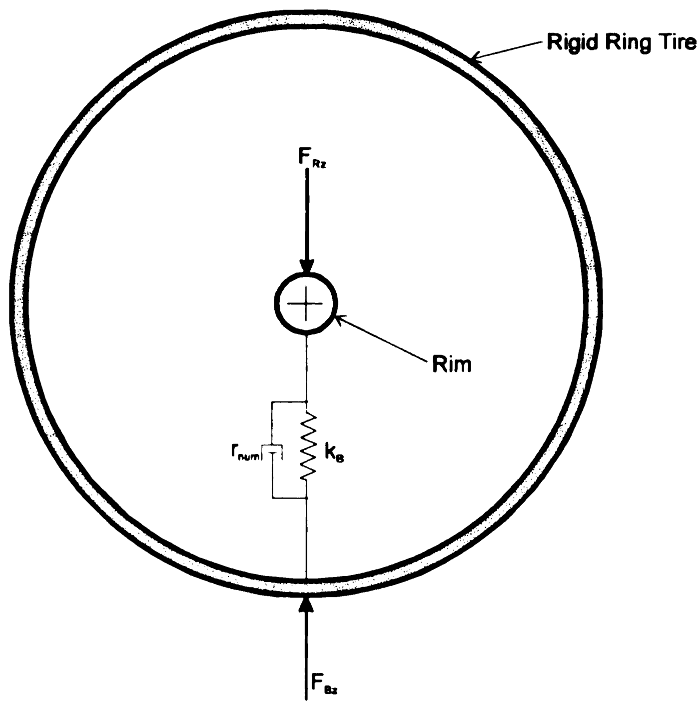

Figure 34: Diagram of modified Unpropelled Rigid Ring Tire Model

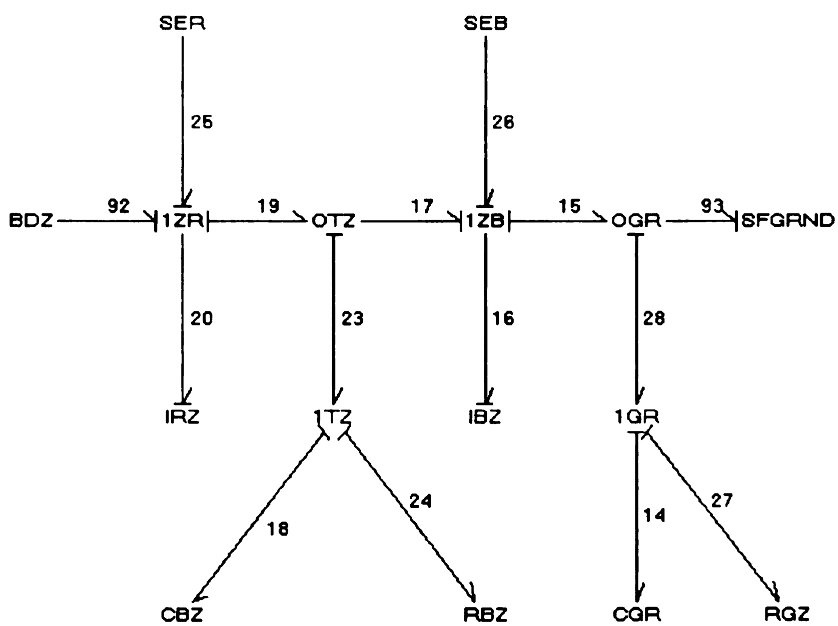

Figure 35: Bond graph submodel of an Unpropelled Rigid Ring Tire Model

Table 10: Unpropelled Rigid Rim Tire Model node descriptions

Name	Type	Primary Coordinate	Associated Subroutine	Description
BDZ	port	z		Rim connection to axle
CBZ	C	z		Tire stiffness
CGR	C	z	ZZSU02	Ground contact stiffness
IBZ	I	z		Tire Inertia
IRZ	I	z		Rim Inertia
RBZ	R	z		Tire/Numerical Damping
RGZ	R	z		Ground contact damping
SEB	SE	z	ZZSU01	Gravitational force of tire
SER	SE	z	ZZSU01	Gravitational force of rim
SFGRND	port	z		Road profile

A.2.2 Ports and Parameters

There are two ports associated with this model. As indicated in Figure 35 and Table 11 the two ports are BDZ and SFGRND. Table 11 describes the ports, their type, and associated units.

The parameters associated with this model are described in Table 12. There the parameter name, a description, associated node, units, and a typical range of usage are listed. The parameters describe the linear characteristics of a smaller 70% tire. (Zegelaar, 1983).

Table 11: Port description for an Unpropelled Rigid Ring Tire Model

Port	Location	Units	Description
BDZ	Bond 92	N m/s	Vertical force to rim Vertical velocity of rim
SFGRND	Bond 93	N m/s	Force transmitted to ground Velocity of ground profile

Table 12: Parameter description for an Unpropelled Rigid Rim Tire Model

Parameter	Node	Units	Typical Range	Description
KB	CBX, CBZ	N/m	1.47×10^6	Translational stiffness of tire
MRIM	IRZ	kg	5.0	Mass of rim
MTIRE	IBZ	kg	4.52	Mass of tire
RTIRE	RTIRE	m	.288	Undeformed tire radius
RNUM	RGZ		100	Tire/Numerical Damping
G	SER, SEB	m/s^2	9.81	Acceleration due to gravity
KGR	CGR	N/m	7.35×10^7	Contact stiffness with ground
RG	RGZ		1×10^4	Contact damping with ground

A.2.3 Verification Results

The verification of this model is rather simple since only the vertical steady state behavior must be checked. This will be accomplished by applying a 2000N load to the port BDZ with the model at initially at rest in a relaxed position. The net load applied to the tire will 2050N and since the tire stiffness is 1.47 MN/m it is anticipated that the net deflection of the tire will be 0.139cm. Figure 36 illustrates the damped dynamic response of the load application and verifies the steady state deflection of 0.139cm.

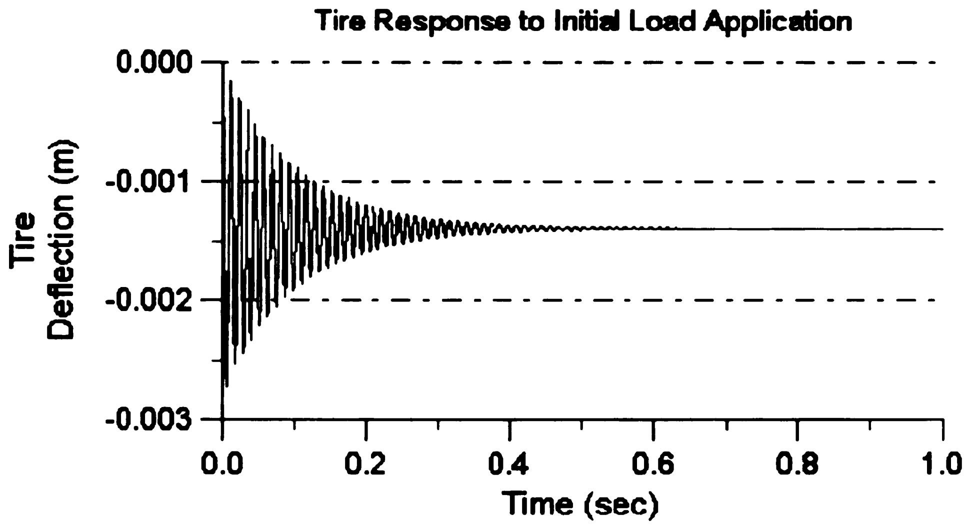

Figure 36: Verification Test - Damped response of vertical tire deflection to initial load application.

A.3 A Simple Open Differential

A.3.1 Model Description and Assumptions

A differential is used in automotive applications to distribute power from the transmission or drive shaft between the driven axles. Further, a differential compensates for speed variations between the driven wheels when a vehicle follows a curve. In this case, the differential is described as open because the torque transmitted to either axle is always the same while the speed of each axle may vary. The result is that if one axle loses traction the other axle can only provide as much traction as the axle which is slipping.

This is a simple model of a differential typically found in automotive applications. Gear backlash, viscous damping, contact stiffness, and inertial effects have been neglected and only the essential characteristics of the gear ratios are considered. Figure 37 below indicates that this model captures two separate stages of gear reduction between the Drive Pinion and Ring Gear and between the Differential Pinion gears and the Side Gears. In

Figure 38 this is represented as two separate transformers TFDIFF and TFPIN correspondingly. These transformers are also indicated in Figure 37.

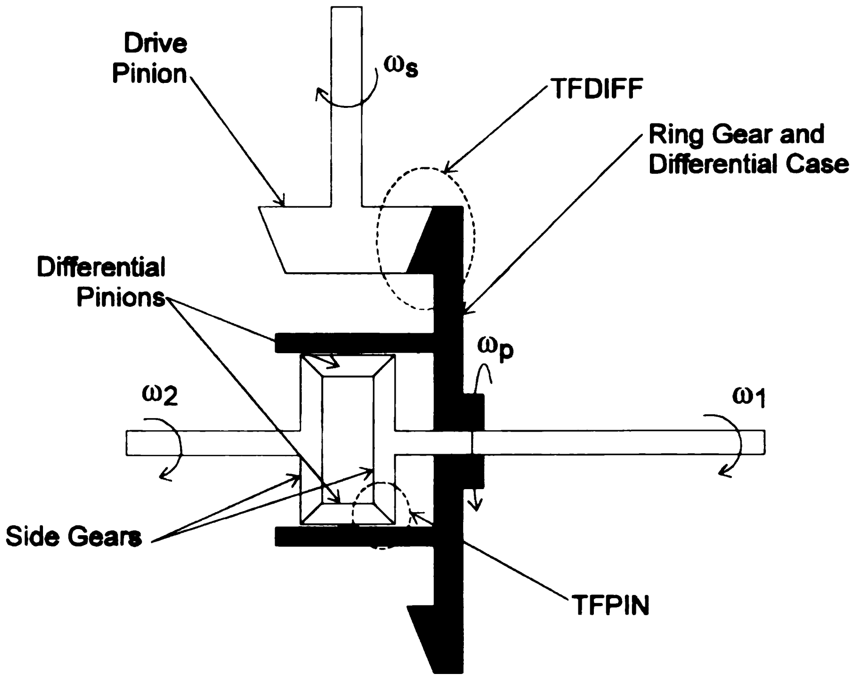

Figure 37: Diagram of a typical open face differential

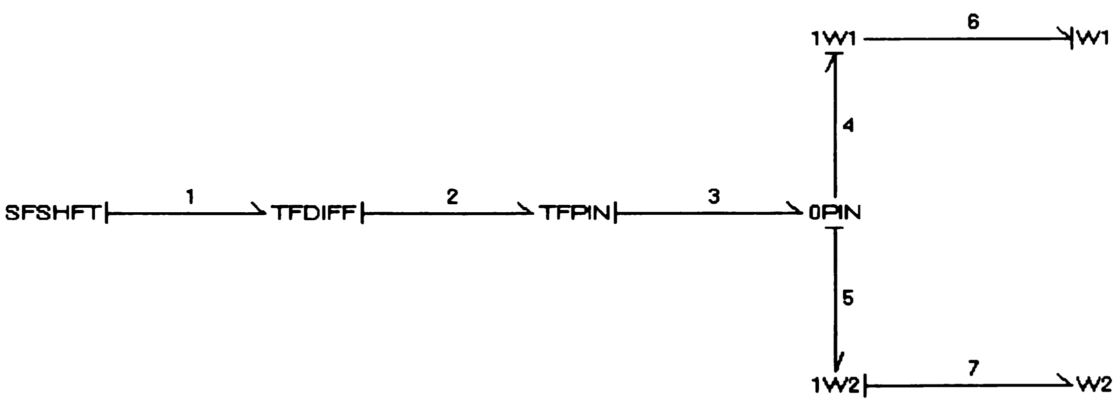

Figure 38: Bond graph submodel of a Simple Open Differential

A.3.2 Ports and Parameters

The ports of the Simple Open Face Differential are indicated in Figure 38 by the nodes SHFTIN, W1, and W2. Each of these nodes are connected to bonds and therefore each carry two pieces of information: effort and flow. Since the ports are all connected to rotating shafts effort corresponds to torque and flow corresponds to rotational velocity. Table 13 below describes the port information.

Table 13: Port description for a Simple Open Differential

Port	Location	Units	Description
SHFTIN	Bond 1	N-m rad/sec	Input shaft torque Input shaft angular velocity
W1	Bond 6	N-m rad/sec	Output shaft #1 torque Output shaft #1 angular velocity
W2	Bond 7	N-m rad/sec	Output shaft #2 torque Output shaft #2 angular velocity

Parameters associated with this model correspond to the gear ratios between the Drive Pinion and Ring Gear (node TFDIFF) and between the Differential Pinion gears and the Side Gears (node TFPIN). Table 14 below describes the parameters, their associated nodes, units, and recommended range of usage.

Table 14: Parameter Description for a Simple Open Differential

Parameter	Node	Units	Typical Range	Description
NDIFF	TFDIFF	-none-	2.73 to 4.11	Drive Pinion and Ring Gear reduction ratio.
NPIN	TFPIN	-none-	2	Two times reduction ratio of differential pinion gear teeth to side gear teeth.

A.3.3 Verification Results

Since this is a relatively simple model its verification is also correspondingly simple. That is to say that only a few tests are required and those tests are largely qualitative in nature. Several aspects of the Simple Open Differential need to be tested:

Test #1 - Proper input-output shaft speed reduction
Test #2 - Appropriate behavior during traction loss to a driven axle
Test #3 - Equal torque provided to each output axle

In all of the validate tests the following parameters were used: NDIFF=4, NPIN=2. The objective of Test #1 was to demonstrate that the speed reduction of the differential was appropriate. In the case of the given parameters, it was expected that the reduction of input shaft speed to output shaft speed was 4:1. The results of Test #1 are shown in Figure 39 below and indicate that this test is satisfied.

The objective of Test #2 was to evaluate the differential's performance when traction was lost to one axle. In this case the traction of W2 was ramped down from full traction to zero traction. It was anticipated that the effect of the traction loss would be two-fold. First, it was expected that as the traction of the axle W2 was decreased the torque applied to W1 would also decrease equivalently. Since the angular velocity of W1 has been set to be proportional to its supplied torque it was expected that as its torque decreased so would its speed. Thus, as the traction of W2 decreased it was expected that the speed of W2 would increase. Figure 40 confirms the anticipated variations in output shaft velocity and Figure **41** confirms the anticipated variations in torque. Further, Figure **41** also resolves the verification of Test 3 because it indicates that the torque applied to each output shaft is equal.

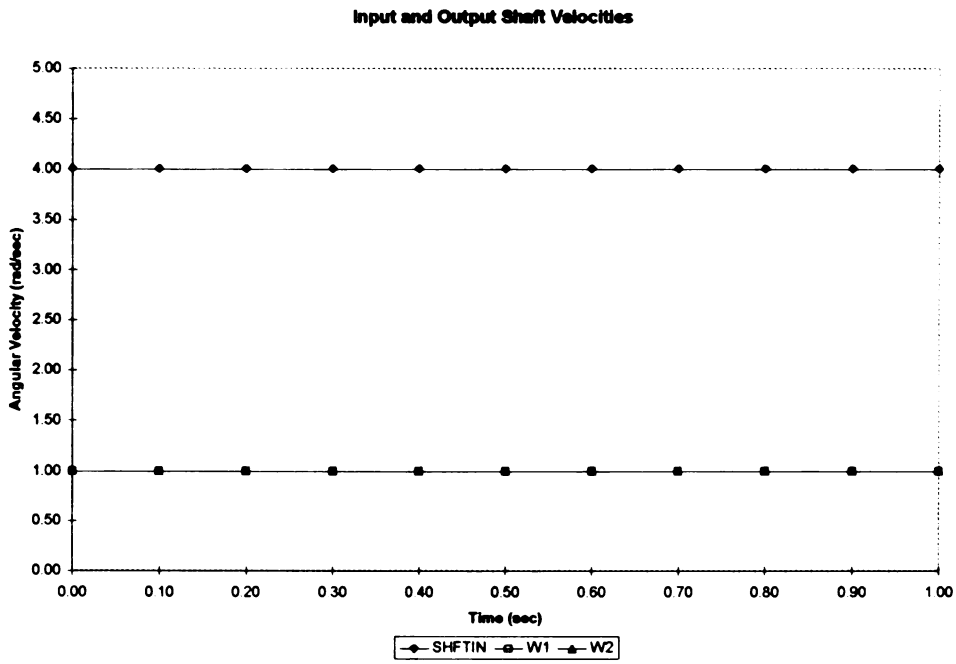

Figure 39: Simple Open Differential Verification Results: Test 1, the comparison of input and output shaft speeds.

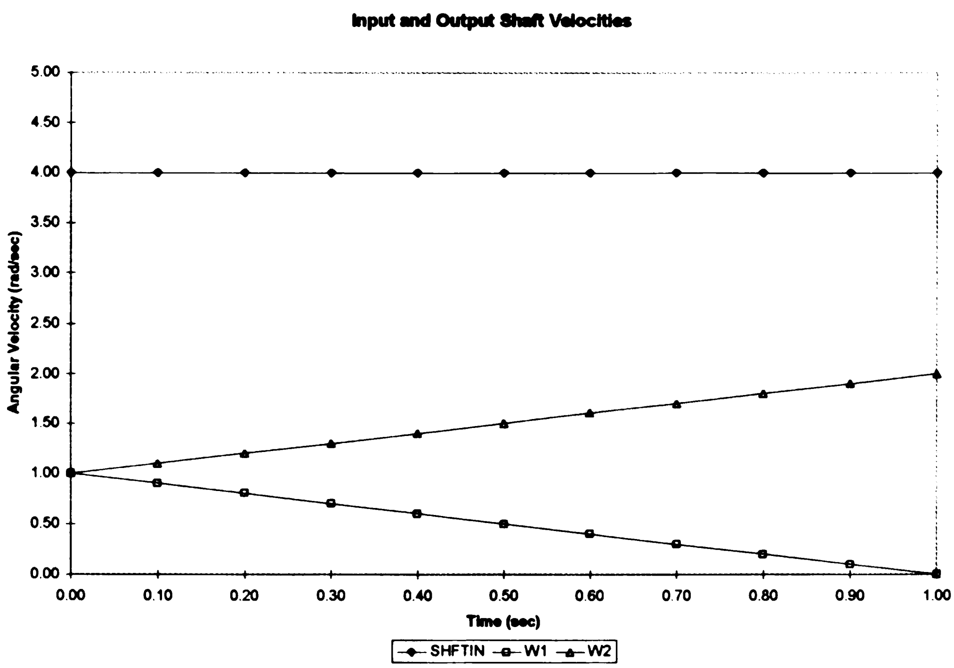

Figure 40: Simple Open Differential Verification Results: Test 2, the loss of traction to W2.

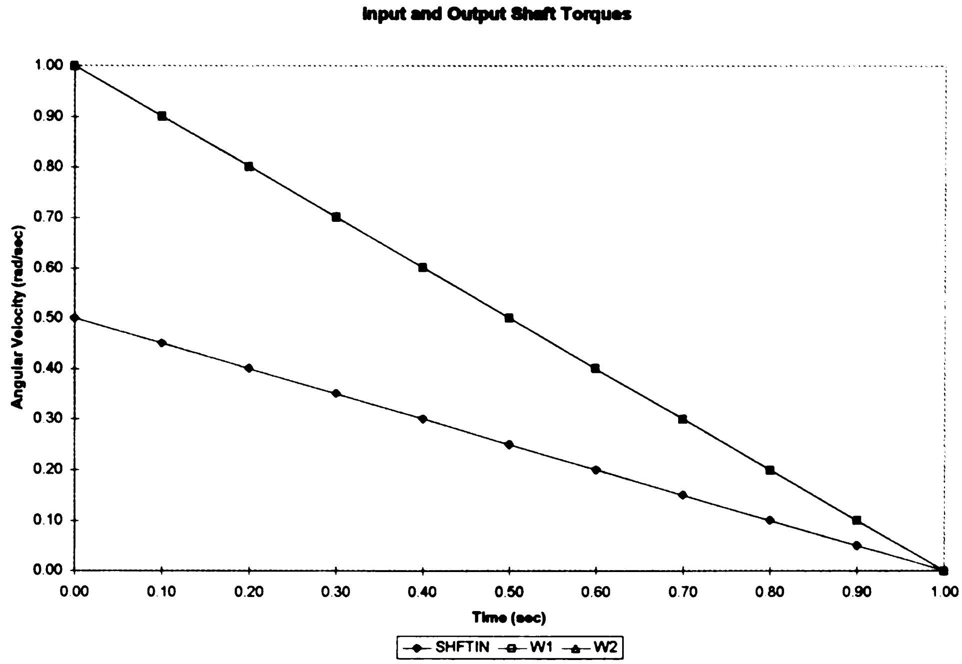

Figure 41: Simple Open Differential Verification Results: Tests 2 and 3, torque applied to each axle.

A.4 A Lumped Mass Manual Transmission with Clutch

A.4.1 Model Description and Assumptions

A generic manual transmission model is being presented which assumes that the stiffness, damping, and inertial effects of a manual transmission can be treated in a lumped fashion. Equivalent stiffness, damping, and inertia are used to capture the rotational dynamics of the transmission. The clutch is treated as having stribeck damping and torsional compliance.

The model is a combination of work completed by Hrovat (Hrovat, 1991) and Runde (Runde, 1986) complemented with work by the author of this thesis. Hrovat contributed the framework for a lumped mass transmission with torsional compliance due to the clutch. Runde's work details the characteristics of clutch during engagement where slip may or may not be present. The author of this thesis extended Hrovat's assumption of lumped mass to equivalent damping and torsional rigidity. Runde's work states that the causality of a clutch switches during slip and stick conditions. His work was modified slightly to include viscous damping such that the causality of the clutch is unchanged during slip and stick conditions. Figure 42 illustrates the viscous effects near zero clutch velocity and the stribeck damping which dominates as the magnitude of slip velocity is increased. Note that the coefficient of viscous damping, bcl, is sufficiently large to minimize slip velocity and simulate stick conditions.

A diagram of the model is shown in Figure 43 and the system bond graph is shown in Figure 44. Note that contact stiffness springs are shown on the pressure plate of the clutch. These springs allow the clutch pad and pressure plate to establish a normal force which balances the forces generated by the clutch springs. The force Fcl is the clutch disengaging force which the driver applies to disengage the clutch. The reduction ratio of the transmission is facilitated via the gear set and the node RATIO in Figure 44 dictates what the actual reduction ratio is based upon driver input. Throughout the model several subroutines have been used to model effects where the ENPORT function library was inadequate. The following subroutines have been used in this model:

ZZSU02 - Establishes the normal force in the clutch as a result of the contact stiffness.
ZZSU04 - Determines the torque transmitted by the clutch.
ZZSU05 - Selects a transmission reduction ratio based upon driver input.

Table 15 highlights the nodes in the bond graph model (Figure 44) and describes their type, associated subroutine, and function.

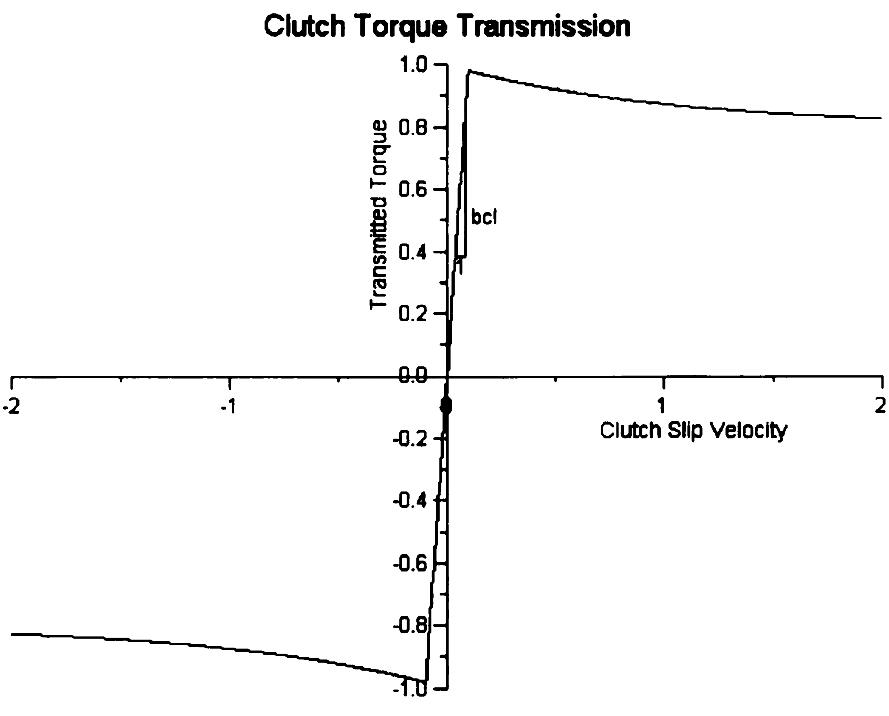

Figure 42: Clutch stick-slip properties.

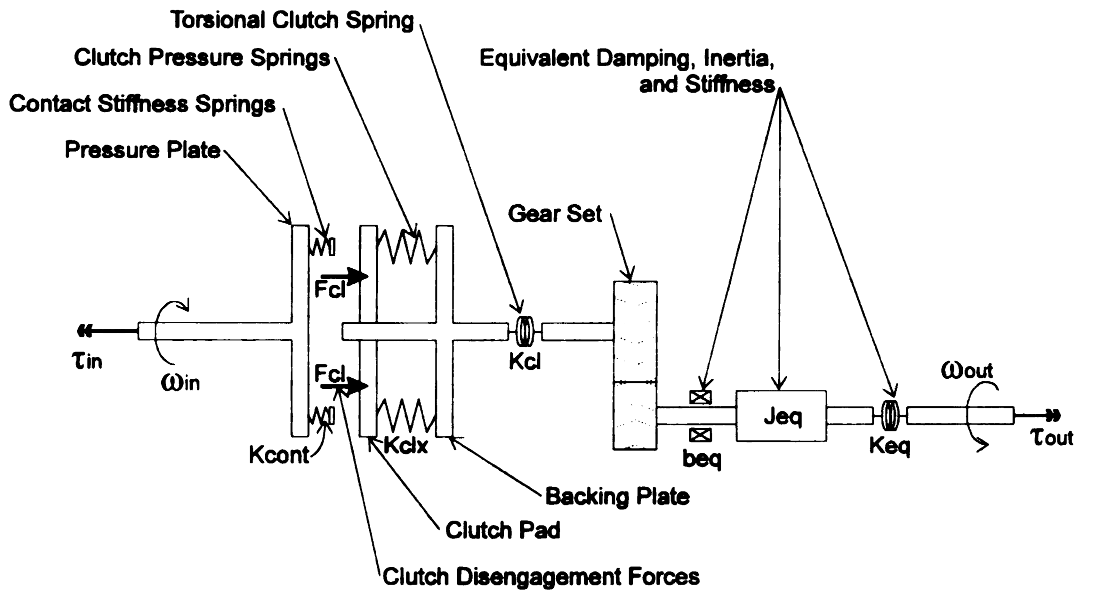

Figure 43: Diagram of a Lumped Mass Manual Transmission with Clutch

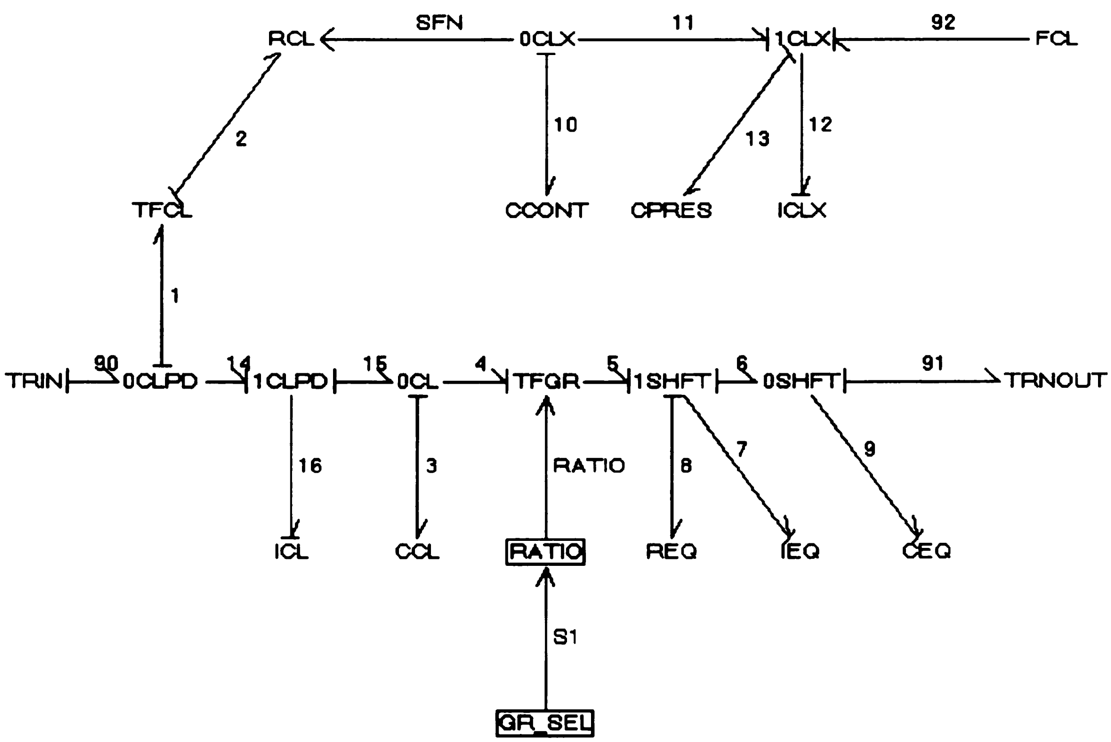

Figure 44: Bond graph of a Lumped Mass Manual Transmission

Table 15: Lumped mass manual transmission model node description.

Name	Type	Associated Subroutine	Description
CCL	C		Clutch torsional rigidity
CCONT	C	zzsu02	Clutch contact stiffness
CEQ	C		Equivalent stiffness
CPRES	C		Clutch pressure springs
FCL	port		Clutch disengagement force
GR_SEL	port		Driver gear selection
ICL	I		Clutch rotational inertia
ICLX	I		Clutch translational inertia
IEQ	I		Equivalent inertia
RATIO	fcn	zzsu05	Determines gear ratio from driver input
RCL	R	zzsu04	Clutch force transmission
REQ	R		Equivalent damping
TFCL	TF		Relates clutch forces to torques
TFGR	TF		Modulus of the transmission
TRIN	port		Input from engine
TRNOUT	port		Output to drive shaft

A.4.2 Ports and Parameters

In the following tables the ports and parameters used in the lumped mass transmission model are described. Table 27 describes the ports and Table 17 describes the parameters. The source of parameters values used in this model are Hrovat (Hrovat, 1991), Runde (Runde, 1986), and derived by the author of this thesis.

Table 16: Port description for a lumped mass manual transmission.

Port	Location	Units	Description
FCL	BOND 92	N m/s	Force applied to clutch Velocity of clutch
GR_SEL	signal S1	none	Driver gear selection
TRIN	BOND 90	N·m rad/sec	Motor torque at input Motor angular velocity
TROUT	BOND 91	N·m rad/sec	Output shaft torque Output shaft angular velocity

Table 17: Parameter description for a lumped mass manual transmission.

Parameter	Node	Units	Typical Range	Description
JCL	ICL	$kg{\cdot}m^2$	0.0296	Rotational inertia of the clutch pad/backing plate
MCL	ICLX	kg	5.93	Mass of clutch pad/backing plate
JEQ	IEQ	$kg{\cdot}m^2$	0.0105	Equivalent inertia of the transmission
KEQ	CEQ	N·m/rad	7000	Equivalent Stiffness of the transmission
REQ	REQ	N·s	0.0027	Equivalent viscous damping of the transmission
KCONT	CCONT	N/m	$1x10^9$	Contact stiffness
KCL	CCL	N·m/rad	678	Torsional stiffness of clutch springs
KCLX	CPRES	N/m	$2.95x10^5$	Stiffness of clutch pressure springs
RCL	TFCL	m	0.1016	Clutch radius
MUSTAT	RCL	-none-	0.4	Static coefficient of friction
MUDYN	RCL	-none-	0.3	Dynamic coefficient of friction
GEAR1	RATIO	-none-	3	1st gear ratio
GEAR2	RATIO	-none-	2	2nd gear ratio
GEAR3	RATIO	-none-	1.5	3rd gear ratio
GEAR4	RATIO	-none-	1	4th gear ratio
GEAR5	RATIO	-none-	0	5th gear ratio or neutral
GEARRV	RATIO	-none-	-3.5	Reverse gear ratio
BCL	RCL	N·s/m	1×10^4	Viscous clutch damping

A.4.3 Verification Results

The lumped mass manual transmission model must pass several tests before it can be treated as a valid model. The major qualities of the transmission operation which must be tested include the proper speed and torque reduction, clutch, and shifting. These qualities will be verified in the following tests:

Test 1 - Steady state input/output torque and velocity.
Test 2 - Affect of clutch engagement/disengagement on transmission input/output.
Test 3 - Influence of shifting gears on transmission input-output.

Test #1 requires that the steady state response of the transmission is evaluated. To facilitate this, an angular velocity step of 1rad/sec is applied to the input of the transmission and the response is observed. Figure 45 illustrates that after an initial transient the steady state output velocity is 0.33 rad/sec. This is expected since the reduction ratio during this test is 1/3. It can be concluded that the steady state throughput characteristics of the transmission are appropriate.

Test # 2 requires that the operation of the clutch is verified. To accomplish this the transmission will operate at a steady initial condition and then the clutch will be disengaged and re-engaged. A small amount of viscous damping has be added to the output of the transmission such that when the clutch is disengaged the output velocity will decrease. Figure 46 contains the results of the trial. The output velocity does decrease when the clutch is disengaged and then there is a slight transient as the output velocity returns to its initial state. Further note that the clutch normal forces also experience a slight transient after re-engagement. This is expected since the contact of the clutch and clutch plate is represented by a stiff spring.

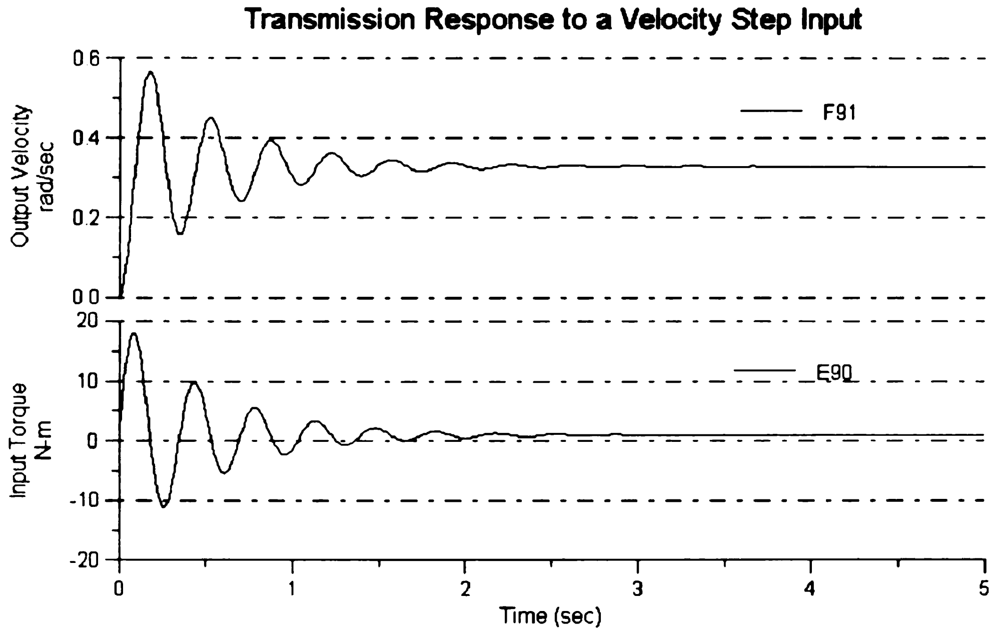

Figure 45: Test 1 - Steady state input torque and output velocity for a lumped mass manual transmission.

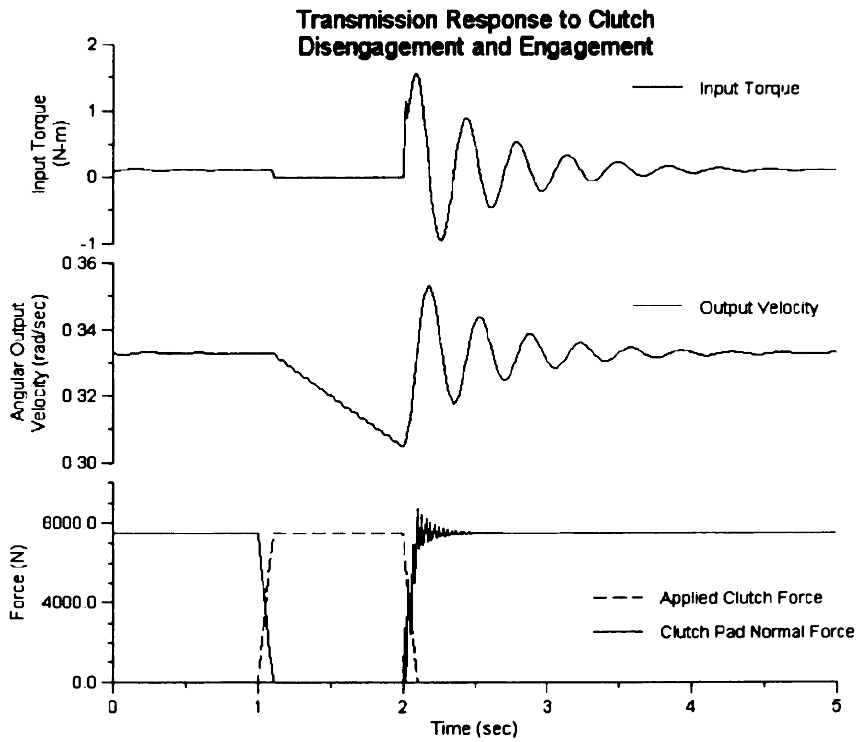

Figure 46: Test 2 - Lumped mass manual transmission response to clutch engagement and disengagement.

Test #3 requires that the shifting characteristics of the transmission are also evaluated. In this test the transmission is initially operating at steady state conditions. A brief description of the test cycle follows:

1. Initial steady state operation
2. At 1.0 seconds the input torque is ramped up.
3. At 3.0 seconds the clutch is disengaged, the motor torque is discontinued, and the transmission shifts gears.
4. From 4.0 to 8.0 seconds the clutch is engaged and the motor torque is ramped up.
5. At 8.0 seconds the clutch is disengaged, the motor torque is discontinued, and the transmission shifts gears.
6. From 8.0 to 12.0 seconds the clutch is engaged and the motor torque is held at constant value.

Figure 47 illustrates the response of the transmission during the above test cycle. There are several key characteristics which determine the proper performance of the transmission. The first quality is that the output velocity decreases when the clutch is disengaged. Figure 47 illustrates this during both shift points. The second quality is the ratio of input speed to output speed. As Figure 47 illustrates, the ratio of input speed to output speed is directly related to the transmission gear ratio. Initially the input speed is 105.2rad/sec and the output speed is 35.0rad/sec which results in a ratio of 3.00 as expected. After the transmission shifts to second gear the output speed is 48.6rad/sec and the input speed is 80.1rad/sec which results in a ratio of 1.97. This ratio is slightly lower than expected but since the vehicle is accelerating the input and output velocities will have a slight phase angle. This confirms that as the driver selects new gears, the transmission changes to the appropriate ratio and the clutch engages and disengages properly.

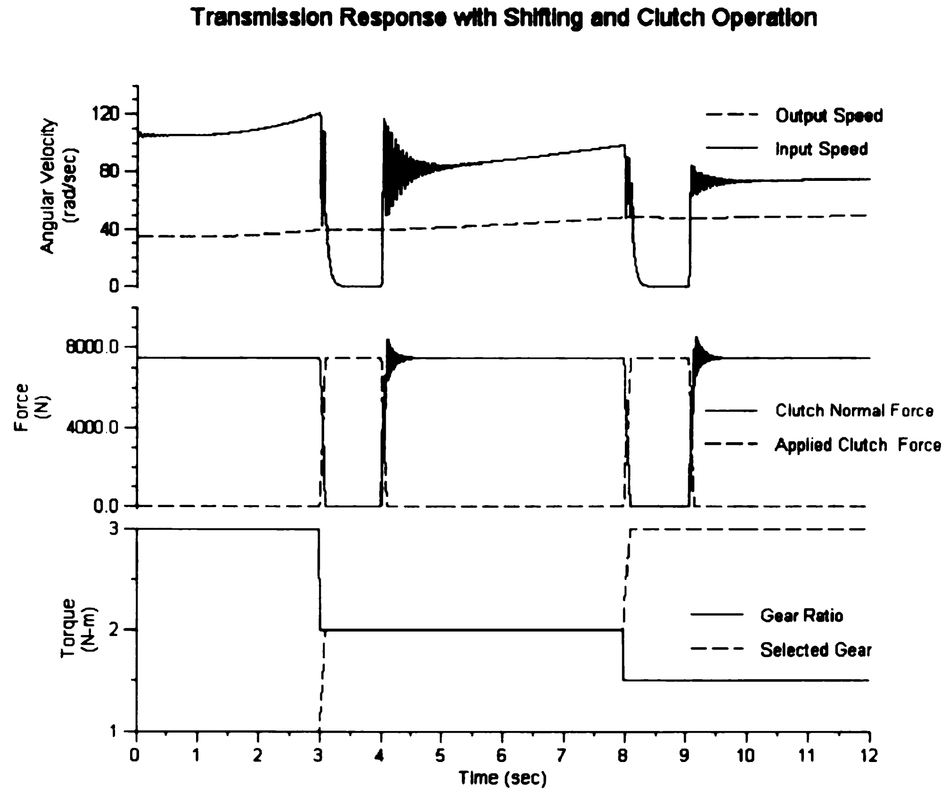

Figure 47: Test 3 - Lumped mass manual transmission response during shifting and clutch operation.

A.5 Hollow Shaft Models

A.5.1 Model Description and Assumptions

The hollow shaft model is used to transmit rotational power between various submodels in the vehicle model. Since there are different causal restrictions between submodels several shaft models must be developed which are capable of linking these components. Three different types of shaft models are described here. Each shaft model is capable of capturing the the zeroth and first modes of a hollow shaft and have identical characteristics. In all cases the user is required to specify shaft geometry in metric units.

Three different types of shaft models will be presented. They will be described by the causal restrictions on their input and output ports. The first model will be described as a flow-flow model since it dictates what flows the ports will have based upon the efforts applied by the outside models. The bond graph of the model can be seen in Figure 48. The second model will be described as an effort-effort model since it enforces effort on its external ports. The bond graph of this model is shown in Figure 49. The third model is described as an effort-flow model since it enforces effort on one port and flow on the other. The bond graph of this model is shown in Figure 50. While each of these shaft models appears to be different, they are each qualitatively identical.

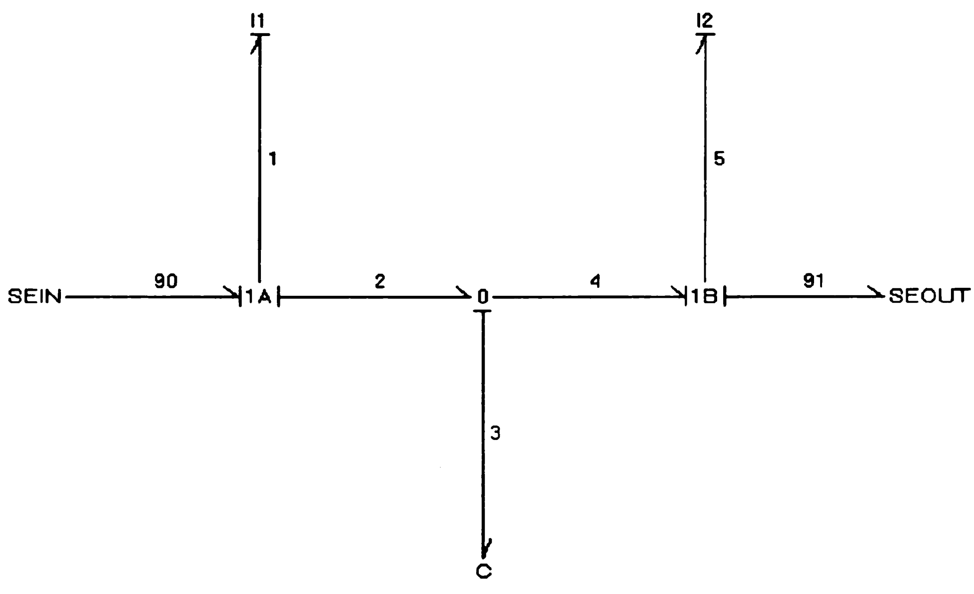

Figure 48: Bond graph of a hollow shaft model with flow-flow external causality.

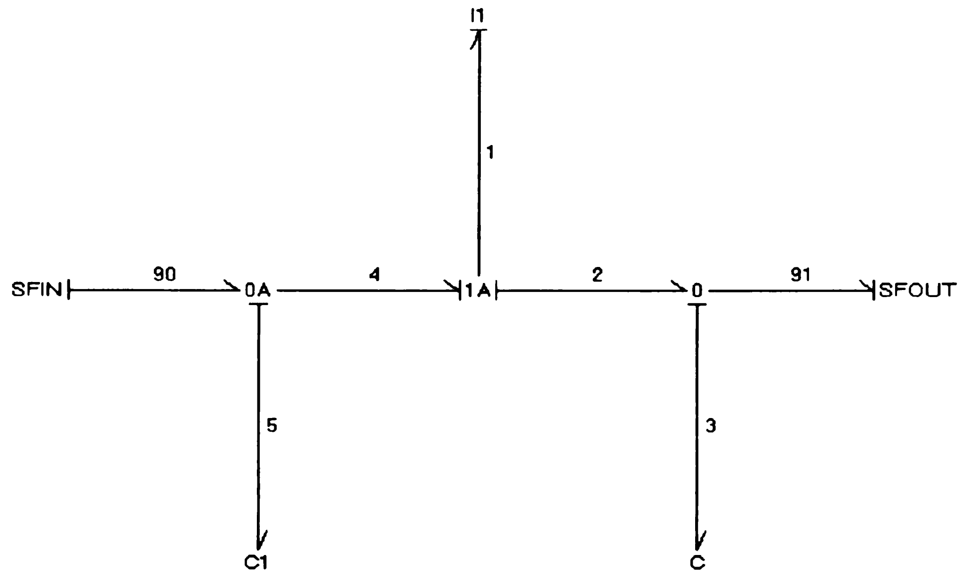

Figure 49: Bond graph of a hollow shaft model with effort-effort causality.

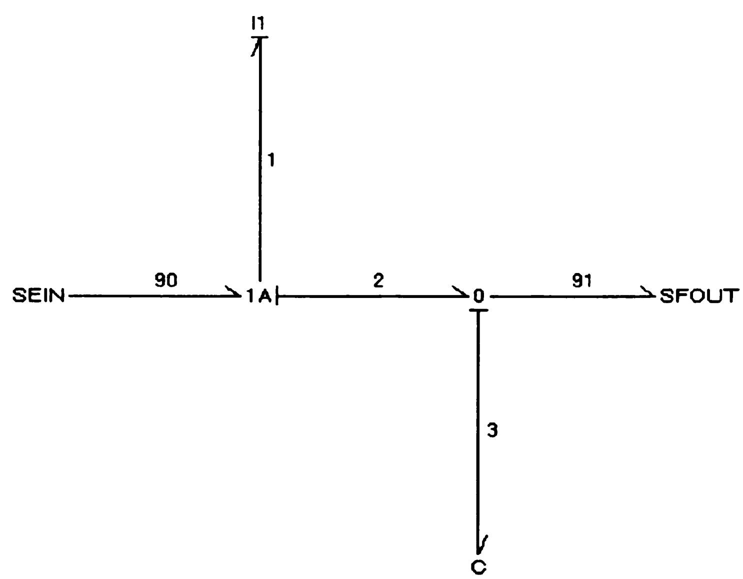

Figure 50: Bond graph of a hollow shaft model with effort-flow causality.

A.5.2 Ports and Parameters

Table 18 describes the ports and Table 19 describes the parameters for the hollow shaft models. All three of the models use the same ports and parameters.

Table 18: Ports for the hollow shaft model.

Port	Type	Units	description
INPUT	Bond	N-m rad/sec	Torque input to shaft Velocity of input to shaft
OUTPUT	Bond	N m/s	Torque input to shaft Velocity of input to shaft

Table 19: Parameters for the hollow shaft model.

Parameter	Node	Units	Typical Range	Description
L	C, I	m		Total shaft length
G	C	Pa	77.9×10^9	Modulus of Rigidity
DI	C,I	m		Inner Diameter
DO	C,I	m		Outer Diameter
rho	I	N/m^2	76.5×10^3	Material Density

A.6 Mean Torque Full Throttle Engine Model

A.6.1 Model Description and Assumptions

The engine model presented is a quasi-static semi-empirical model capable of predicting the mean value engine torque over a range of operating speeds. The range of speeds is dependent upon user supplied engine data. The user can choose between two modes of operation which can be described as being an idle mode and a operating mode. The idle mode gives the user the opportunity to specify an idle speed and then the engine will supply sufficient torque to maintain the steady state speed given engine damping. When the model is in "operating mode" the engine supplies torque as a function of engine speed. The engine torque is determined by a polynomial equation of up to order 9 and is determined by the subroutine ZZSU08 shown in appendix B. The model assumes that the engine inertia and damping can be lumped and treated linearly where the engine torque, output, and damping are applied to the engine inertia as shown in Figure 51. The bond graph of the model is shown in Figure 52 and the nodes are explained in Table 20.

Engine data used in this study is based upon published data for a GM 4.3L V6 internal combustion engine (Graham, 1992). A seventh order polynomial was fit through the torque data and the coefficients were entered as parameters for the model. The parameter values are shown in the next section and the torque curve is shown with the verification results.

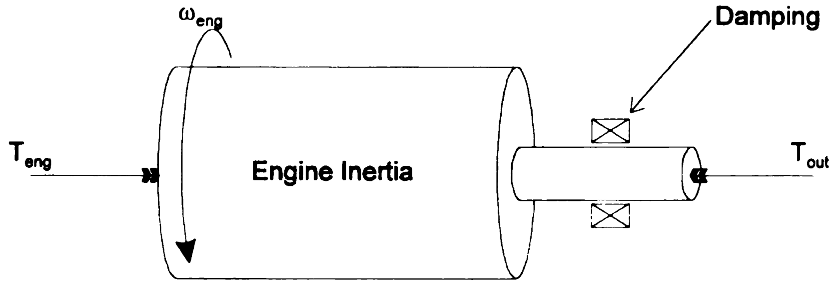

Figure 51: Diagram of a mean torque full throttle engine model.

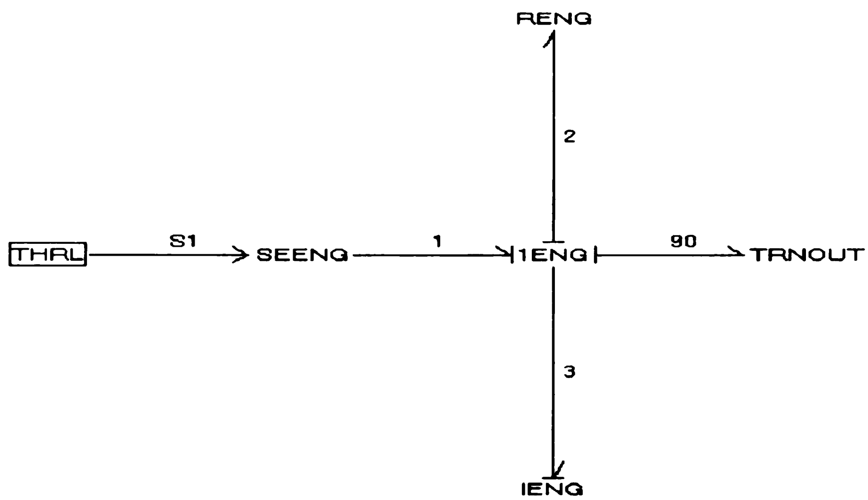

Figure 52: Bond graph of a mean torque full throttle engine model

Table 20: Node description for a mean torque full throttle engine model.

Name	Type	Associated Subroutine	Description
IENG	I		Lumped engine inertia
RENG	R		Lumped engine damping
SEENG	SE	ZZSU08	Determines the applied engine torque as a function of engine speed and operating mode
THRL	port		Determines engine mode of operation
TRNOUT	port		Engine output.

A.6.2 Ports and Parameters

The ports and parameters used in this model are shown in Tables 21 and 22 respectively.

Table 21: Ports for a mean torque full throttle engine model.

Port	Type	Units	Description
THRL	signal		Determines operation mode of engine. 0 ⇒ idle mode, 1 ⇒ operation mode.
TRNOUT	bond	N·m rad/sec	Output torque Output speed.

Table 22: Parameters for a mean torque full throttle model.

Parameter	Node	Units	Typical Range	Description
jeng	IENG	kg·m^2	0.1354	Equivalent inertia
reng	RENG	N·m·s	0.2714	Equivalent damping
X0	SEENG	-none-	-570.6165	0th order polynomial term.
X1	SEENG	-none-	24.11288	1st order polynomial term.
X2	SEENG	-none-	-2.749187e-01	2nd order polynomial term.
X3	SEENG	-none-	1.636347e-03	3rd order polynomial term.
X4	SEENG	-none-	-5.470921e-06	4th order polynomial term.
X5	SEENG	-none-	1.039598e-08	5th order polynomial term.
X6	SEENG	-none-	-1.052086e-11	6th order polynomial term.
X7	SEENG	-none-	4.408587e-15	7th order polynomial term.
X8	SEENG	-none-	0	8th order polynomial term.
X9	SEENG	-none-	0	9th order polynomial term.

A.6.3 Verification

The mean torque engine model will be validated for proper torque output and operating mode performance. Figure 53 shows the mean torque output as a function of engine speed when the model is in operating mode. The curve shown is a seventh order polynomial fit through data publish by General Motors (Graham, 1992). The coefficients of the curve are shown in Table 22. The idle mode performance is shown in Figure 54 where the system settles to 100 rad/sec (idle speed) from 200rad/sec. The model satisfies both of these tests successfully.

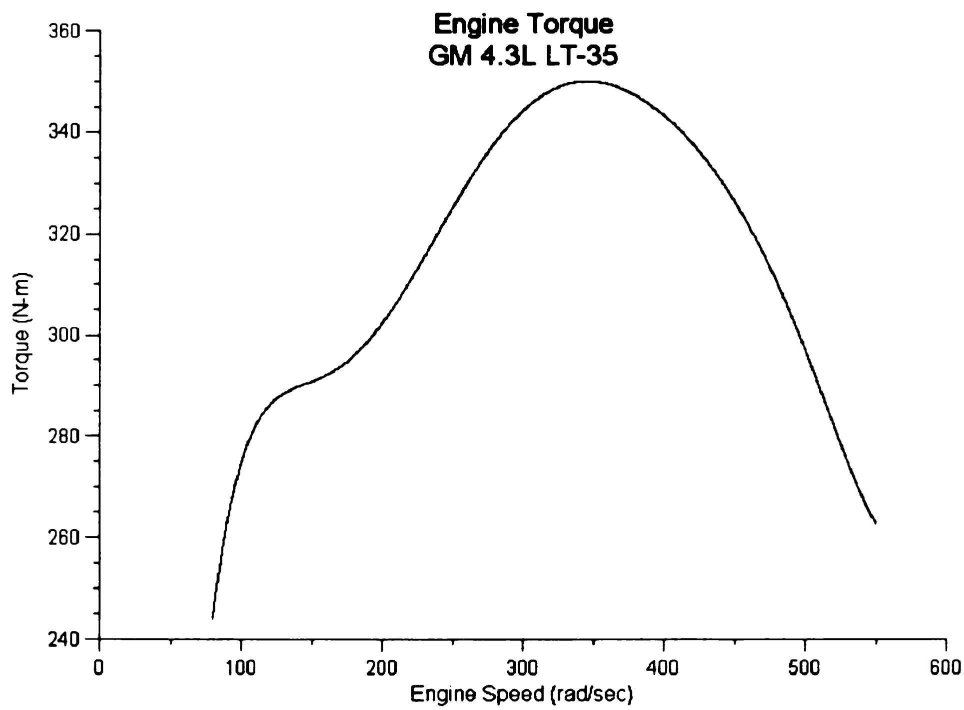

Figure 53: Torque as a function of engine speed for a mean torque engine model based upon a GM 4.3L V6 engine.

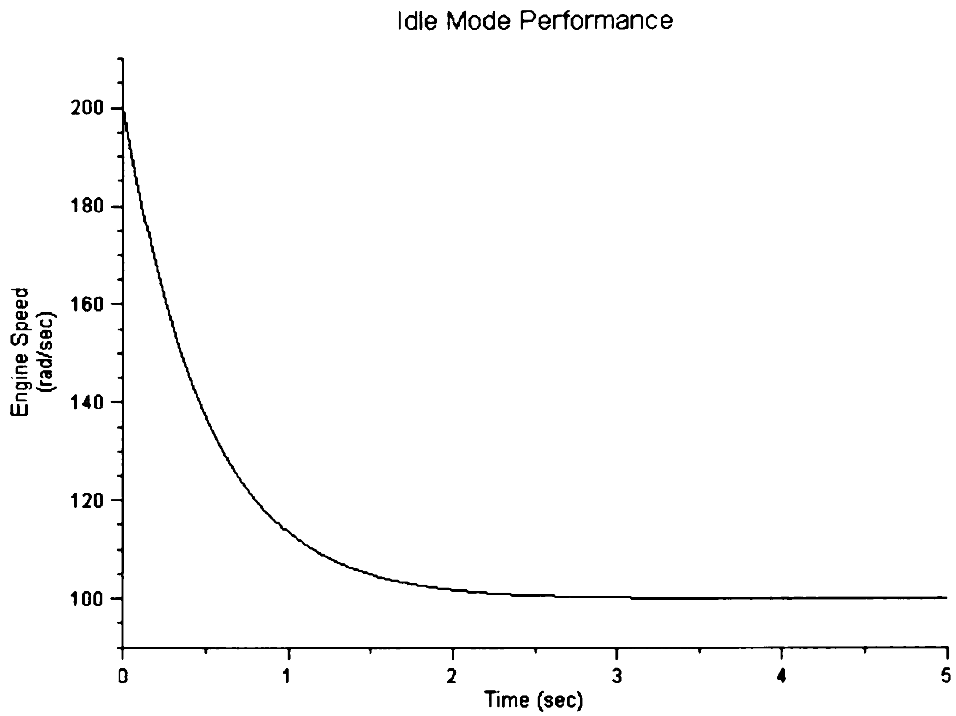

Figure 54: Engine speed during idle mode operation.

A.7 Longitudinal Wind Effects

A.7.1 Model Presentation and Assumptions

Drag on the vehicle resulting from wind is calculated based upon information presented by Gillespie (Gillespie, 1992). This model only considers wind effects in the longitudinal direction of the vehicle and is based upon the dynamic pressure of the wind in conjunction with a drag coefficient. The net forces which the vehicle feels are determined by the RWIND node in Figure 55 which calculates force as a function of relative wind speed. Varying wind speed and gusts are ported to the model through the SFWIND node and vehicle speed and forces are ported to the model through the BODY node. The RWIND node is based upon the following equation,

$$F = R_{eq}V^2 \tag{2}$$

where R_{eq} is the equivalent wind damping and V is the wind speed relative to the vehicle.

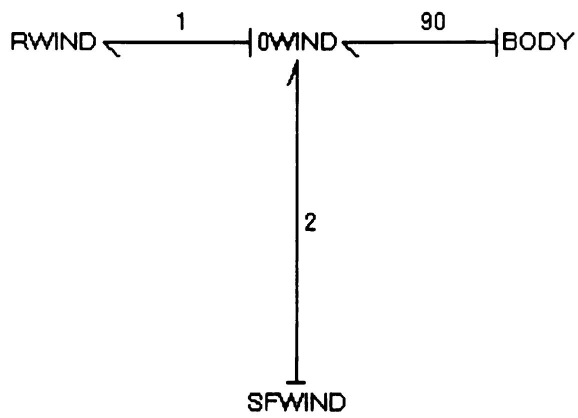

Figure 55: Bond graph of wind effects model.

A.7.2 Ports and Parameters

The ports associated with the longitudinal wind effects model are shown in Table 23 along with their associated information. The only parameter associated with the wind effects model is R_{eq} which is based upon work presented by Gillespie (Gillespie, 1992). The equation for R_{eq} is,

$$R_{eq} = \tfrac{1}{2}\rho \cdot A \cdot C_d \tag{3}$$

where ρ is the density of the air, A is the frontal area of the vehicle, and C_d is the drag coefficient. In this study R_{eq} = 0.3983 N·s/m. Often the drag coefficient is based upon experimental results, but typical values for a particular vehicle body style can be used as an initial value. In this study C_d=0.35 was used as a typical value for an aerodynamic sedan.

Table 23: Ports for the longitudinal wind effects model.

Port	Location	Units	Description
BODY	bond 90	N	Force exerted on body
		m/s	Velocity of body
SFWIND	bond 2	N	Force exerted by additional wind
		m/s	Absolute velocity of wind

A.7.3 Verification

The proper functioning of the model will be evaluated by studying the forces exerted as a function of relative wind speed. Figure 56 shows the wind forces where R_{eq} was set equal to 0.3983 N·s/m. It can be seen that at 0 m/s the force is zero Newtons and that at 50 m/s the force is 996 N which is valid for this model.

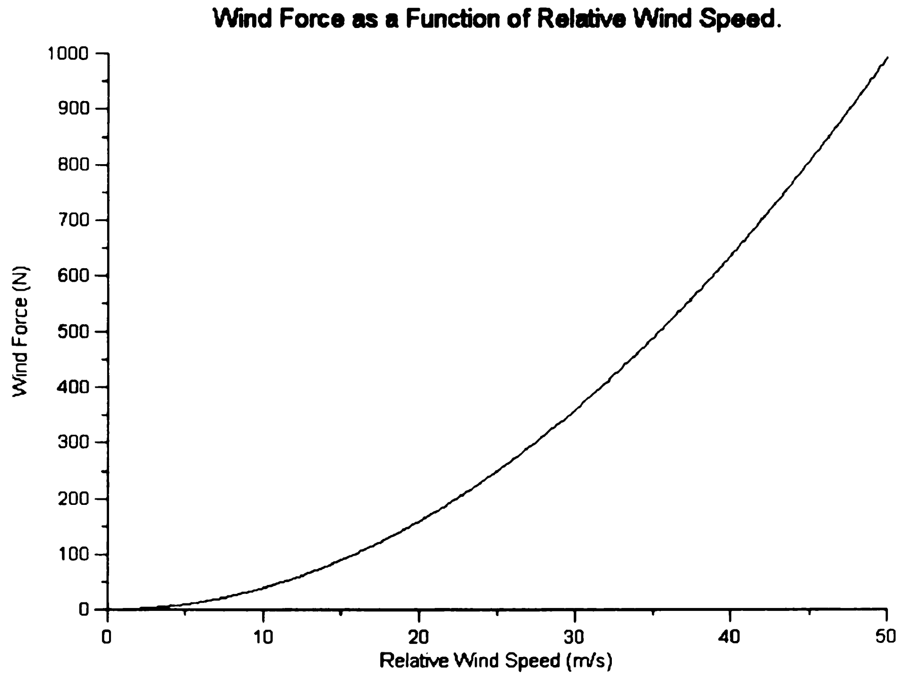

Figure 56: Wind force as a function of relative wind speed.

Appendix B

FORTRAN Subroutines

The FORTRAN subroutines used by ENPORT are listed below. References to these subroutines are made throughout Appendix A.

B.1 ZZSU01 - Parameter Multiplication

```
      SUBROUTINE ZZSU01(TIME,X,P,Y,STAT)
C---- PROGRAMMING:  Mark Minor    3/5/96
C---- DESCRIPTION:  Multiplies two parameters
C---- INPUTS:  TIME,    current time
C              X,       input_variable values
C              P,       parameter values
C              STAT(1), =1 iff 1ST time subrtn is called,  =0 else
C              STAT(2), =1 iff last time subrtn is called, =0 else
C              STAT(3), =1 iff last time subrtn is called
C                            for this storage interval, =0 else
C
C---- OUTPUTS: Y,       output_variable values
C              STAT(4)  =1, stop the integration,  =0 continue
C
C---- DECLARATIONS:
      CHARACTER         STR*80
      DOUBLE PRECISION TIME, X(20), P(20), Y(20)
      INTEGER           STAT(10)
C
      EXTERNAL          ZZWRIT
C
C     P(1) - P1a
C     P(2) - P1b
C
C***ZZSU01************************************************************
C
C---- Description section
      IF (STAT(10).EQ.1) THEN
        STR= ' A function to multiply multiple parameters and vars and'
        CALL ZZWRIT(STR)
        STR= ' sum it all up.'
```

```
        CALL ZZWRIT(STR)
        RETURN
      ENDIF
C
C---- Multipling two parameters....
C
      Y(1) = P(1)*P(2)
      RETURN
      END
```

B.2 ZZSU02 - Ground Contact Force Function

```
      SUBROUTINE ZZSU02(TIME,X,P,Y,STAT)
C---- PROGRAMMING:  Mark Minor    2/26/96
C---- DESCRIPTION:  A contact function which only establishes a
tranmitted force when contact is made
C
C---- INPUTS:  TIME,     current time
C             X,        input_variable values
C             P,        parameter values
C             STAT(1),  =1 iff 1ST time subrtn is called,  =0 else
C             STAT(2),  =1 iff last time subrtn is called, =0 else
C             STAT(3),  =1 iff last time subrtn is called
C                          for this storage interval, =0 else
C
C---- OUTPUTS: Y,        output_variable values
C             STAT(4)   =1, stop the integration,  =0 continue
C
C---- DECLARATIONS:
      CHARACTER        STR*80
      DOUBLE PRECISION TIME, X(20), P(20), Y(20)
      INTEGER          STAT(10)
C
      EXTERNAL         ZZWRIT

c     P(1) - Contact Stiffness
C     P(2) - P(2)>0 : Compression,  P(2)<0 : Tension forces only
C     X(1) - Displacement of spring from Free Length
C     Y(1) - Contact force
C
C***ZZSU02************************************************************
C
C---- Description section
      IF (STAT(10).EQ.1) THEN
        STR= ' A function which determines whether forces are'
        CALL ZZWRIT(STR)
        STR= ' transmitted.  P(1) is the contact stiffness'
        CALL ZZWRIT(STR)
        STR= ' P(2) >< 0 => compr/tension contact forces only.'
```

```
        CALL ZZWRIT(STR)
        RETURN
      ENDIF
C
C---- Contact stiffness subroutine
C
      if (p(2) .gt. 0) then
        if (x(1) .ge. 0) then
          y(1) = abs(p(1))*x(1)
        else
          y(1) = 0
        endif
      else
        if (x(1) .le. 0) then
          y(1) = abs(p(1))*x(1)
        else
          y(1) = 0
        endif
      endif
      RETURN
      END
```

B.3 ZZSU03 - Multi Parameter and Variable Multiplication

```
      SUBROUTINE ZZSU03(TIME,X,P,Y,STAT)
C---- PROGRAMMING:  Mark Minor    3/5/96
C---- DESCRIPTION:  Multiplies two parameters and a variable for 2
channels and sums it all to give the output result
C
C---- INPUTS:  TIME,    current time
C              X,       input_variable values
C              P,       parameter values
C              STAT(1), =1 iff 1ST time subrtn is called,  =0 else
C              STAT(2), =1 iff last time subrtn is called, =0 else
C              STAT(3), =1 iff last time subrtn is called
C                           for this storage interval, =0 else
C
C---- OUTPUTS: Y,       output_variable values
C              STAT(4)  =1, stop the integration,  =0 continue
C
C---- DECLARATIONS:
      CHARACTER        STR*80
      DOUBLE PRECISION TIME, X(20), P(20), Y(20)
      INTEGER          STAT(10)
C
      EXTERNAL         ZZWRIT
C
C     P(1) - P1a
```

```
C     P(2) - P1b
C     X(1) - X1
C     P(3) - P2a
C     P(4) - P2b
C     X(2) - X2
C
C***ZZSU01************************************************************
C
C---- Description section
      IF (STAT(10).EQ.1) THEN
        STR= ' A function to multiply multiple parameters and vars and'
        CALL ZZWRIT(STR)
        STR= ' sum it all up.'
        CALL ZZWRIT(STR)
        RETURN
      ENDIF
C
C---- Multipling two parameters....
C
      Y(1) = P(1)*P(2)*X(1)+P(3)*P(4)*X(2)
      RETURN
      END
```

B.4 ZZSU04 - Coulomb Damping Function

```
      SUBROUTINE ZZSU04(TIME,X,P,Y,STAT)
C---- PROGRAMMING:  Mark Minor 3/17/96
C---- DESCRIPTION:  Coulomb Damping Function
C---- INPUTS:  TIME,     current time
C              X,        input_variable values
C              P,        parameter values
C              STAT(1), =1 iff 1ST time subrtn is called,  =0 else
C              STAT(2), =1 iff last time subrtn is called, =0 else
C              STAT(3), =1 iff last time subrtn is called
C                           for this storage interval, =0 else
C
C---- OUTPUTS: Y,        output_variable values
C              STAT(4)  =1, stop the integration,  =0 continue
C
C---- DECLARATIONS:
      CHARACTER         STR*80
      DOUBLE PRECISION TIME, X(20), P(20), Y(20),fd,fd_break,vr,fd_max
      DOUBLE PRECISION fsp, fds, fdf
      INTEGER           STAT(10)
C
      EXTERNAL          ZZWRIT
C
C     P(1)    Static Coefficient of Frictin
C     P(2)    Dynamic Coefficient of Friction
```

```
C     P(3)    Viscous damping which allows evaluation of torque when
vr<>0
C     X(1)    Normal Force
C     X(2)    Velocity of slip
C     Y(1)    Damping Force
C
C***ZZSU04************************************************************
C
C---- Description section
      IF (STAT(10).EQ.1) THEN
        STR= ' Coulomb Damping Function'
        CALL ZZWRIT(STR)
        RETURN
      ENDIF
C
C---- Stribeck Coulomb Damping Subroutine
C
      vr = X(2)
      fd_break = P(1)*x(1)
      fd_max   = P(2)*x(1)
      fsp = X(1)

      fds = p(3) * vr          ! Forces due to slip

c  Forces due to stick friction
      fdf=dsign(1,vr)*(fd_max+(fd_break-fd_max)*exp(-abs(vr)))
      if (abs(fds) .le. abs(fdf)) then
        fd = fds
      else
        fd = fdf
      end if
      Y(1) = fd
      RETURN
      END
```

B.5 ZZSU05 - Parameter Selection Based Upon Signal

```
      SUBROUTINE ZZSU05(TIME,X,P,Y,STAT)
C---- PROGRAMMING:  Mark Minor
C---- DESCRIPTION:  Gear selection subroutine....
C---- INPUTS:  TIME,    current time
C              X,       input_variable values
C              P,       parameter values
C              STAT(1), =1 iff 1ST time subrtn is called,  =0 else
C              STAT(2), =1 iff last time subrtn is called, =0 else
C              STAT(3), =1 iff last time subrtn is called
C                          for this storage interval, =0 else
C
C---- OUTPUTS: Y,       output_variable values
```

```
C              STAT(4)  =1, stop the integration,  =0 continue
C
C---- DECLARATIONS:
      CHARACTER        STR*80
      DOUBLE PRECISION TIME, X(20), P(20), Y(20)
      INTEGER          STAT(10)
C
      EXTERNAL         ZZWRIT
C     P(1)    First Gear Ratio
C     P(2)    Second Gear Ratio
C     P(3)    Third Gear ratio
C     P(4)    Fourth Gear Ratio
C     P(5)    Fifth Gear Ratio
C     P(6)    Reverse Gear Ratio (should be less than zero)
C     X(1)    Driver Gear Selection
C     Y(1)    Output gear ratio
C
C***ZZSU05*************************************************************
C
C---- Description section
      IF (STAT(10).EQ.1) THEN
        STR= ' Subroutine to select transmission gear ratio.'
        CALL ZZWRIT(STR)
        RETURN
      ENDIF
C
C---- The Subroutine...
C
      if (X(1) .le. 1) then
        Y(1) = P(1)
      else if (X(1) .le. 2) then
        Y(1) = P(2)
      else if (X(1) .le. 3) then
        Y(1) = P(3)
      else if (X(1) .le. 4) then
        Y(1) = P(4)
      else if (X(1) .le. 5) then
        Y(1) = P(5)
      else if (X(1) .le. 6) then
        Y(1) = P(6)
      end if

      RETURN
      END
```

B.6 ZZSU08 - Engine Torque-Speed Curve

```
SUBROUTINE ZZSU08(TIME,X,P,Y,STAT)
C
C---- PROGRAMMING:  Mark Minor, 3/24/96
C
C---- DESCRIPTION:  Determines engine torque as a function of speed
C
C---- INPUTS:  TIME,    current time
C              X,       input_variable values
C              P,       parameter values
C              STAT(1), =1 iff 1ST time subrtn is called,  =0 else
C              STAT(2), =1 iff last time subrtn is called, =0 else
C              STAT(3), =1 iff last time subrtn is called
C                          for this storage interval, =0 else
C
C---- OUTPUTS: Y,       output_variable values
C              STAT(4)  =1, stop the integration,  =0 continue
C
C---- DECLARATIONS:
      CHARACTER        STR*80
      DOUBLE PRECISION TIME, X(20), P(20), Y(20), W
      INTEGER          STAT(10)
C
      EXTERNAL         ZZWRIT

c      X(1) - Engine speed, rad/sec
C      X(2) - 1 => engaged, 0=>disengaged
c      Y(1) - Engine torque, N-m
c      P(1) - X^0 coeff
c      P(2) - X^2 coeff
c      P(3) - X^3 coeff
c      P(4) - X^4 coeff
c      P(5) - X^5 coeff
c      P(6) - X^6 coeff
c      P(7) - X^7 coeff
c      P(8) - X^8 coeff
c      P(9) - X^9 coeff
c      P(10) - offset coeff
C      P(11) - idle speed
C      P(12) - equivalent motor damping
C
C***ZZSU08*************************************************************
C
C---- Description section
      IF (STAT(10).EQ.1) THEN
        STR= ' Engine subroutine'
        CALL ZZWRIT(STR)
        RETURN
      ENDIF
C
C---- Engine subroutine
```

```
C

      if (X(1) .lt. 85) then
       W = 85
      elseIF (X(1) .GT. 550) THEN
       W = 550
      ELSE
       W = X(1)
      endIf

      if (X(2) .gt. 0) then
        Y(1) = W*P(1)+P(2)*W**2+P(3)*W**3+P(4)*W**4+P(10)+
     /  P(5)*W**5+P(6)*W**6+P(7)*W**7+P(8)*W**8+P(9)*W**9
        Y(1) = Y(1) * 0.70
      else
        Y(1) = P(11)*P(12)
      end if

      RETURN
      END
```

B.7 ZZSU23 - Tire Slip Function

```
      SUBROUTINE ZZSU23(TIME,X,P,Y,STAT)
C  ---- PROGRAMMING:
C       ver     date         who     what
c       1.0     9/25/95      Minor   Initial creation for testing.
c       1.1     10/9/95      Minor   Modify variable notation.
C       2.1     10/14/95     Minor   Adapted original single power port
model
c                                      to two-power port version.
C       2.2     10/14/95     Minor   Added ability to assign Yss and
Ypk.
c                                      Removed assignment of shape
function.
C
C---- DESCRIPTION:  Two power port tire traction function.
C
C---- INPUTS:      X(1) Traction velocity
c                  X(2) Wheel velocity
C                  X(3) Normal Force (FNORM)
C
C                  P(1) Asymptotic FTR/FNORM typical for high slip.
C                  P(2) Peak value of FTR/FNORM
C                  P(3) Slip where peak occurs.
C                  P(4) SLOPE AT ORIGIN (DEGREES)
C
C                  STAT(1), =1 iff 1ST time subrtn is called,  =0 else
C                  STAT(2), =1 iff last time subrtn is called, =0 else
C                  STAT(3), =1 iff last time subrtn is called
C                           for this storage interval, =0 else
```

```
C                  STAT(4)  =1, stop the integration,  =0 continue
C
C---- OUTPUTS:     Y(1) Traction Force (FTR)
C                  Y(2) % SLIP


C
C---- DECLARATIONS:
      CHARACTER         STR*80
      DOUBLE PRECISION TIME, X(20), P(20), Y(20), E, SLIP, YSS, YPK
      DOUBLE PRECISION THETA, VTR, FNORM, FTR,PI
      INTEGER           STAT(10)
C
      EXTERNAL          ZZWRIT

      YSS   = P(1)
      YPK   = P(2)
      XPK   = P(3)
      THETA = P(4)

      VTR   = X(1)
      VWHL  = X(2)
      FNORM = X(3)
      PI = 3.1415927
C
C***ZZSU23************************************************************
C
C---- Description section
      IF (STAT(10).EQ.1) THEN
      STR= ' Tire Traction-Handling Model'
      CALL ZZWRIT(STR)
      STR= ' Based upon the Magic Formula Traction model'
      CALL ZZWRIT(STR)
      STR= ' developed by Pacejka, Delft University'
      CALL ZZWRIT(STR)
      RETURN
      ENDIF
C
C---- Subroutine...
C
C CHECKING FOR APPLIED NORMAL FORCE...

      IF (X(3) .LT. 0) THEN
      Y(1) = 0
      Y(2) = 0
      GOTO 999
      END IF
C CALUCLATING COEFFICIENTS...
      IF (ABS(VTR) .LT. .1) THEN
      VTR = 0
      ENDIF

      IF (ABS(VHWL) .LT. .1) THEN
      VHWL=0
```

```
      ENDIF

      IF (VTR .EQ. 0) THEN
      IF (VWHL .EQ. 0) THEN
      SLIP = 0
      ELSEIF (VWHL .GT. 0) THEN
      SLIP =-10
      ELSE
      SLIP = 10
      ENDIF
      ELSE
      SLIP = (VTR-VWHL)/VTR
      ENDIF

      SHAPE =((PI-ASIN(YSS/YPK))*2/PI)
      B = TAN(THETA/180*PI)/(SHAPE*YPK)
      E = (B*XPK-TAN(PI/2/SHAPE))/(B*XPK-ATAN(B*XPK))

C CALCULATING THE OUTPUT

      FTR = FNORM*YPK*SIN(SHAPE*ATAN(B*SLIP-E*(B*SLIP-ATAN(B*SLIP))))
      Y(1) = FTR
      Y(2) = FTR
 999  RETURN
      END
```

B.8 ZZSU50 - Automatic Tranmission Torque Converter

This torque converter model is based upon one used by Runde [Runde, 1986].

```
SUBROUTINE ZZSU50(TIME,X,P,Y,STAT)
C---- PROGRAMMING:  Mark Minor    4/18/96
C---- DESCRIPTION:  Torque converter subroutine
C---- INPUTS:  TIME,    current time
C              X,       input_variable values
C              P,       parameter values
C              STAT(1), =1 iff 1ST time subrtn is called,  =0 else
C              STAT(2), =1 iff last time subrtn is called, =0 else
C              STAT(3), =1 iff last time subrtn is called
C                          for this storage interval, =0 else
C---- OUTPUTS: Y,       output_variable values
C              STAT(4)  =1, stop the integration,  =0 continue
C---- DECLARATIONS:
      CHARACTER         STR*80
      DOUBLE PRECISION TIME, X(20), P(20), Y(20), wp,wt,Tp,Tt
      INTEGER           STAT(10)
C
```

```
      EXTERNAL          ZZWRIT
c
C     x(1) = wp => pump speed
C     x(2) = wt => turbine speed
c     y(1) = Tp => pump torque
C     y(2) = Tt => turbine torque
C
C***ZZSU50************************************************************
C
C---- Description section
      IF (STAT(10).EQ.1) THEN
        STR= ' Torque converter subroutine.'
        CALL ZZWRIT(STR)
        RETURN
      ENDIF
C
C---- The subroutine
C
      wp=X(1)
      wt=X(2)

      Tp=3.4325e-3*wp**2+2.2210e-3*wp*wt-4.6041e-3*wt**2
      Tt=5.7656e-3*wp**2+3.107e-4*wp*wt-5.4323e-3*wt**2

      Y(1)=Tp
      Y(2)=Tt


      RETURN
      END
```

B.9 ZZSU51 - Determination of CVT Ratio

```
SUBROUTINE ZZSU51(TIME,X,P,Y,STAT)
C
C---- PROGRAMMING:  Mark Minor    4/18/96
C
C---- DESCRIPTION:  CVT Model
C
C---- INPUTS:  TIME,    current time
C              X,       input_variable values
C              P,       parameter values
C              STAT(1), =1 iff 1ST time subrtn is called,  =0 else
C              STAT(2), =1 iff last time subrtn is called, =0 else
C              STAT(3), =1 iff last time subrtn is called
C                          for this storage interval, =0 else
C
C---- OUTPUTS: Y,       output_variable values
C              STAT(4)  =1, stop the integration,  =0 continue
```

```
C
C---- DECLARATIONS:
      CHARACTER        STR*80
      DOUBLE PRECISION TIME, X(20), P(20), Y(20)
      INTEGER          STAT(10)
C
      EXTERNAL         ZZWRIT

c     X(1) - Engine Speed
c     X(2) - Transmission Speed
C     Y(1) - Gear ratio
C     P(1) - Proportionality to engine speed
C     P(2) - Proportionality to transmission speed
C     P(3) - Offset
C     ie: Y(1)=X(1)P(1)+X(2)P(2)+P(3)
C
C***ZZSU51**************************************************************
C
C---- Description section
      IF (STAT(10).EQ.1) THEN
        STR= ' CVT Ratio model'
        CALL ZZWRIT(STR)
        RETURN
      ENDIF
C
C---- CVT Ratio Subroutine
C
      Y(1) = X(1)*P(1)+X(2)*P(2)+P(3)

      RETURN
      END
```

Literature Cited

7. Literature Cited

Broenink, 1995. PC Version of the Bond Graph Modeling, Analysis, and Simulation Tool CAMAS. *1995 International Conference on Bond Graph Modeling and Simulation.* 203-8. San Diego: Society for Computer Simulation

Gillespie, T. D. 1992. *Fundamentals of Vehicle Dynamics.* 4th Printing. Warrendale, PA: Society for Automotive Engineers, Inc.

Graham, C. R. 1992. General Motors High Performance 4.3L V6 Engine. *SAE Transactions.* Vol. 101. Sect 3. 1305-1320. Warrendale, Pa: Society of Automotive Engineers, Inc.

Hales, M.K. 1995. A Design Environment for the Graphical Representation of Hierarchical Engineering Models. Master of Science Thesis. Michigan State University.

Hrovat, D. 1991. Bond Graph Modeling of Automotive Power Trains. *Journal of the Franklin Institute.* Elmsford, NY: Pergamon Press.

Karnopp, D.C., D.L. Margolis, and R.C. Rosenberg. 1990. *System Dynamics: A Unified Approach.* 2nd ed. Canada: John Wiley and Sons, Inc.

Margolis, D.L. and J. Asgari. 1989. Sophisticated Yet Insightful Models of Vehicle Dynamics Using Bond Graphs. *Advanced Automotive Technologies, Automotive Society of Mechanical Engineers, DSC Volume 13.* 155-168. New York, N.Y.: American Society of Mechanical Engineers.

Pacejka, H.B. and E. Bakker. 1991. The Magic Formula Tyre Model. *Tyre Models for Vehicle Dynamic Analysis: proceeding of the 1st International Colloquium on Tyre Models for Vehicle Dynamics Analysis held in Delft, The Netherlands. Supplement to Vehicle System Dynamics, Volume 21.* 1-18. Amsterdam/Lisse, The Netherlands: Swets and Zeitlinger B.V.

Runde, J. K. 1986. Modeling and Control of an Automatic Transmission. Master's Thesis. Massachusetts Institute of Technology, Department of Mechanical Engineering.

Top, J.L., A.P.J. Breuneuse, J.F.Broenink, J.M. Akkermans. 1995. Structure and Use of a Library for Physical System Models. *1995 International Conference on Bond Graph Modeling and Simulation. (ICBGM '95).* 97-102. San Diego: The Society for Computer Simulation.

Wagner, J.R. 1995. Optimization of a Tire Traction Model for Antilock Brake System Simulations. *Transactions of the ASME, Journal of Dynamic Systems, Measurement, and Control.* Vol. 117. 199-204. New York, N.Y.: American Society of Mechanical Engineers.

Zegelaar, P.W.A., S. Gong, and H.B. Pacejka. 1993. Tyre Model for the Study of In-plane Dynamics. *The Dynamics of Vehicles on Roads and on Tracks. Supplement to Vehicle System Dynamics, Volume 23.* 578-590. Alblasserdam, The Netherlands: Offsetdrukkerij Kanters B.V.